

Effective Bayesian Modeling of Large Spatiotemporal Count Data Using Autoregressive Gamma Processes

Yifan Cheng * and Cheng Li †

Department of Statistics and Data Science, National University of Singapore

Abstract

We put forward a new Bayesian modeling strategy for spatiotemporal count data that enables efficient posterior sampling. Most previous models for such data decompose logarithms of the response Poisson rates into fixed effects and spatial random effects, where the latter is typically assumed to follow a latent Gaussian process, the conditional autoregressive model, or the intrinsic conditional autoregressive model. Since log-Gaussian is not conjugate to Poisson, such implementations must resort to either approximation methods like INLA or Metropolis moves on latent states in MCMC algorithms for model fitting and exhibit several approximation and posterior sampling challenges. Instead of modeling logarithms of spatiotemporal frailties jointly as a Gaussian process, we construct a spatiotemporal autoregressive gamma process guaranteed stationary across the time dimension. We decompose latent Poisson variables to permit fully conjugate Gibbs sampling of spatiotemporal frailties and design a sparse spatial dependence structure to get a linear computational complexity that facilitates efficient posterior computation. Our model permits convenient Bayesian predictive machinery based on posterior samples that delivers satisfactory performance in predicting at new spatial locations and time intervals. We have performed extensive simulation experiments and real data analyses, which corroborated our model’s accurate parameter estimation, model fitting, and out-of-sample prediction capabilities.

Keywords: spatiotemporal count data, Gibbs sampler, autoregressive gamma process, Vecchia approximation.

*y.cheng@u.nus.edu

†stalic@nus.edu.sg

Contents

1	Introduction	3
2	A Bayesian Spatiotemporal Model for Count Data	6
3	Posterior Sampling Algorithm	13
4	Spatial and Temporal Predictions	17
5	Simulation Experiments	19
6	World Weekly COVID-19 Data	26
7	Discussion	33
A	Deductions Leading to Posterior Sampling Steps for the Model Given by (2.1), (2.13), and (2.14)	34
B	Spatiotemporal Frailty Process Stationarity Condition for the Third Simulation Group Mentioned at the Start of Section 5	39
C	Simulation Results Complementary to Section 5	41
D	World Weekly COVID-19 Data Results Complementary to Section 6	73

1 Introduction

Spatial and spatiotemporal count data are ubiquitous in many scientific fields, such as ecology (Estes et al., 2018), epidemiology (Ward et al., 2023), and transcriptomics (Zhao et al., 2021). Bayesian models for such data enable flexible hierarchical structures, convenient posterior sampling, and robust uncertainty quantification. A classic statistical model for spatial and spatiotemporal count data is the latent Gaussian model (LGP, Diggle et al. 1998; Christensen and Waagepetersen 2004), where the count data is assumed to follow a standard generalized linear model such as the log-linear model, whose log-transformed parameters are specified as a linear combination of fixed effects and spatial random effects. For point-referenced spatial data, the spatial random effects are typically assumed to follow a continuous latent Gaussian process, characterizing the spatial or spatiotemporal dependence and leading to a well-defined stochastic process over continuous domains. For areal data, the spatial random effects are typically assumed to follow the conditional autoregressive model (CAR) or the intrinsic conditional autoregressive model (ICAR, Besag 1974; Mardia 1988; Besag et al. 1991; Besag and Kooperberg 1995). Computationally, both LGP and CAR models are often fit by either the integrated nested Laplace approximation (INLA, Rue et al. 2009; Blangiardo et al. 2013) or Markov chain Monte Carlo (MCMC) algorithms that require Metropolis moves for latent states (Lee et al., 2018). For example, a recent survey on the spatial and spatiotemporal analysis of COVID-19 epidemiology reveals that almost all statistical models adopted in practice belong to either the LGP or ICAR class of models and used either INLA or MCMC for model fitting (Nazia et al., 2022).

While the LGP and CAR models have achieved considerable empirical success in statistical applications, there exist several potential drawbacks in current statistical models and computational strategies. First, modeling the spatial random effects as Gaussian processes implies that the rate parameter of a Poisson response variable follows a log-Gaussian

process, which is not conjugate to the Poisson distribution. Therefore, to compute the posterior distribution, one has to rely on either approximation methods such as INLA or Metropolis moves on latent states in an MCMC algorithm. INLA typically depends on tessellation of the spatial domain and incurs an approximation error that does not necessarily vanish with large samples. For MCMC algorithms, the dimension of latent states gets large as the number of spatial locations becomes large, and thus, the Metropolis moves may result in slow mixing of posterior chains and low effective sample sizes. Second, the log-Gaussian process is known to lead to potentially large gradients of log-likelihoods with respect to the latent states and model parameters in the covariance functions ([Christensen and Waagepetersen, 2004](#)), which makes exploration of the full posterior difficult and requires numerical truncation. Third, realizations of an LGP model often demonstrate the whitening effect ([Morales-Navarrete et al., 2024](#)), due to implicit restrictions on the correlation structure caused by the nugget for spatial count data ([De Oliveira, 2013](#)). The literature offers many alternative strategies to overcome the aforementioned modeling and computational challenges. For instance, [De Oliveira \(2013, 2014\)](#) studied several classes of transformed covariance functions to remove discontinuity in the covariance function caused by the nugget and reduce the whitening effect. More recently, new efficient MCMC algorithms based on the Pólya-Gamma sampler have been proposed in [D'Angelo and Canale \(2023\)](#) for the Poisson model and in [Bansal et al. \(2021\)](#) for spatial negative binomial model. [Bradley et al. \(2018\)](#) and [Bradley and Clinch \(2025\)](#) introduced new classes of multivariate log-gamma distributions as a fully conjugate prior of the Poisson model for spatial count data, which results in a fully conjugate posterior that does not require MCMC sampling.

This work focuses on Bayesian modeling of spatiotemporal count data and proposes a new modeling strategy that enables efficient and fully conjugate Gibbs sampling of spatiotemporal frailties and model parameters. Instead of assuming a log-Gaussian process on the spatial random effects as in most of the previous literature, we take the Poisson frailties

associated with all spatial locations corresponding to each time interval as a vector and generalize scalar autoregressive gamma processes for time series (Gourieroux and Jasiak 2006, Creal 2017) to model the spatiotemporal frailties, thus extending prior applications of autoregressive gamma processes from the time series setting and the time-to-event network setting (Zhai et al., 2025) to the spatiotemporal setting. We make four main contributions, as follows. First, we establish a spatiotemporal autoregressive gamma process provably stationary across the time dimension. Different from LGP and CAR, our construction does not involve any Gaussian latent variables. Second, we adopt a novel decomposition of latent Poisson variables that allows fully conjugate Gibbs sampling of the frailties and scalar parameters c , κ , ρ in Section 2. Third, we design a spatial dependence structure built on a sparse neighborhood graph that leads to a computational complexity linear in both the number of spatial locations and the number of time intervals in each posterior sampling iteration, thus facilitating efficient posterior computation. Fourth, we develop a complete set of Bayesian predictive machinery for new points in both spatial and temporal dimensions, based on posterior samples of spatiotemporal frailties and model parameters.

The rest of this paper is organized as follows. Section 2 introduces our Bayesian spatiotemporal count model with prior specification and a rigorous theory on the stationarity condition for the spatiotemporal frailty process. Section 3 details the posterior sampling steps for all model parameters. Section 4 elaborates on procedures for predicting at future time intervals and unseen spatial locations. Section 5 conducts extensive simulation experiments that justify our model’s accurate parameter estimation, model fitting, and prediction capabilities on par with alternative methods. Section 6 analyzes world weekly COVID-19 cases and deaths data using our framework and competitive spatiotemporal count models, validating our model’s effectiveness and satisfactory performance in both in-sample and out-of-sample predictions. Section 7 concludes with pointers towards potential future work. Finally, the supplementary material provides deduction details of the MCMC sam-

pler in Section 3, presents a theorem that justifies stationarity of the spatiotemporal frailty process for the third simulation group in Section 5, and displays complementary results for simulation experiments and the COVID-19 real data example in Sections 5 and 6.

2 A Bayesian Spatiotemporal Model for Count Data

Let $m, T \in \mathbb{N}$ be the numbers of spatial locations and time intervals of equal length, respectively. For each $(i, t) \in \{1, \dots, m\} \times \{1, \dots, T\}$, we denote $y_t(\mathbf{s}_i) \in \mathbb{N}$ as our observed counts at the spatial location \mathbf{s}_i during the t^{th} time interval. Then $\{y_t(\mathbf{s}_i) : t = 1, \dots, T, i = 1, \dots, m\}$ consists of all the observed count data. We assume

$$y_t(\mathbf{s}_i) \mid U^t(\mathbf{s}_i), \boldsymbol{\beta}, \mathbf{x}_t(\mathbf{s}_i) \stackrel{\text{ind}}{\sim} \text{Poisson}(U^t(\mathbf{s}_i) \exp\{\mathbf{x}_t(\mathbf{s}_i)^T \boldsymbol{\beta}\}), \quad (2.1)$$

where $\text{Poisson}(\lambda)$ denotes the Poisson distribution with rate parameter λ , $U^t(\mathbf{s}_i)$ is a positive spatiotemporal frailty term, $\mathbf{x}_t(\mathbf{s}_i) \in \mathbb{R}^p$ is a vector of observed spatiotemporal covariates, and $\boldsymbol{\beta} \in \mathbb{R}^p$ is the vector of regression coefficients.

Our Bayesian modeling strategy differs from the prior literature primarily in the model for frailties $U^{1:T}(\mathbf{s}_{1:m}) = \{U^t(\mathbf{s}_i) : t = 1, \dots, T, i = 1, \dots, m\}$. Instead of modeling their logarithms jointly as a Gaussian process, as in the classic latent Gaussian model (Christensen and Waagepetersen, 2004), we construct a spatiotemporal autoregressive gamma process for $U^{1:T}(\mathbf{s}_{1:m})$, extending previous applications of such processes in the time series setting (Gourieroux and Jasiak 2006, Creal 2017) and the time-to-event network setting (Zhai et al., 2025). Specifically, for each $t = 2, \dots, T$ and \mathbf{s}_i , we assume that each $U^t(\mathbf{s}_i)$ is associated with a latent space $Z^{t-1}(\mathbf{s}_i)$, such that

$$\begin{aligned} U^t(\mathbf{s}_i) \mid Z^{t-1}(\mathbf{s}_i) &\stackrel{\text{ind}}{\sim} \text{Gamma}\left(\alpha + Z^{t-1}(\mathbf{s}_i), \frac{1}{c}\right), \\ Z^{t-1}(\mathbf{s}_i) \mid \{U^{t-1}(\mathbf{s}_j) : j = 1, \dots, m\} &\stackrel{\text{ind}}{\sim} \text{Poisson}\left(\frac{1}{c} \sum_{j=1}^m v_{ij} U^{t-1}(\mathbf{s}_j)\right) \end{aligned} \quad (2.2)$$

for some hyperparameter $\alpha > 1$, parameter $c > 0$, and nonnegative weights $\mathbf{V} = \{v_{ij} : i, j = 1, \dots, m\}$ such that $\sum_{j=1}^m v_{ij} > 0$ for all i , where $\stackrel{\text{ind}}{\sim}$ indicates the independence

of all concerned distributions, and the $\text{Gamma}(a, b)$ distribution has density $f(x; a, b) = \frac{b^a}{\Gamma(a)} x^{a-1} \exp(-bx)$ for $x > 0$. As a result of the conditional distributions in (2.2), for a given set of α, c, \mathbf{V} , the conditional distribution of $U^t(\mathbf{s}_i)$ given 1-lag values $U^{t-1}(\mathbf{s}_{1:m})$ is a noncentral gamma distribution with density

$$p(U^t(\mathbf{s}_i) | U^{t-1}(\mathbf{s}_{1:m})) = \left(\frac{U^t(\mathbf{s}_i)}{\sum_{j=1}^m v_{ij} U^{t-1}(\mathbf{s}_j)} \right)^{\frac{\alpha-1}{2}} \times \frac{1}{c} \exp \left(-\frac{U^t(\mathbf{s}_i) + \sum_{j=1}^m v_{ij} U^{t-1}(\mathbf{s}_j)}{c} \right) \times I_{\alpha-1} \left(2 \sqrt{\frac{U^t(\mathbf{s}_i) \sum_{j=1}^m v_{ij} U^{t-1}(\mathbf{s}_j)}{c^2}} \right), \quad (2.3)$$

where $I_{\alpha-1}(\cdot)$ is the modified Bessel function of the first kind. From (2.2), by the law of iterated expectations and the law of total variance, the conditional mean and variance of the vector $U^t(\mathbf{s}_{1:m})$ given $U^{t-1}(\mathbf{s}_{1:m})$ are

$$\begin{aligned} \mathbb{E}[U^t(\mathbf{s}_{1:m}) | U^{t-1}(\mathbf{s}_{1:m})] &= \mathbf{1}_m \alpha c + \mathbf{V} U^{t-1}(\mathbf{s}_{1:m}) \text{ and} \\ \text{Var}[U^t(\mathbf{s}_{1:m}) | U^{t-1}(\mathbf{s}_{1:m})] &= \mathbf{1}_m \alpha c^2 + 2c \mathbf{V} U^{t-1}(\mathbf{s}_{1:m}), \end{aligned} \quad (2.4)$$

respectively, where $\mathbf{1}_m = (1, \dots, 1)^T \in \mathbb{R}^m$.

The process defined by (2.2) along the temporal dimension is a vector generalization of the original autoregressive gamma process for time series, as in Gourieroux and Jasiak (2006) and Creal (2017). We can show the following result regarding the stationarity condition for this process.

Theorem 1. Suppose that for any fixed $m \in \mathbb{N}$, \mathbf{V} is an $m \times m$ matrix whose entries are all nonnegative with $\sum_{j=1}^m v_{ij} > 0$ for all $i = 1, \dots, m$. Assume \mathbf{V} satisfies at least one of the two following conditions.

- **Condition 1:** $\sum_{i=1}^m v_{ij} \leq 1$ for all $j = 1, \dots, m$;
- **Condition 2:** $\sum_{j=1}^m v_{ij} \leq 1$ for all $i = 1, \dots, m$.

Then the process $\{U^t(\mathbf{s}_{1:m}) : t = 1, 2, \dots, T\}$ defined in (2.2) is a stationary process with an invariant distribution as $T \rightarrow \infty$.

Proof of Theorem 1. We show the stationarity condition using the theory on Laplace transform of compound autoregressive processes in [Darolles et al. \(2006\)](#). We first verify that for a fixed m and given spatial locations $\{\mathbf{s}_1, \dots, \mathbf{s}_m\}$, the vector process $\{U^t(\mathbf{s}_{1:m}) : t = 1, 2, \dots\}$ is a temporal compound autoregressive process of order 1. For any vector $\mathbf{x} = (x_1, \dots, x_m)^\top \in \mathbb{R}^m$ such that $x_i \geq 0$ for all $i = 1, \dots, m$, we have

$$\begin{aligned}
& \mathbb{E} [\exp \{-\mathbf{x}^\top U^t(\mathbf{s}_{1:m})\} \mid U^{t-1}(\mathbf{s}_{1:m})] \\
&= \mathbb{E} (\mathbb{E} [\exp \{-\mathbf{x}^\top U^t(\mathbf{s}_{1:m})\} \mid Z^{t-1}(\mathbf{s}_{1:m})] \mid U^{t-1}(\mathbf{s}_{1:m})) \\
&= \mathbb{E} \left(\prod_{i=1}^m \mathbb{E} [\exp \{-x_i U^t(\mathbf{s}_i)\} \mid Z^{t-1}(\mathbf{s}_i)] \mid U^{t-1}(\mathbf{s}_{1:m}) \right) \\
&= \mathbb{E} \left(\prod_{i=1}^m \frac{1}{(cx_i + 1)^{\alpha + Z^{t-1}(\mathbf{s}_i)}} \mid U^{t-1}(\mathbf{s}_{1:m}) \right) \\
&= \prod_{i=1}^m \mathbb{E} \left(\frac{1}{(cx_i + 1)^{\alpha + Z^{t-1}(\mathbf{s}_i)}} \mid U^{t-1}(\mathbf{s}_{1:m}) \right) \\
&= \prod_{i=1}^m \sum_{k=0}^{\infty} \frac{\left(\frac{1}{c} \sum_{j=1}^m v_{ij} U^{t-1}(\mathbf{s}_j)\right)^k}{k!} \exp \left\{ -\frac{1}{c} \sum_{j=1}^m v_{ij} U^{t-1}(\mathbf{s}_j) \right\} \cdot \frac{1}{(cx_i + 1)^{\alpha+k}} \\
&= \prod_{i=1}^m \frac{1}{(cx_i + 1)^\alpha} \times \exp \left\{ -\frac{1}{c} \sum_{j=1}^m v_{ij} U^{t-1}(\mathbf{s}_j) \left[1 - \frac{1}{cx_i + 1} \right] \right\} \\
&= \exp \left\{ -\sum_{j=1}^m \left(\sum_{i=1}^m \frac{x_i v_{ij}}{cx_i + 1} \right) U^{t-1}(\mathbf{s}_j) - \alpha \sum_{i=1}^m \log(cx_i + 1) \right\}. \tag{2.5}
\end{aligned}$$

If we define vector-valued function $a(\mathbf{x}) = \left(\sum_{i=1}^m \frac{x_i v_{i1}}{cx_i + 1}, \dots, \sum_{i=1}^m \frac{x_i v_{im}}{cx_i + 1} \right)^\top \in \mathbb{R}^m$ and scalar-valued function $b(\mathbf{x}) = -\alpha \sum_{i=1}^m \log(cx_i + 1) \in \mathbb{R}$, then (2.5) implies

$$\mathbb{E} [\exp \{-\mathbf{x}^\top U^t(\mathbf{s}_{1:m})\} \mid U^{t-1}(\mathbf{s}_{1:m})] = \exp \{-a(\mathbf{x})^\top U^{t-1}(\mathbf{s}_{1:m}) + b(\mathbf{x})\}.$$

Since $v_{ij} \geq 0$ for all (i, j) and $\sum_{j=1}^m v_{ij} > 0$ for all i , $a(\mathbf{x}) \neq \mathbf{0}_{m \times 1}$ for all $\mathbf{x} \in \mathbb{R}^m$ with $x_i \geq 0$ for all i and $\sum_{i=1}^m x_i > 0$. Hence, based on Definition 1 in [Darolles et al. \(2006\)](#), $\{U^t(\mathbf{s}_{1:m}) : t = 1, 2, \dots\}$ is a temporal compound autoregressive process of order 1.

By Proposition 6 in [Darolles et al. \(2006\)](#), the process $\{U^t(\mathbf{s}_{1:m}) : t = 1, 2, \dots\}$ converges to a stationary distribution as $T \rightarrow \infty$ if and only if $\lim_{h \rightarrow \infty} a^{\circ h}(\mathbf{x}) = \mathbf{0}_{m \times 1}$ for all $\mathbf{x} \in \mathbb{R}^m$

with $x_i \geq 0$ for all $i = 1, \dots, m$ and $\sum_{i=1}^m x_i > 0$, where $a^{\circ h}(\mathbf{x})$ represents the function $a(\mathbf{x})$ compounded h times with itself. In this case, if we define the m -dimensional function $K(\mathbf{x}) = (K_1(\mathbf{x}), \dots, K_m(\mathbf{x}))^\top = \left(\frac{x_1}{cx_1+1}, \dots, \frac{x_m}{cx_m+1} \right)^\top$ for any $\mathbf{x} \in \mathbb{R}^m$ with $x_i \geq 0$ for all $i = 1, \dots, m$ and $\sum_{i=1}^m x_i > 0$, then for any $h \in \mathbb{N}$, $h \geq 1$, it is straightforward to see that

$$a^{\circ h}(\mathbf{x}) = \mathbf{V}^\top K(a^{\circ(h-1)}(\mathbf{x})).$$

In particular, for any $j = 1, \dots, m$, the j th entry of $a^{\circ h}(\mathbf{x})$ is

$$a_j^{\circ h}(\mathbf{x}) = \sum_{i=1}^m v_{ij} K_i(a^{\circ(h-1)}(\mathbf{x})).$$

Condition 1: Suppose $\sum_{i=1}^m v_{ij} \leq 1$ for all $j = 1, \dots, m$. For each $h \in \mathbb{N}$, let $i_{\max}^{(h)} = \arg \max_{1 \leq i \leq m} K_i(a^{\circ h}(\mathbf{x}))$. Since v_{ij} 's are all nonnegative, for any $j = 1, \dots, m$,

$$\begin{aligned} 0 \leq a_j^{\circ h}(\mathbf{x}) &\leq \left(\sum_{i=1}^m v_{ij} \right) K_{i_{\max}^{(h-1)}}(a^{\circ(h-1)}(\mathbf{x})) \\ &\stackrel{(i)}{\leq} 1 \cdot \frac{a_{i_{\max}^{(h-1)}}^{\circ(h-1)}(\mathbf{x})}{c a_{i_{\max}^{(h-1)}}^{\circ(h-1)}(\mathbf{x}) + 1} \stackrel{(ii)}{=} \frac{\max_{1 \leq k \leq m} a_k^{\circ(h-1)}(\mathbf{x})}{c \max_{1 \leq k \leq m} a_k^{\circ(h-1)}(\mathbf{x}) + 1}, \end{aligned} \quad (2.6)$$

where (i) follows from $0 \leq \sum_{i=1}^m v_{ij} \leq 1$ for all $j = 1, \dots, m$ and (ii) from the fact that the function $x/(cx + 1)$ increases in x for $x \geq 0$. The relation (2.6) implies that $a_{\max}^h(\mathbf{x}) := \max_{1 \leq j \leq m} a_j^{\circ h}(\mathbf{x})$ is a nonnegative sequence that strictly decreases in h when strictly positive for any fixed \mathbf{x} and satisfies

$$0 \leq a_{\max}^h(\mathbf{x}) \leq \frac{a_{\max}^{h-1}(\mathbf{x})}{c a_{\max}^{h-1}(\mathbf{x}) + 1} \leq a_{\max}^{h-1}(\mathbf{x}). \quad (2.7)$$

By the increasing property of the function $f(x) = x/(cx + 1)$ for $x \geq 0$, we can apply the second inequality in (2.7) $h - 1$ times iteratively to obtain

$$0 \leq a_{\max}^h(\mathbf{x}) \leq f(a_{\max}^{h-1}(\mathbf{x})) \leq f^{\circ(h-1)}(a_{\max}^1(\mathbf{x})) = \frac{a_{\max}^1(\mathbf{x})}{c a_{\max}^1(\mathbf{x}) \cdot (h-1) + 1}. \quad (2.8)$$

Therefore, $\lim_{h \rightarrow \infty} a_{\max}^h(\mathbf{x}) = 0$. This further implies that $\lim_{h \rightarrow \infty} a_j^{\circ h}(\mathbf{x}) = 0$ for all $j = 1, 2, \dots, m$, i.e., $\lim_{h \rightarrow \infty} a^{\circ h}(\mathbf{x}) = \mathbf{0}_{m \times 1}$, as $a_j^{\circ h}(\mathbf{x}) \geq 0$ for all $j \in \{1, \dots, m\}$ and $h \in \mathbb{N}$.

Condition 2: Suppose $\sum_{j=1}^m v_{ij} \leq 1$ for all $i = 1, \dots, m$. Since v_{ij} 's are all nonnegative, we have that for any $j = 1, \dots, m$,

$$\begin{aligned} 0 &\leq \frac{1}{m} \sum_{j=1}^m a_j^{\circ h}(\mathbf{x}) = \frac{1}{m} \sum_{j=1}^m \sum_{i=1}^m v_{ij} K_i(a^{\circ(h-1)}(\mathbf{x})) = \frac{1}{m} \sum_{i=1}^m \left(\sum_{j=1}^m v_{ij} \right) K_i(a^{\circ(h-1)}(\mathbf{x})) \\ &\stackrel{(i)}{\leq} \frac{1}{m} \sum_{i=1}^m 1 \cdot \frac{a_i^{\circ(h-1)}(\mathbf{x})}{ca_i^{\circ(h-1)}(\mathbf{x}) + 1} = \frac{1}{m} \sum_{j=1}^m \frac{a_j^{\circ(h-1)}(\mathbf{x})}{ca_j^{\circ(h-1)}(\mathbf{x}) + 1} \stackrel{(ii)}{\leq} \frac{\frac{1}{m} \sum_{j=1}^m a_j^{\circ(h-1)}(\mathbf{x})}{c \cdot \frac{1}{m} \sum_{j=1}^m a_j^{\circ(h-1)}(\mathbf{x}) + 1}, \end{aligned} \quad (2.9)$$

where (i) follows from $0 < \sum_{j=1}^m v_{ij} \leq 1$ for all $i = 1, \dots, m$ and (ii) from the concavity of the function $f(x) = x/(cx + 1)$ for $x \geq 0$, as $c > 0$ and thus $f''(x) = -\frac{2c}{(cx+1)^3} < 0$ for all $x \geq 0$. The relation (2.9) implies that $a_{\text{mean}}^h(\mathbf{x}) := \frac{1}{m} \sum_{j=1}^m a_j^{\circ h}(\mathbf{x})$ is a nonnegative sequence that strictly decreases in h when strictly positive for any fixed \mathbf{x} and satisfies

$$0 \leq a_{\text{mean}}^h(\mathbf{x}) \leq \frac{a_{\text{mean}}^{h-1}(\mathbf{x})}{ca_{\text{mean}}^{h-1}(\mathbf{x}) + 1} \leq a_{\text{mean}}^{h-1}(\mathbf{x}). \quad (2.10)$$

By the increasing property of the function $f(x) = x/(cx + 1)$ for $x \geq 0$, we can apply the second inequality in (2.10) $h - 1$ times iteratively to obtain

$$0 \leq a_{\text{mean}}^h(\mathbf{x}) \leq f(a_{\text{mean}}^{h-1}(\mathbf{x})) \leq f^{\circ(h-1)}(a_{\text{mean}}^1(\mathbf{x})) = \frac{a_{\text{mean}}^1(\mathbf{x})}{ca_{\text{mean}}^1(\mathbf{x}) \cdot (h-1) + 1}. \quad (2.11)$$

Therefore, $\lim_{h \rightarrow \infty} a_{\text{mean}}^h(\mathbf{x}) = 0$, which is equivalent to $\lim_{h \rightarrow \infty} \sum_{j=1}^m a_j^{\circ h}(\mathbf{x}) = 0$. Since $a_j^{\circ h}(\mathbf{x}) \geq 0$ for all $j \in \{1, \dots, m\}$ and $h \in \mathbb{N}$, we have $\lim_{h \rightarrow \infty} a_j^{\circ h}(\mathbf{x}) = 0$ for all $j = 1, 2, \dots, m$, i.e., $\lim_{h \rightarrow \infty} a^{\circ h}(\mathbf{x}) = \mathbf{0}_{m \times 1}$. \square

Under the joint framework specified by (2.1) and (2.2), the conditional posterior distribution of each $U^t(\mathbf{s}_i)$ ($t = 2, \dots, T$) does not immediately follow a closed-form parametric distribution, even with a fixed set of α, c, \mathbf{V} . The fundamental issue lies in the weighted sum of $U^{t-1}(\mathbf{s}_{1:m})$ in the second equation of (2.2). Using the additive property of independent Poisson random variables, we can further decompose each $Z^{t-1}(\mathbf{s}_i)$ into a sum of latent Poisson variables with rates $v_{ij} U^{t-1}(\mathbf{s}_j)/c$, $j = 1, \dots, m$ so that $v_{ij} > 0$, such that the conditional posterior of $U^t(\mathbf{s}_i)$ can be made conjugate as a gamma distribution. If all

entries in the $m \times m$ weighting matrix \mathbf{V} are strictly positive, however, this strategy will introduce $m^2(T - 1)$ latent variables, which incurs exceptionally high posterior sampling cost for spatiotemporal count data with a large number of spatial locations m .

To reduce this computational cost quadratic in m , we consider a sparse weighting matrix \mathbf{V} for practical implementation. In the following, we construct a \mathbf{V} that satisfies Condition 2 in Theorem 1 by making each row of \mathbf{V} sparse. That is, each $Z^{t-1}(\mathbf{s}_i)$ only depends on a small number of neighboring spatial locations in the $t - 1^{\text{th}}$ time interval. This modeling strategy is fundamentally similar to the Vecchia approximation in the Gaussian process literature (Vecchia 1988, Datta et al. 2016, Katzfuss and Guinness 2021, Zhu et al. 2024), where the conditional distribution of the response variable at each spatial location is made only dependent on a small set of neighboring locations.

Specifically, for each \mathbf{s}_i ($i = 1, \dots, m$), we let the neighboring set of \mathbf{s}_i be $N(\mathbf{s}_i)$, which usually consists of the $|N(\mathbf{s}_i)|$ “nearest” neighbors of \mathbf{s}_i in $\{\mathbf{s}_1, \dots, \mathbf{s}_m\} \setminus \{\mathbf{s}_i\}$. We denote $h_s \in \mathbb{N}$, $h_s \ll m$ as the maximum number of neighbors for each spatial location; thus, $1 \leq |N(\mathbf{s}_i)| \leq h_s$ for all $i = 1, \dots, m$. It is permitted that some spatial locations’ numbers of nearest neighbors are strictly smaller than h_s . Let us fix any arbitrary $i \in \{1, 2, \dots, m\}$ and consider the i^{th} row in the $m \times m$ weighting matrix \mathbf{V} in (2.2). We assume the following parametric form of \mathbf{V} :

$$\begin{aligned} v_{ii} &= \rho, \\ v_{ij} &= \kappa \cdot w_{ik_i(\mathbf{s}_j)}, \quad \text{for all } j \text{ such that } \mathbf{s}_j \in N(\mathbf{s}_i), \\ v_{ij} &= 0, \quad \text{for all } j \neq i \text{ such that } \mathbf{s}_j \notin N(\mathbf{s}_i), \end{aligned} \tag{2.12}$$

where $k_i(\mathbf{s}_j) \in \{1, \dots, |N(\mathbf{s}_i)|\}$ satisfies $\mathbf{s}_j = N(\mathbf{s}_i)[k_i(\mathbf{s}_j)]$, i.e., \mathbf{s}_j is the $k_i(\mathbf{s}_j)^{\text{th}}$ spatial location in $N(\mathbf{s}_i)$. $\{w_{ik_i(\mathbf{s}_j)}\}_{j: \mathbf{s}_j \in N(\mathbf{s}_i)} = \{w_{ik}\}_{1 \leq k \leq |N(\mathbf{s}_i)|}$ consists of prespecified constants in $(0, 1]$ with $\sum_{k=1}^{|N(\mathbf{s}_i)|} w_{ik} = 1$. In real applications, for $\mathbf{s}_j \in N(\mathbf{s}_i)$, $w_{ik_i(\mathbf{s}_j)}$ can either be inversely related to the distance between \mathbf{s}_i and \mathbf{s}_j or set to $w_{ik_i(\mathbf{s}_j)} = 1/|N(\mathbf{s}_i)|$ as uniform over all neighboring locations of \mathbf{s}_i . Following Theorem 1, we have the following corollary

regarding the parameters ρ and κ in the model (2.12).

Corollary 1. Assume the weighting matrix $\mathbf{V} = \{v_{ij} \geq 0 : i, j = 1, \dots, m\}$ is specified in (2.12) with known constants $w_{ik_i(\mathbf{s}_j)} \in (0, 1]$ for all $\mathbf{s}_j \in N(\mathbf{s}_i)$ and $i = 1, \dots, m$ that satisfy $\sum_{j: \mathbf{s}_j \in N(\mathbf{s}_i)} w_{ik_i(\mathbf{s}_j)} = \sum_{k=1}^{|N(\mathbf{s}_i)|} w_{ik} = 1$ for all $i = 1, \dots, m$. Suppose that the parameters (ρ, κ) satisfy $\rho \geq 0$, $\kappa \geq 0$, $0 < \rho + \kappa \leq 1$. Then $\{U^t(\mathbf{s}_{1:m}) : t = 1, 2, \dots, T\}$ defined in (2.2) is a stationary process with an invariant distribution as $T \rightarrow \infty$.

Proof of Corollary 1. The construction (2.12) ensures that all entries in \mathbf{V} are nonnegative.

For any $i = 1, 2, \dots, m$,

$$\sum_{j=1}^m v_{ij} = \rho + \sum_{j: \mathbf{s}_j \in N(\mathbf{s}_i)} \kappa w_{ik_i(\mathbf{s}_j)} + 0 = \rho + \kappa \cdot \sum_{k=1}^{|N(\mathbf{s}_i)|} w_{ik} = \rho + \kappa \in (0, 1].$$

Hence, Condition 2 of Theorem 1 is satisfied, and the conclusion follows. \square

We introduce $(T - 1) \sum_{i=1}^m |N(\mathbf{s}_i)| \leq mh_s(T - 1) \ll m^2(T - 1)$ latent variables $\{Z_{ij}^t : t = 1, \dots, T - 1, i = 1, \dots, m, j = 0, 1, \dots, |N(\mathbf{s}_i)|\}$ that lead to fully conjugate Gibbs sampling steps of $U^t(\mathbf{s}_i)$'s, c, κ, ρ for the model specified by (2.1), (2.2), and (2.12). For each spatial location \mathbf{s}_i , we let $U^1(\mathbf{s}_i) \mid c \stackrel{\text{ind}}{\sim} \text{Gamma}(\alpha, \frac{1}{c})$ and for each $t = 2, \dots, T$,

$$U^t(\mathbf{s}_i) \mid Z_{i0}^{t-1}, Z_{i1}^{t-1}, Z_{i2}^{t-1}, \dots, Z_{i|N(\mathbf{s}_i)|}^{t-1}, c \stackrel{\text{ind}}{\sim} \text{Gamma}\left(\alpha + \sum_{j=0}^{|N(\mathbf{s}_i)|} Z_{ij}^{t-1}, \frac{1}{c}\right), \quad (2.13)$$

where $Z^{t-1}(\mathbf{s}_i)$ in (2.2) equals $\sum_{j=0}^{|N(\mathbf{s}_i)|} Z_{ij}^{t-1}$ in (2.13) and

$$\begin{aligned} Z_{ij}^{t-1} \mid U_{N(\mathbf{s}_i)[j]}^{t-1}, \kappa, c &\stackrel{\text{ind}}{\sim} \text{Poisson}\left(\frac{\kappa}{c} \cdot w_{ij} U_{N(\mathbf{s}_i)[j]}^{t-1}\right), \quad j = 1, 2, \dots, |N(\mathbf{s}_i)| \text{ independent of} \\ Z_{i0}^{t-1} \mid U^{t-1}(\mathbf{s}_i), \rho, c &\stackrel{\text{ind}}{\sim} \text{Poisson}\left(\frac{\rho}{c} \cdot U^{t-1}(\mathbf{s}_i)\right). \end{aligned} \quad (2.14)$$

Hence, for each (t, i) with $t \in \{2, \dots, T\}$,

$$Z^{t-1}(\mathbf{s}_i) = \sum_{j=0}^{|N(\mathbf{s}_i)|} Z_{ij}^{t-1} \mid c, U^{t-1}(\mathbf{s}_i), \rho, U_{N(\mathbf{s}_i)}^{t-1}, \kappa \sim \text{Poisson}(\lambda_{it}), \quad (2.15)$$

where $\lambda_{it} = \frac{\kappa}{c} \cdot \sum_{j=1}^{|N(\mathbf{s}_i)|} w_{ij} U_{N(\mathbf{s}_i)[j]}^{t-1} + \frac{\rho}{c} \cdot U^{t-1}(\mathbf{s}_i)$ and $U_{N(\mathbf{s}_i)}^{t-1} = \left\{U_{N(\mathbf{s}_i)[j]}^{t-1}, j = 1, 2, \dots, |N(\mathbf{s}_i)|\right\}$. $U^t(\mathbf{s}_i) \mid c, U^{t-1}(\mathbf{s}_i), \rho, U_{N(\mathbf{s}_i)}^{t-1}, \kappa \sim \text{Non-Central Gamma}(\alpha, \frac{1}{c}, \lambda_{it})$, with mean $(\alpha + \lambda_{it})c$ and variance $(\alpha + 2\lambda_{it})c^2$. See Figure 1 for the structure and flow of our model.

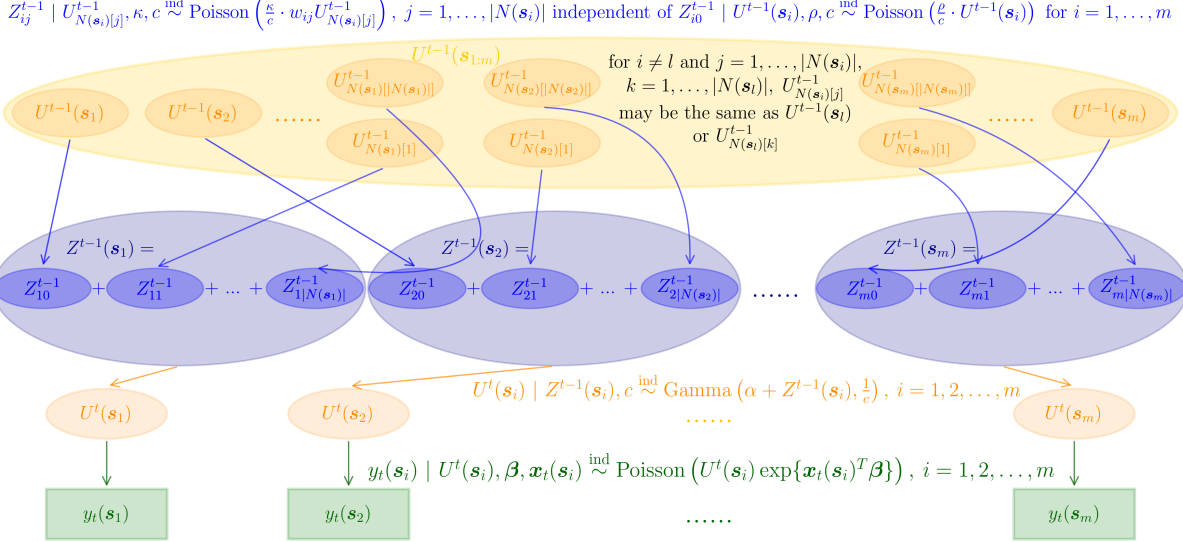


Figure 1: A schematic diagram of our model specified by (2.1), (2.13), and (2.14).

The hyperparameter α satisfies the Feller condition (Creal, 2017) $\alpha > 1$; w_{ij} 's are positive constants satisfying $\sum_{k=1}^{|N(\mathbf{s}_i)|} w_{ik} = 1$ for all $i = 1, \dots, m$; positive parameters ρ, κ satisfy $\rho + \kappa \leq 1$. Therefore, Corollary 1 applies and thus the process $\{U^t(\mathbf{s}_{1:m}) : t = 1, 2, \dots, T\}$ is guaranteed stationary. ρ is imposed a conjugate truncated gamma prior $\pi(\rho) \sim \text{Truncated Gamma}(a_\rho, b_\rho, 0, 1)$, and κ is imposed a conjugate truncated gamma prior $\pi(\kappa) \sim \text{Truncated Gamma}(a_\kappa, b_\kappa, 0, 1 - \rho)$. The Truncated Gamma($a, b, \text{lo}, \text{hi}$) distribution is a Gamma(a, b) distribution restricted to a specific interval (lo, hi), where $0 \leq \text{lo} < \text{hi} \leq \infty$. $c > 0$ is assigned a conjugate inverse gamma prior $\pi(c) \sim \mathcal{IG}(\alpha_c, \theta_c)$. In presence of spatiotemporal covariates $\mathbf{x}_t(\mathbf{s}_i)$'s, the coefficient vector $\boldsymbol{\beta} \in \mathbb{R}^p$ is imposed a standard p -variate normal prior $\pi(\boldsymbol{\beta}) \sim N_p(\boldsymbol{\mu}_{0\boldsymbol{\beta}}, \Sigma_{0\boldsymbol{\beta}})$.

3 Posterior Sampling Algorithm

We detail below posterior sampling steps for the model (2.1) with spatiotemporal frailties $U^{1:T}(\mathbf{s}_{1:m}) = \{U^t(\mathbf{s}_i) : t = 1, \dots, T, i = 1, \dots, m\}$ modeled as in (2.13) and (2.14). Our parameter set is $\Theta = \{\boldsymbol{\beta}, c, U^{1:T}(\mathbf{s}_i), \kappa, \rho, Z_{ij}^{1:(T-1)}, i = 1, \dots, m, j = 0, 1, \dots, |N(\mathbf{s}_i)|\}$ when

$m > 1$ and $T > 1$. Θ simplifies to $\{\beta, c, U^{1:T}(\mathbf{s}_1), \rho, Z_{10}^{1:(T-1)}\}$ when $m = 1$ and $T > 1$, and to $\{\beta, c, U^1(\mathbf{s}_{1:m})\}$ when $T = 1$. If we do not consider $U^t(\mathbf{s}_i)$ directly affected by $U^{t-1}(\mathbf{s}_i)$, then ρ and $\{Z_{i0}^t : t = 1, \dots, T-1, i = 1, \dots, m\}$ are not required anymore, i.e., $\rho = 0$ in (2.12). All parameters have full conditional densities corresponding to standard distributions except for the coefficient vector $\beta \in \mathbb{R}^p$, which requires a Metropolis step in posterior sampling. See Appendix A for full deduction details of this algorithm.

1. Sampling from the full conditional distribution of c :

If $m > 1$ and $T > 1$, then

$$\begin{aligned} f(c|\cdot) &\propto \pi(c) \times \prod_{i=1}^m f(U^1(\mathbf{s}_i) | c) \times \prod_{t=2}^T \prod_{i=1}^m f(U^t(\mathbf{s}_i) | Z_{i0}^{t-1}, Z_{i1}^{t-1}, \dots, Z_{i|N(\mathbf{s}_i)|}^{t-1}, c) \times \\ &\quad \prod_{t=2}^T \prod_{i=1}^m f(Z_{i0}^{t-1} | U^{t-1}(\mathbf{s}_i), \rho, c) \times \prod_{t=2}^T \prod_{i=1}^m \prod_{j=1}^{|N(\mathbf{s}_i)|} f(Z_{ij}^{t-1} | U_{N(\mathbf{s}_i)[j]}^{t-1}, \kappa, c) \\ &\sim \mathcal{IG} \left(\alpha_c + Tm\alpha + 2 \sum_{t=1}^{T-1} \sum_{i=1}^m \sum_{j=0}^{|N(\mathbf{s}_i)|} Z_{ij}^t, \theta_c^{\text{post}} \right), \end{aligned} \quad (3.1)$$

$$\text{where } \theta_c^{\text{post}} = \theta_c + \sum_{t=1}^T \sum_{i=1}^m U^t(\mathbf{s}_i) + \rho \cdot \sum_{t=1}^{T-1} \sum_{i=1}^m U^t(\mathbf{s}_i) + \kappa \cdot \sum_{i=1}^m \sum_{j=1}^{|N(\mathbf{s}_i)|} w_{ij} \sum_{t=1}^{T-1} U_{N(\mathbf{s}_i)[j]}^t.$$

If $T = 1$, then

$$f(c|\cdot) \propto \pi(c) \times \prod_{i=1}^m f(U^1(\mathbf{s}_i) | c) \sim \mathcal{IG} \left(m\alpha + \alpha_c, \sum_{i=1}^m U^1(\mathbf{s}_i) + \theta_c \right).$$

If $m = 1$ and $T > 1$, then

$$\begin{aligned} f(c|\cdot) &\propto \pi(c) \times f(U^1(\mathbf{s}_1) | c) \times \prod_{t=2}^T f(U^t(\mathbf{s}_1) | Z_{10}^{t-1}, c) \times \prod_{t=1}^{T-1} f(Z_{10}^t | U^t(\mathbf{s}_1), \rho, c) \\ &\sim \mathcal{IG} \left(T\alpha + 2 \sum_{t=1}^{T-1} Z_{10}^t + \alpha_c, \sum_{t=1}^T U^t(\mathbf{s}_1) + \rho \cdot \sum_{t=1}^{T-1} U^t(\mathbf{s}_1) + \theta_c \right). \end{aligned}$$

2. Sampling from the full conditional distributions of $U^{1:T}(\mathbf{s}_{1:m})$:

Fix any arbitrary $i \in \{1, 2, \dots, m\}$. For each $l \in \{1, 2, \dots, m\}$ such that $\mathbf{s}_i \in N(\mathbf{s}_l)$, we denote $k_l(\mathbf{s}_i)$ as the positive integer less than or equal to h_s such that $\mathbf{s}_i = N(\mathbf{s}_l)[k_l(\mathbf{s}_i)]$.

If $m > 1$ and $T > 1$, then for any $t \in \{2, 3, \dots, T - 1\}$,

$$\begin{aligned} f(U^t(\mathbf{s}_i)|\cdot) &\propto f(y_t(\mathbf{s}_i) | U^t(\mathbf{s}_i), \boldsymbol{\beta}) \times f(U^t(\mathbf{s}_i) | Z_{i0}^{t-1}, Z_{i1}^{t-1}, \dots, Z_{i|N(\mathbf{s}_i)|}^{t-1}, c) \times \\ &f(Z_{i0}^t | U^t(\mathbf{s}_i), \rho, c) \times \prod_{l:\mathbf{s}_i \in N(\mathbf{s}_l)}^{1 \leq l \leq m} f(Z_{lk_l(\mathbf{s}_i)}^t | U^t(\mathbf{s}_i), \kappa, c) \\ &\sim \text{Gamma} \left(y_t(\mathbf{s}_i) + \alpha + \sum_{j=0}^{|N(\mathbf{s}_i)|} Z_{ij}^{t-1} + Z_{i0}^t + \sum_{l:\mathbf{s}_i \in N(\mathbf{s}_l)}^{1 \leq l \leq m} Z_{lk_l(\mathbf{s}_i)}^t, \text{rate}_{U^t(\mathbf{s}_i)} \right), \quad (3.2) \end{aligned}$$

where $\text{rate}_{U^t(\mathbf{s}_i)} = e^{\mathbf{x}_t(\mathbf{s}_i)^T \boldsymbol{\beta}} + \frac{1}{c} \left(1 + \rho + \kappa \sum_{l:\mathbf{s}_i \in N(\mathbf{s}_l)}^{1 \leq l \leq m} w_{lk_l(\mathbf{s}_i)} \right)$.

$$\begin{aligned} f(U^t(\mathbf{s}_i)|\cdot) &\sim \text{Gamma} \left(y_t(\mathbf{s}_i) + \alpha + Z_{i0}^t + \sum_{l:\mathbf{s}_i \in N(\mathbf{s}_l)}^{1 \leq l \leq m} Z_{lk_l(\mathbf{s}_i)}^t, \text{rate}_{U^t(\mathbf{s}_i)} \right) \text{ for } t = 1, \text{ and} \\ f(U^t(\mathbf{s}_i)|\cdot) &\sim \text{Gamma} \left(y_t(\mathbf{s}_i) + \alpha + \sum_{j=0}^{|N(\mathbf{s}_i)|} Z_{ij}^{t-1}, e^{\mathbf{x}_t(\mathbf{s}_i)^T \boldsymbol{\beta}} + \frac{1}{c} \right) \text{ for } t = T. \end{aligned}$$

If $T = 1$, then $f(U^1(\mathbf{s}_i)|\cdot) \sim \text{Gamma} \left(y_1(\mathbf{s}_i) + \alpha, e^{\mathbf{x}_1(\mathbf{s}_i)^T \boldsymbol{\beta}} + \frac{1}{c} \right)$.

If $m = 1$ and $T > 1$, then for any $t \in \{2, \dots, T - 1\}$,

$$\begin{aligned} f(U^t(\mathbf{s}_1)|\cdot) &\sim \text{Gamma} \left(y_t(\mathbf{s}_1) + \alpha + Z_{10}^{t-1} + Z_{10}^t, e^{\mathbf{x}_t(\mathbf{s}_1)^T \boldsymbol{\beta}} + \frac{1}{c}(1 + \rho) \right). \\ f(U^t(\mathbf{s}_1)|\cdot) &\sim \text{Gamma} \left(y_t(\mathbf{s}_1) + \alpha + Z_{10}^t, e^{\mathbf{x}_t(\mathbf{s}_1)^T \boldsymbol{\beta}} + \frac{1}{c}(1 + \rho) \right) \text{ for } t = 1, \text{ and} \\ f(U^t(\mathbf{s}_1)|\cdot) &\sim \text{Gamma} \left(y_t(\mathbf{s}_1) + \alpha + Z_{10}^{t-1}, e^{\mathbf{x}_t(\mathbf{s}_1)^T \boldsymbol{\beta}} + \frac{1}{c} \right) \text{ for } t = T. \end{aligned}$$

3. Sampling from the full conditional distribution of ρ when $T > 1$:

$$\begin{aligned} f(\rho|\cdot) &\propto \pi(\rho) \times \prod_{t=1}^{T-1} \prod_{i=1}^m f(Z_{i0}^t | U^t(\mathbf{s}_i), \rho, c) \\ &\sim \text{Truncated Gamma} \left(a_\rho + \sum_{t=1}^{T-1} \sum_{i=1}^m Z_{i0}^t, b_\rho + \frac{1}{c} \sum_{t=1}^{T-1} \sum_{i=1}^m U^t(\mathbf{s}_i), 0, 1 \right). \quad (3.3) \end{aligned}$$

4. Sampling from the full conditional distribution of κ when $m > 1$ and $T > 1$:

$$\begin{aligned} f(\kappa|\cdot) &\propto \pi(\kappa) \times \prod_{t=1}^{T-1} \prod_{i=1}^m \prod_{j=1}^{|N(\mathbf{s}_i)|} f(Z_{ij}^t | U_{N(\mathbf{s}_i)[j]}^t, \kappa, c) \\ &\sim \text{Truncated Gamma} \left(a_\kappa + \sum_{t=1}^{T-1} \sum_{i=1}^m \sum_{j=1}^{|N(\mathbf{s}_i)|} Z_{ij}^t, \text{rate}_\kappa^{\text{post}}, 0, 1 - \rho \right), \quad (3.4) \end{aligned}$$

where $\text{rate}_\kappa^{\text{post}} = b_\kappa + \frac{1}{c} \sum_{i=1}^m \sum_{j=1}^{|N(\mathbf{s}_i)|} w_{ij} \sum_{t=1}^{T-1} U_{N(\mathbf{s}_i)[j]}^t$.

5. Sampling from the full conditional distributions of Z_{ij}^t 's when $T > 1$:

Fix any arbitrary $t \in \{1, 2, \dots, T-1\}$, $i \in \{1, 2, \dots, m\}$. Then

$$\begin{aligned} f(Z_{i0}^t | \cdot) &\propto f(U^{t+1}(\mathbf{s}_i) | Z_{i0}^t, Z_{i1}^t, \dots, Z_{i|N(\mathbf{s}_i)|}^t, c) \times f(Z_{i0}^t | U^t(\mathbf{s}_i), \rho, c) \\ &\sim \text{Bessel} \left(\alpha + \sum_{k=1}^{|N(\mathbf{s}_i)|} Z_{ik}^t - 1, \frac{2}{c} \sqrt{\rho \cdot U^{t+1}(\mathbf{s}_i) U^t(\mathbf{s}_i)} \right). \end{aligned} \quad (3.5)$$

When $m > 1$, we further fix any arbitrary $j \in \{1, 2, \dots, |N(\mathbf{s}_i)|\}$. Then

$$\begin{aligned} f(Z_{ij}^t | \cdot) &\propto f(U^{t+1}(\mathbf{s}_i) | Z_{i0}^t, Z_{i1}^t, \dots, Z_{i|N(\mathbf{s}_i)|}^t, c) \times f(Z_{ij}^t | U_{N(\mathbf{s}_i)[j]}^t, \kappa, c) \\ &\sim \text{Bessel} \left(\alpha + \sum_{k=0, k \neq j}^{|N(\mathbf{s}_i)|} Z_{ik}^t - 1, \frac{2}{c} \sqrt{\kappa w_{ij} U^{t+1}(\mathbf{s}_i) U_{N(\mathbf{s}_i)[j]}^t} \right), \end{aligned} \quad (3.6)$$

where $X \sim \text{Bessel}(\nu, a)$ has the probability mass function $\mathbb{P}(X = n | a, \nu) = \frac{(a/2)^{2n+\nu}}{I_\nu(a) \Gamma(n+\nu+1)n!}$

for $n \in \mathbb{N}$, $a > 0$, $\nu > -1$, and $I_\nu(\cdot)$ is the modified Bessel function of the first kind.

We generate Bessel random variables via the efficient rejection sampling algorithms in Section 3 of [Devroye \(2002\)](#).

6. Sampling from the full conditional distribution of $\boldsymbol{\beta}_{p \times 1}$ via a Metropolis step:

$$\begin{aligned} f(\boldsymbol{\beta} | \cdot) &\propto \pi(\boldsymbol{\beta}) \times \prod_{i=1}^m \prod_{t=1}^T f(y_t(\mathbf{s}_i) | U^t(\mathbf{s}_i), \boldsymbol{\beta}) \\ &\propto \exp \left\{ -\frac{1}{2} (\boldsymbol{\beta} - \boldsymbol{\mu}_{0\boldsymbol{\beta}})^T \Sigma_{0\boldsymbol{\beta}}^{-1} (\boldsymbol{\beta} - \boldsymbol{\mu}_{0\boldsymbol{\beta}}) + \sum_{i=1}^m \sum_{t=1}^T \left[y_t(\mathbf{s}_i) \cdot \mathbf{x}_t(\mathbf{s}_i)^T \boldsymbol{\beta} - U^t(\mathbf{s}_i) e^{\mathbf{x}_t(\mathbf{s}_i)^T \boldsymbol{\beta}} \right] \right\} \end{aligned} \quad (3.7)$$

is not a standard parametric family, and we resort to a Metropolis step for sampling $\boldsymbol{\beta}$.

We consider a symmetric Markov kernel $Q : \mathbb{R}^p \times \mathbb{R}^p \rightarrow \mathbb{R}^+$ with $Q(\boldsymbol{\beta}_a, \boldsymbol{\beta}_b) = Q(\boldsymbol{\beta}_b, \boldsymbol{\beta}_a)$ for all $\boldsymbol{\beta}_a, \boldsymbol{\beta}_b \in \mathbb{R}^p$. $Q(\boldsymbol{\beta}_a, \boldsymbol{\beta}_b)$ equals the density of a $N_p(\boldsymbol{\beta}_a, V)$ random variable evaluated at $\boldsymbol{\beta}_b$ with probability p and the density of a $N_p(\boldsymbol{\beta}_a, 100V)$ random variable evaluated at $\boldsymbol{\beta}_b$ with probability $1-p$, where V is an estimate of the inverse Hessian of $\ln[f(\boldsymbol{\beta} | \cdot)]$ and $p \in (0, 1)$ should be quite large to give less probability to big moves in

the parameter space. At each MCMC iteration $w \in \mathbb{N}$, we let the current parameter estimate for β be $\beta^{(w)}$. Since

$$\frac{\partial^2}{\partial \beta \partial \beta^T} \ln f(\beta | \cdot) = -\Sigma_{0\beta}^{-1} - \sum_{i=1}^m \sum_{t=1}^T U^t(\mathbf{s}_i) e^{\mathbf{x}_t(\mathbf{s}_i)^T \beta} \mathbf{x}_t(\mathbf{s}_i) \mathbf{x}_t(\mathbf{s}_i)^T, \quad (3.8)$$

we set $V^{(w)} = \left[\Sigma_{0\beta}^{-1} + \sum_{i=1}^m \sum_{t=1}^T U^t(\mathbf{s}_i) e^{\mathbf{x}_t(\mathbf{s}_i)^T \beta^{(w)}} \mathbf{x}_t(\mathbf{s}_i) \mathbf{x}_t(\mathbf{s}_i)^T \right]^{-1}$. We propose a new parameter value β^* from the density $q(\beta | \beta^{(w)}) = Q(\beta^{(w)}, \beta)$ and then set

$$\beta^{(w+1)} = \begin{cases} \beta^*, & \text{with probability } \alpha(\beta^{(w)}, \beta^*) \\ \beta^{(w)}, & \text{with probability } 1 - \alpha(\beta^{(w)}, \beta^*) \end{cases},$$

where $\alpha(\beta^{(w)}, \beta^*) = \min \left\{ \frac{f(\beta^* | \cdot)}{f(\beta^{(w)} | \cdot)}, 1 \right\}$ is the acceptance probability for this multivariate random walk Metropolis algorithm.

4 Spatial and Temporal Predictions

Bayesian predictions at any arbitrary future time intervals and unseen spatial locations under our modeling framework are straightforward. We can decompose the integral representation of the posterior predictive distribution (PPD) into several known densities and then obtain the PPD via composition sampling. Suppose we have an arbitrary number $q \in \mathbb{N}, q \geq 1$ of future time periods $T+1, \dots, T+q$ of the same length and $r \in \mathbb{N}, r \geq 1$ new spatial locations $\mathbf{s}_{(m+1):(m+r)}$. Then for Bayesian predictions given the corresponding covariates matrices $[X_{(T+1):(T+q)}(\mathbf{s}_{1:m})]_{qm \times p}$ and $X_{1:(T+q)}(\mathbf{s}_{(m+1):(m+r)})_{(T+q)r \times p}$, if any, we can write the PPD as

$$\begin{aligned} & f(\mathbf{y}_{(T+1):(T+q)}(\mathbf{s}_{1:m}), \mathbf{y}_{1:(T+q)}(\mathbf{s}_{(m+1):(m+r)}) \mid \mathbf{y}_{1:T}(\mathbf{s}_{1:m}), X^{\text{new}}) \\ &= \int_{\Theta} f(\mathbf{y}_{(T+1):(T+q)}(\mathbf{s}_{1:m}), \mathbf{y}_{1:(T+q)}(\mathbf{s}_{(m+1):(m+r)}) \mid \Theta, \mathbf{y}_{1:T}(\mathbf{s}_{1:m}), X^{\text{new}}) \\ & \quad \times \pi(\Theta \mid \mathbf{y}_{1:T}(\mathbf{s}_{1:m})) d\Theta, \end{aligned} \quad (4.1)$$

where $\Theta = (\beta, U^{(T+1):(T+q)}(\mathbf{s}_{1:m}), U^{1:(T+q)}(\mathbf{s}_{(m+1):(m+r)}), U^{1:T}(\mathbf{s}_{1:m}), \kappa, \rho, c)$ and $X^{\text{new}} = \{X_{(T+1):(T+q)}(\mathbf{s}_{1:m}), X_{1:(T+q)}(\mathbf{s}_{(m+1):(m+r)})\}$. We can then partition the integral in (4.1)

into

$$\begin{aligned}
& \int_{\Theta} \underbrace{f(\mathbf{y}_{(T+1):(T+q)}(\mathbf{s}_{1:m}), \mathbf{y}_{1:(T+q)}(\mathbf{s}_{(m+1):(m+r)}) \mid \boldsymbol{\beta}, U^{(T+1):(T+q)}(\mathbf{s}_{1:m}), U^{1:(T+q)}(\mathbf{s}_{(m+1):(m+r)}), X^{\text{new}})}_{T_1} \\
& \times \underbrace{f(U^{1:(T+q)}(\mathbf{s}_{(m+1):(m+r)}) \mid U^{1:(T+q-1)}(\mathbf{s}_{1:m}), \kappa, \rho, c)}_{T_2} \\
& \times \underbrace{f(U^{(T+1):(T+q)}(\mathbf{s}_{1:m}) \mid U^T(\mathbf{s}_{1:m}), \kappa, \rho, c)}_{T_3} \times \underbrace{\pi(\boldsymbol{\beta}, U^{1:T}(\mathbf{s}_{1:m}), \kappa, \rho, c \mid \mathbf{y}_{1:T}(\mathbf{s}_{1:m}))}_{T_4} d\Theta,
\end{aligned}$$

where T_1 is the likelihood, T_4 is the parameters' posterior distribution obtained from the original model fit's MCMC sampler, $\hat{U}^{1:(T+q)}(\mathbf{s}_{(m+1):(m+r)})$ conditioning on $U^{1:T}(\mathbf{s}_{1:m}), \kappa, \rho, c$, $\hat{U}^{(T+1):(T+q-1)}(\mathbf{s}_{1:m})$ can be predicted based on (4.3) for T_2 , and T_3 is

$$\begin{aligned}
& f(U^{(T+1):(T+q)}(\mathbf{s}_{1:m}) \mid U^T(\mathbf{s}_{1:m}), \kappa, \rho, c) = \prod_{t=T+1}^{T+q} f(U^t(\mathbf{s}_{1:m}) \mid U^{t-1}(\mathbf{s}_{1:m}), \kappa, \rho, c) \\
& = \prod_{t=T+1}^{T+q} \prod_{i=1}^m f(U^t(\mathbf{s}_i) \mid U_{N(\mathbf{s}_i)}^{t-1}, \kappa, U^{t-1}(\mathbf{s}_i), \rho, c) \\
& = \prod_{t=T+1}^{T+q} \prod_{i=1}^m \text{Non-Central Gamma}\left(\alpha, \frac{1}{c}, \lambda_{it}\right),
\end{aligned} \tag{4.2}$$

where $\lambda_{it} = \frac{\kappa}{c} \cdot \sum_{j=1}^{|N(\mathbf{s}_i)|} w_{ij} U_{N(\mathbf{s}_i)[j]}^{t-1} + \frac{\rho}{c} \cdot U^{t-1}(\mathbf{s}_i)$. Assume $m > h_s$. For each new location \mathbf{s} outside of the training set $\mathcal{S} = \{\mathbf{s}_1, \mathbf{s}_2, \dots, \mathbf{s}_m\}$, we let $N(\mathbf{s})$ consist of the h_s nearest neighbors of \mathbf{s} in \mathcal{S} with the attached weights $\{w_j(\mathbf{s}) : j = 1, \dots, h_s\}$ that satisfy $w_j(\mathbf{s}) \in (0, 1]$ for all $j = 1, \dots, h_s$ and $\sum_{k=1}^{h_s} w_k(\mathbf{s}) = 1$. Independently for all new locations, we let $U^1(\mathbf{s}) \mid c \sim \text{Gamma}(\alpha, \frac{1}{c})$, and for $t = 2, 3, \dots, T+q$,

$$\begin{aligned}
& U^t(\mathbf{s}) \mid Z^{t-1}(\mathbf{s}), c \sim \text{Gamma}\left(\alpha + Z^{t-1}(\mathbf{s}), \frac{1}{c}\right), \\
& Z^{t-1}(\mathbf{s}) \mid U_{N(\mathbf{s})}^{t-1}, \kappa, U^{t-1}(\mathbf{s}), \rho, c \sim \text{Poisson}\left(\frac{\kappa}{c} \cdot \sum_{j=1}^{h_s} w_j(\mathbf{s}) U_{N(\mathbf{s})[j]}^{t-1} + \frac{\rho}{c} \cdot U^{t-1}(\mathbf{s})\right).
\end{aligned} \tag{4.3}$$

Then each $U^t(\mathbf{s}) \mid U_{N(\mathbf{s})}^{t-1}, \kappa, U^{t-1}(\mathbf{s}), \rho, c \sim \text{Non-Central Gamma}\left(\alpha, \frac{1}{c}, \lambda_t(\mathbf{s})\right)$, where $\lambda_t(\mathbf{s}) = \frac{\kappa}{c} \sum_{j=1}^{h_s} w_j(\mathbf{s}) U_{N(\mathbf{s})[j]}^{t-1} + \frac{\rho}{c} U^{t-1}(\mathbf{s})$, whose mean and variance are $\alpha c + \kappa \sum_{j=1}^{h_s} w_j(\mathbf{s}) U_{N(\mathbf{s})[j]}^{t-1} + \rho U^{t-1}(\mathbf{s})$ and $\alpha c^2 + 2c \left[\kappa \sum_{j=1}^{h_s} w_j(\mathbf{s}) U_{N(\mathbf{s})[j]}^{t-1} + \rho U^{t-1}(\mathbf{s}) \right]$, respectively.

5 Simulation Experiments

This section first verifies the satisfactory parameter estimation and model fitting performance of our proposed model in (2.1) and (2.2) through extensive simulation experiments. This section then compares computational efficiency, modeling and prediction performance of our framework with alternative Bayesian spatiotemporal count methods on simulated data from our MCMC model and from MCMC models in CARBayesST (Lee et al., 2018).

We first performed three groups of simulation experiments that all simulated data from (2.1) without external covariates $\mathbf{x}_t(\mathbf{s}_i)$'s and differ in variations of (2.2) modeling spatiotemporal frailties $U^{1:T}(\mathbf{s}_{1:m}) = \{U^t(\mathbf{s}_i) : t = 1, \dots, T, i = 1, \dots, m\}$ with the fixed hyperparameter $\alpha = 1.0001$. We specified $T = 100$ time intervals of equal length and $m = 11^2 = 121$ spatial locations $\mathbf{s}_i = (i_1, i_2)$ for $i = 1, \dots, m$ on an equispaced 2-dimensional grid, where $(i_1, i_2) \in \{1, \dots, 11\} \times \{1, \dots, 11\}$. Within each group, various sets of true parameter values for ρ (only for the first group), κ , c , and a few hyperparameter combinations were adopted. We ran each MCMC chain for 3×10^4 burn-in iterations and 2×10^4 post-burn-in iterations, which were thinned to 10^4 posterior samples for analysis.

The first group adopted our standard spatiotemporal frailty model (2.13) and (2.14) for data simulation and model fitting. For each spatial location \mathbf{s}_i , $N(\mathbf{s}_i)$ consists of the $h_s = 12$ nearest neighbors of \mathbf{s}_i in $\{\mathbf{s}_1, \dots, \mathbf{s}_m\} \setminus \{\mathbf{s}_i\}$ and $w_{ij} = 1/h_s$, $j = 1, \dots, h_s$ in (2.14). For entries of the i th row in the matrix $\mathbf{V} = \{v_{ij} : i, j = 1, \dots, m\}$ in (2.2), $v_{ii} = \rho > 0$, $v_{ij} = \kappa/h_s > 0$ for all j such that $\mathbf{s}_j \in N(\mathbf{s}_i)$, and $v_{ij} = 0$ for all $j \neq i$ such that $\mathbf{s}_j \notin N(\mathbf{s}_i)$.

The second group used our spatiotemporal frailty model (2.2) with entries in the matrix $\mathbf{V} = \{v_{ij} : i, j = 1, \dots, m\}$ in (2.2) given as follows for data simulation and model fitting. For each spatial location \mathbf{s}_i , $N(\mathbf{s}_i)$ consists of \mathbf{s}_i itself and the $h_s - 1 = 12 - 1 = 11$ nearest neighbors of \mathbf{s}_i in $\{\mathbf{s}_1, \dots, \mathbf{s}_m\} \setminus \{\mathbf{s}_i\}$. $v_{ij} = \kappa/h_s > 0$ for all j such that $j = i$ or $\mathbf{s}_j \in N(\mathbf{s}_i)$ to weight \mathbf{s}_i and each of its neighbors equally, and $v_{ij} = 0$ for all j such that $j \neq i$ and

$\mathbf{s}_j \notin N(\mathbf{s}_i)$. Hence, $\sum_{j=1}^m v_{ij} = h_s \times \kappa/h_s + 0 = \kappa \in (0, 1)$. As $v_{ij} \geq 0$ for all (i, j) and $0 < \sum_{j=1}^m v_{ij} < 1$ for all $i = 1, \dots, m$, Condition 2 in Theorem 1 applies and the process $\{U^t(\mathbf{s}_{1:m}) : t = 1, 2, \dots, T\}$ is guaranteed temporally stationary.

The third group assumed that the m spatial locations are labeled as $\mathbf{s}_1, \dots, \mathbf{s}_m$, starting from the central location \mathbf{s}_1 and going clockwise in the 2-dimensional grid, and employed a slightly varied version of our spatiotemporal frailty model (2.2) with no autocorrelation detailed as follows for data simulation and model fitting. We let $N(\mathbf{s}_1) = \emptyset$ and define for each $i \in \{2, 3, \dots, m\}$ location \mathbf{s}_i 's neighboring set $N(\mathbf{s}_i)$ as the $\min\{h_s, i - 1\}$ nearest neighbors of \mathbf{s}_i in $\{\mathbf{s}_1, \dots, \mathbf{s}_{i-1}\}$. We assume (2.2) for all \mathbf{s}_i with $i = 2, \dots, m$, $U^t(\mathbf{s}_1) \sim \text{Gamma}(\alpha, 1/c)$, and set all m entries in the first row of $\mathbf{V} = \{v_{ij} : i, j = 1, \dots, m\}$ as 0. For each $i = 2, \dots, m$, $v_{ij} = \kappa/|N(\mathbf{s}_i)|$ for all $j < i$ such that $\mathbf{s}_j \in N(\mathbf{s}_i)$, where $|N(\mathbf{s}_i)| = \min\{h_s, i - 1\} = \min\{12, i - 1\}$, and $v_{ij} = 0$ for all j such that $\mathbf{s}_j \notin N(\mathbf{s}_i)$. Hence, $\sum_{j=1}^m v_{ij} = |N(\mathbf{s}_i)| \times \kappa/|N(\mathbf{s}_i)| + 0 = \kappa \in (0, 1)$. As $v_{ij} \geq 0$ for all (i, j) and $0 < \sum_{j=1}^m v_{ij} < 1$ for all $i = 2, \dots, m$, Theorem 2 in Appendix B, a theorem similar to Theorem 1, applies and guarantees the temporal stationarity of the process $\{U^t(\mathbf{s}_{1:m}) : t = 1, 2, \dots, T\}$.

We calculate Mean Absolute Error (MAE) = $\frac{1}{mT} \sum_{t=1}^T \sum_{i=1}^m |y_t(\mathbf{s}_i) - \hat{y}_t(\mathbf{s}_i)|$, where $\hat{y}_t(\mathbf{s}_i)$ is the posterior mean of the estimated expectation of the response in time interval t and spatial location \mathbf{s}_i for each (t, i) (Tables 1 and 8 and Figures 4 and 5), and present summary statistics for posterior samples of parameters ρ (for the first group only), κ , c , $U_t(\mathbf{s}_i)$'s, and the actual observed counts $y_t(\mathbf{s}_i)$'s corresponding to true parameter values $(\rho, \kappa, c) \in \{0.4\} \times \{0.4\} \times \{5, 10, 15, 20, 50, 100, 500, 1000, 2000, 5000\}$ and hyperparameter combinations `hypara1` and `hypara2` for the first simulation group and true parameter values $(\kappa, c) \in \{0.35, 0.7\} \times \{5, 10, 15, 20, 50, 100, 500, 1000, 2000, 5000\}$ and hyperparameter combinations `hypara3` and `hypara4` for the second and the third simulation groups.

1. `hypara1`: $(\alpha_c, \theta_c) = (2, 10)$ for c , $(a_\kappa, b_\kappa) = (0.55, 1)$ for κ , $(a_\rho, b_\rho) = (0.4, 1)$ for ρ ;
2. `hypara2`: $(\alpha_c, \theta_c) = (2, 50)$ for c , $(a_\kappa, b_\kappa) = (0.4, 1)$ for κ , $(a_\rho, b_\rho) = (0.55, 1)$ for ρ .

3. **hypara3**: $(\alpha_c, \theta_c) = (2, 10)$ for c and $(a_\kappa, b_\kappa) = (0.9, 1)$ for κ ;
4. **hypara4**: $(\alpha_c, \theta_c) = (2, 50)$ for c and $(a_\kappa, b_\kappa) = (0.4, 1)$ for κ .

The obtained results presented in Tables 1 and 8 to 60 and Figures 4 and 5 corroborate our model's accurate parameter estimation and in-sample prediction capabilities for spatiotemporal count data spanning a wide range.

True c Value	Posterior Mean of c		Posterior Mean of κ		Posterior Mean of ρ		MAE	
	hypara1	hypara2	hypara1	hypara2	hypara1	hypara2	hypara1	hypara2
$c = 5$	4.987	4.997	0.4023	0.4030	0.4040	0.4031	1.272418	1.269910
$c = 10$	9.936	9.949	0.4031	0.4025	0.4035	0.4040	1.33638	1.334743
$c = 15$	14.91	14.92	0.4088	0.4074	0.3979	0.3991	1.350147	1.348748
$c = 20$	19.89	19.87	0.4064	0.4072	0.4001	0.3995	1.363482	1.362761
$c = 50$	49.86	49.84	0.4061	0.4069	0.3998	0.3991	1.380839	1.379167
$c = 100$	99.57	99.53	0.4061	0.4068	0.4002	0.3995	1.387671	1.389354
$c = 500$	497.5	497.7	0.4065	0.4062	0.3999	0.4001	1.429515	1.433766
$c = 1000$	996.9	994.9	0.4067	0.4073	0.3993	0.3991	1.483429	1.477110
$c = 2000$	1990	1994	0.4061	0.4072	0.4001	0.3989	1.570770	1.590506
$c = 5000$	4983	4973	0.4072	0.4064	0.3989	0.3999	1.816319	1.821356

Table 1: MAE and Mean value of the kept 10^4 posterior samples of c , κ , ρ for each of the $2 \times 10 = 20$ settings for the first simulation group with true parameter values $\kappa = \rho = 0.4$.

We then implemented our model with hyperparameter combination **hypara1** given earlier and six MCMC models—**ST.CARlinear**, **ST.CARanova**, **ST.CARsepspatial**, **ST.CARar**, **ST.CARadaptive**, and **ST.CARlocalised**—from the R package **CARBayesST** (Lee et al., 2018) and used the [R-INLA package](#) to fit the last two models for spatiotemporal areal data (Equations 7 and 8 in Section 3.3 of Blangiardo et al. 2013), denoted as **INLA.ST1** and **INLA.STint**, on data simulated from our model with the same mechanism as the first of the three simulation groups mentioned earlier in this section, where we specified $h_s = 4$, $c = 50$, $\kappa = 0.4$, $\rho = 0.1$, and on data generated from the aforementioned **CARBayesST**

models with the same mechanisms as in the package manual examples (Lee et al., 2018), where `ST.CARlocalised` and `ST.CARadaptive` share a common mechanism. We set $T = 50$ with two choices of the number of spatial locations— $m = 30^2 = 900$ and $m = 40^2 = 1600$.

When fitting `CARBayesST` models, we specified `AR=1` for `ST.CARar` and `interaction = TRUE` for `ST.CARanova`. On data generated from our model, we specified the $m \times m$ adjacency matrix $W = (w_{lj})$ as binary, where $w_{lj} = 1$ if and only if $\mathbf{s}_l \in N(\mathbf{s}_j)$ or $\mathbf{s}_j \in N(\mathbf{s}_l)$, and `G=6` for `ST.CARlocalised`, where `G` is the maximum number of distinct clusters permitted, indicated as 3 on data simulated from `ST.CARlocalised` itself. When fitting our model, we specified $|N(\mathbf{s}_i)| = h_s = 4$ and $w_{ij} = 1/h_s$, $j = 1, \dots, h_s$ in (2.14) for all $i = 1, \dots, m$. We ran each MCMC chain for 10^4 burn-in iterations and 10^4 post-burn-in iterations, thinned to 5000 posterior samples for analysis. For both `INLA.ST1` and `INLA.STint`, the `graph` input for the spatial structured and unstructured components under a Besag-York-Mollie (BYM) specification (Besag et al., 1991) is produced from the W adjacency matrix for `CARBayesST` models. A `logGamma(1, 0.1)` prior is imposed on the four precisions in `INLA.ST1` and the five precisions in `INLA.STint`.

Model \ Measure	runtime	$\overline{\text{ESS}}$	MAE	DIC	p.d.	WAIC	p.w.
Model							
our model	5976	≈ 5000	0.8700	629253.4	76748.78	631860.1	40400.18
<code>ST.CARar</code>	810.5	1831.7	0.6561196	634740.50	77915.41	615289.45	42213.60
<code>ST.CARanova</code>	632.6	1815.29	0.1972	631168.50	79178.71	607686.27	40153.84
<code>ST.CARsepspatial</code>	781.5	1834.9	0.7036909	634851.46	77972.09	615489.38	42307.94
<code>ST.CARadaptive</code>	26339.3	1830.7	0.7262935	634386.92	77719.66	614979.23	42107.87
<code>ST.CARlocalised</code>	5421.9	1825.8	1.393124	589610.92	27372.65	625742.84	45768.54
<code>INLA.STint</code>	0.49	N.A.	0.7418	637908.4	78591.9	627063.6	47732.64

Table 2: Data simulated from our model with $T = 50$ and $m = 1600$: overall computation time (`runtime`) in seconds, mean response ESS ($\overline{\text{ESS}}$) at the 5000 kept post-burn-in MCMC iterations, and diagnostics metrics from our model and adequate `CARBayesST`, `INLA` models. `ST.CARlinear` and `INLA.ST1` perform very poorly and are thus excluded from the table.

Measure Model	runtime	$\bar{\text{ESS}}$	MAE	DIC	p.d.	WAIC	p.w.
ST.CARlinear	376.9	1758.5	0.7615936	203867.457	1245.449	203877.468	1231.952
our model	7164	1780.7	0.5877898	206284.7	16745.43	227533.2	19548.92
INLA.ST1	0.012	N.A.	0.7784977	206559.4	1063.286	206561.6	1051.365
INLA.STint	0.37	N.A.	0.7676521	206537.9	2131.546	206562.2	2098.806
ST.CARsepspatial	743.2	312.18	0.8648668	229463.915	1759.231	229485.080	1727.627
our model	5472	≈ 5000	0.41761	240632.6	36262.85	250083.2	23388.25
INLA.ST1	0.08	N.A.	0.8761719	228936.3	506.5141	228947.8	514.6062
INLA.STint	0.29	N.A.	0.8522007	227920.5	2151.013	227970.1	2141.197
ST.CARanova	571.4	1674.8	0.8549369	225248.6631	931.3869	225253.3885	925.1672
our model	6732	1889.0	0.6350912	229445.7	19782.83	251996.4	21661.22
INLA.ST1	0.08	N.A.	0.8306218	219293.5	517.8178	219295.3	516.1339
INLA.STint	0.29	N.A.	0.8192538	219275.8	1580.859	219299.1	1572.868
ST.CARar	732.6	168.17	0.7703520	213100.853	6325.963	213398.226	6088.797
our model	6444	2025	0.5986256	213717.5	19371.1	243104.1	24950.1
INLA.ST1	0.08	N.A.	0.8936	226253.8	871.5126	226446	1051.778
INLA.STint	0.41	N.A.	0.7496993	223827	13036.55	224140.1	11520.21
ST.CARadaptive	26260.2	592.73	2.626	466999.97	28277.32	468224.07	23389.50
ST.CARlocalised	4322.2	1101.763	2.152	468133.15	32165.86	473010.07	28313.31
our model	6372	4183	1.610672	483729	58051.67	493412.3	34472.09
INLA.STint	1.08	N.A.	1.566	490315.3	54133.67	484575.3	35720.6

Table 3: Data simulated from five CARBayesST settings (ST.CARadaptive and ST.CARlocalised share the same simulated data set) with $T = 50$ and $m = 1600$: overall computation time (`runtime`) in seconds, mean response ESS ($\bar{\text{ESS}}$) at the 5000 kept post-burn-in MCMC iterations, and diagnostics metrics from the corresponding CARBayesST models, our model, INLA.ST1, and INLA.STint. INLA.ST1 performs poorly on the last simulated data set, and that row is thus excluded from the table.

For each MCMC model, we recorded the overall computation time for 2×10^4 MCMC iterations, denoted as `runtime`, and calculated the Effective Sample Size (ESS) for fitted response count values at the kept 5000 posterior iterations. Then, computation time per

effective response sample, obtained by the `runtime`/4 $\overline{\text{ESS}}$, where $\overline{\text{ESS}}$ denotes the mean of the mT effective sample sizes corresponding to $y_t(\mathbf{s}_i)$ s, would be an adequate metric to gauge the model's computational efficiency. We calculated MAE and considered model fit criteria including the Deviance Information Criterion (DIC), the Watanabe-Akaike Information Criterion (WAIC), and their estimated effective numbers of parameters (p.d for DIC and p.w. for WAIC) to evaluate model fitting performance. Tables 2, 3, 63 and 64 suggest that our MCMC model is comparable in computation time and modeling performance to and yields in all settings clearly higher ESS than **CARBayesST** MCMC models. Our framework also performs better than or comparably to **INLA.ST1** and **INLA.STint**.

We further investigate the prediction capabilities of these Bayesian spatiotemporal count models. Our package, **spatempBayesCounts**, has a function `predictNewLocTime()` for out-of-sample predictions executing our methodology in Section 4, which takes a fitted model object as one of its arguments and thus needs not refit a model. The **CARBayesST** package contains no built-in functions for out-of-sample predictions and can only obtain predictions on new data by refitting a model with new responses set to `NA`. Among the six models, only `ST.CARlinear`, `ST.CARanova`, and `ST.CARar` permit missing (`NA`) values in the response data and thus support out-of-sample predictions, as they are the simplest in terms of parsimony. `ST.CARsepspatial`, `ST.CARadaptive`, and `ST.CARlocalised` exhibit more complex forms and cannot recover missing data well (Lee et al., 2018). **INLA.ST1** and **INLA.STint** also require refitting the model with response data corresponding to new spatial locations and/or time intervals set to `NA` in order to make out-of-sample predictions.

We simulated data from `ST.CARlinear`, `ST.CARanova`, and `ST.CARar` with the same mechanisms as in the previous simulation experiments. We considered a total of $N = 50$ consecutive time intervals of equal length and $K = 39^2 = 1521$ spatial locations $\mathbf{s} = (i_1, i_2)$ on an equispaced 2-dimensional grid, where $(i_1, i_2) \in \{1, \dots, 39\} \times \{1, \dots, 39\}$. The last $h = 2$ of the $N = 50$ time intervals were taken as future time periods and had their corresponding

generated responses at all locations set to NA when fitting the three **CARBayesST** models and the two **R-INLA** models. $r = 21$ out of the $K = 1521$ locations, whose set of coordinates is $\{10, 20, 30\} \times \{10, 20, 30\} \cup \{5, 15, 25, 35\} \times \{15, 25\} \cup \{15, 25\} \times \{5, 35\}$, were set as testing locations (see Figure 2A) and had their corresponding generated responses at all time intervals set to NA when fitting the three **CARBayesST** models and the two **R-INLA** models. Simulated response data corresponding to the first $T = N - h = 48$ time intervals and the $m = K - r = 1500$ training locations were used to fit our model. The function `predictNewLocTime()` in our package, which takes in the fitted model object and the distance matrix between the $m = 1500$ reference and the $r = 21$ testing locations, then predicts at the 2 future time intervals and the r testing locations following Section 4.

Model	$i = 1 : m$		$i = (m + 1) : (m + r)$		$t = T + 1, T + 2, i = 1 : m; t = 1 : (T + 2), i = (m + 1) : (m + r)$	
	$t = 1 : T$	$t = T + 1$	$t = (T + 1) : (T + 2)$	$t = 1 : T$	$t = 1 : (T + 2)$	
ST.CARlinear	0.7525225	0.759521	0.7533761	0.7884273	0.7929358	0.7636323
our model	0.5759387	0.7593725	0.7522299	0.794803	0.798284	0.7641698
INLA.ST1	0.754968	1.0900247	1.0911743	1.1091403	1.1122884	1.0966483
INLA.STint	0.7442695	1.1031692	1.1060514	1.1167986	1.1204805	1.1097923
ST.CARanova	0.7715878	0.89888	0.89300	0.7825770	0.7818363	0.8641791
our model	0.5662226	0.8951150	0.8867734	0.786961	0.785446	0.8605033
INLA.ST1	0.7730499	1.2358673	1.2379976	1.07116	1.07961	1.1969354
INLA.STint	0.7624068	1.2450	1.248512	1.075794	1.084680	1.206037
ST.CARar	0.7835062	0.871665	0.874366	0.8882452	0.8947664	0.8796553
our model	0.6192472	0.8716193	0.8795939	0.936035	0.938046	0.8947482
INLA.ST1	0.8894	1.0689401	1.1037297	1.1291291	1.1471930	1.1149979
INLA.STint	0.7428802	1.209911	1.2661711	1.1727726	1.1981913	1.2485467

Table 4: Data simulated from **ST.CARlinear**, **ST.CARanova**, and **ST.CARar** with $T + h = 48 + 2 = 50$ consecutive time periods and $m + r = 1500 + 21 = 1521 = 39^2$ spatial locations: MAEs for in-sample (the second column) and out-of-sample (the third column to the last column) predictions from the corresponding **CARBayesST** models, our model, **INLA.ST1**, and **INLA.STint**. The last column presents MAE for all testing response data.

As the prediction MAEs in Table 4 and Figures 2B, 6 and 7 demonstrate, our model matches the performance of ST.CARlinear, ST.CARanova, and ST.CARar and significantly outperforms INLA.ST1 and INLA.STint in predicting responses at future time intervals and unseen spatial locations on data simulated from the three CARBayesST models that support out-of-sample predictions. Despite the fast computation speed and adequate in-sample prediction performance, INLA appears to introduce an approximation error that may not disappear with large samples, thus producing evidently higher MAEs for out-of-sample predictions.

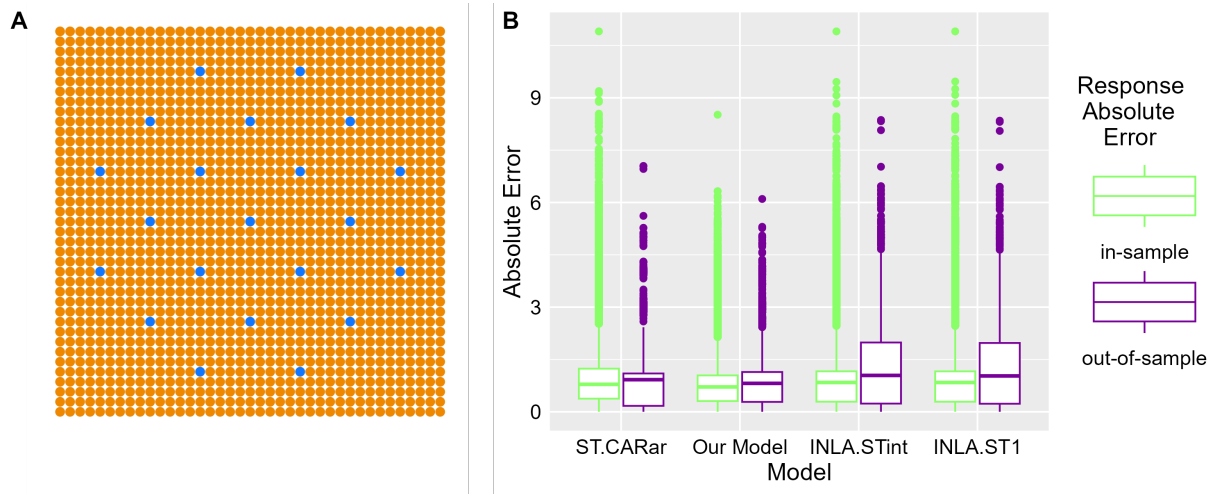


Figure 2: (A) Data simulated from ST.CARlinear, ST.CARanova, and ST.CARar with 50 consecutive time periods and $m + r = 1521 = 39^2$ spatial locations: the $r = 21$ blue locations are testing ones, and the $m = 1500$ orange locations are training ones. (B) Boxplot for the last of the three simulated data sets from A (from ST.CARar): distribution of the absolute errors $|y_t(\mathbf{s}_i) - \hat{y}_t(\mathbf{s}_i)|$, where $\hat{y}_t(\mathbf{s}_i)$ is the posterior mean for each (t, i) .

6 World Weekly COVID-19 Data

We compare the performance of our proposed Bayesian spatiotemporal count model with several popular LGP-based and CAR-based models in the literature, including two methods fit by INLA (Rue et al., 2009; Blangiardo et al., 2013) and six models from the R package CARBayesST (Lee et al., 2018), which also adopts MCMC simulation, on COVID-19 data.

We downloaded from [the WHO website](#) Weekly COVID-19 Cases and Deaths data of 240 countries/territories since January 2020. We considered the 145 countries/territories

with neither NA cases nor NA deaths in all 123 weeks from May 24, 2020, to September 25, 2022, both ends included. Negative counts for weekly new cases/deaths were taken as recording errors and changed to their absolute values. After extensive trials, population turned out to be an external covariate that should be included in the model, and yearly population by country/territory data was obtained from [the World Bank website](#).

As geographical proximity does not amount to heavy bilateral human traffic between two countries, it is likely inappropriate to specify each country's neighbor set based on geographical distances between countries, which was corroborated by our tests and experiments. Instead, we retrieved from [World Integrated Trade Solution \(WITS\)](#) all products' import & export data in the latest available year for all countries of interest and specified for each country \mathbf{s}_i its $h_s = 8$ neighbor countries as the ones among our retained $m = 123$ countries that contribute the most to \mathbf{s}_i 's import dollars. For each country \mathbf{s}_i , w_{ij} in (2.14) was calculated as \mathbf{s}_i 's latest available year import dollars from its j th neighbor $N(\mathbf{s}_i)[j]$ divided by \mathbf{s}_i 's latest available year import dollars from all its h_s neighbor countries.

Due to zero new COVID-19 cases for many consecutive weeks since May 24, 2020, suspicious new counts fluctuations, a lack of reliable population data, and/or unavailable recent yearly WITS import & export data, we excluded 22 countries/territories, whose ISO 3 codes are WLF, XKX, COK, NIU, PCN, TKL, ASM, PRK, MHL, NRU, FSM, SLB, TON, TUV, VUT, PLW, WSM, KIR, GUM, PRI, MNP, and HTI, from the 145 originally retained countries/territories. Our training data contain weekly new COVID-19 cases and deaths of $m = 123$ countries/territories in $T = 105$ weeks, from May 24, 2020, to May 22, 2022, both ends included. After comprehensive tests and detailed analyses, we decided to include fixed scaled population as the only external covariate by fixing $\boldsymbol{\beta}$ and setting $\exp\{\mathbf{x}_t(\mathbf{s}_i)\boldsymbol{\beta}\} = N_t(\mathbf{s}_i)/k$ in (2.1), where $N_t(\mathbf{s}_i)$ denotes country/territory \mathbf{s}_i 's population in the year among 2020, 2021, and 2022 within which the t th week falls, and k is a constant specified as 5000 for new cases and 5×10^5 for new deaths.

For each training data set of either weekly new cases or weekly new deaths, we fit our model with $2 \times 2 = 4$ settings for spatiotemporal frailties $U^t(\mathbf{s}_i)$'s – with ($\rho > 0$, `autoreg`) or without ($\rho = 0$, `noself`) autoregression; specify each country \mathbf{s}_i 's neighbor set and w_{ij} 's in (2.14) either based on the country's latest available year import data as detailed in the third paragraph of this section (WITS) or based on the correlations of the actual observed responses in the T weeks between \mathbf{s}_i and the other $m - 1$ countries (Cor). The four settings are denoted as `autoregWITS`, `autoregCor`, `noselfWITS`, `noselfCor`, respectively. We set $h_s = 8$, $\alpha = 1.0001$, and $(\alpha_c, \theta_c) = (2, 10)$. For `autoreg`, i.e., we follow our standard spatiotemporal frailty model (2.13) and (2.14) so that all m diagonal entries in the \mathbf{V} matrix in (2.2) equal $\rho > 0$, we specified $(a_\kappa, b_\kappa) = (0.55, 1)$ and $(a_\rho, b_\rho) = (0.4, 1)$; for `noself`, i.e., $\rho = 0$ in (2.12) so that all m diagonal entries in \mathbf{V} equal 0, we specified $(a_\kappa, b_\kappa) = (0.9, 1)$. We ran each MCMC chain for 2×10^4 burn-in iterations and 10^4 post-burn-in iterations, thinned to 5000 posterior samples for analysis.

Tables 66 and 67 present summary statistics of actual and predicted count responses and posterior samples of scalar parameters c , κ , and ρ . All four settings of our model produce good fits, as demonstrated by the close alignment between the estimated responses and the actual counts and the consistent and adequate scalar parameter estimates. Figures 3 and 8 further showcase our model setting `noselfWITS`'s decent in-sample prediction performance in all 123 training countries/territories in the week with reporting date December 20, 2020. The other three settings of our model lead to satisfactory outcomes, too.

As a comparison, we implemented the eight alternative Bayesian spatiotemporal count models carried out in Section 5 on the two data sets, which all included population (in 2022, 2023, and 2024) by country/territory as the only external covariate and adopted the Poisson family. For all six CARBayesST models, we ran 3×10^4 MCMC iterations, with the first 2×10^4 discarded as burn-in, and specified two choices for the $m \times m$ adjacency or weight matrix W , which is required by CARBayesST to be symmetric, nonnegative, and produce a positive

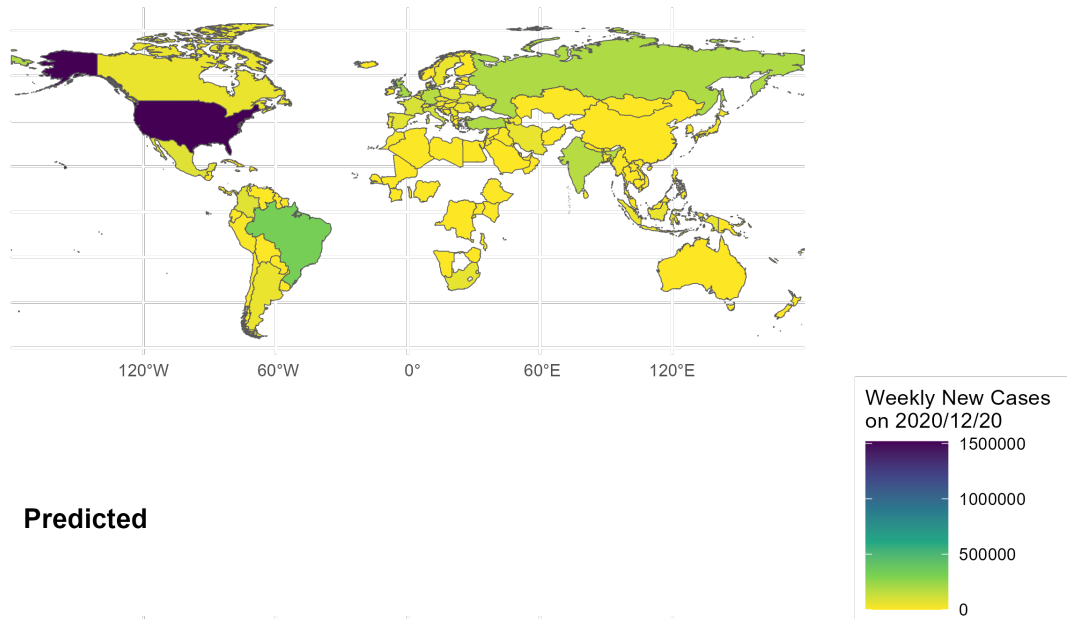
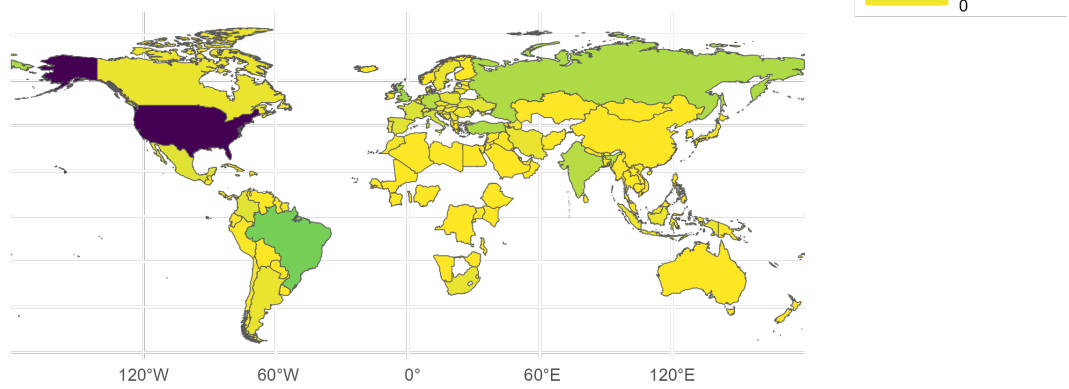
Actual**Predicted**

Figure 3: Actual and predicted (from the `noselfWITS` setting) new COVID-19 cases in the $m = 123$ training countries/territories in the week reported on December 20, 2020. The shapefile is obtained from [Opendatasoft](#).

sum for each row. For each of the two data sets, we first calculate the $m \times m$ correlation matrix (ρ_{lj}) of the actual observed counts in the T weeks for the m countries/territories. One $W_{m \times m}$ choice simply replaces all negative entries in the correlation matrix by 0 and is denoted as `Wcorr`. The other $W = (w_{lj})$ choice, denoted as `Wbinary`, is an $m \times m$ binary matrix whose diagonal entries are all 0. For all $l \neq j$, $w_{lj} = 1$ if and only if ρ_{lj} is among the $h_s = 8$ largest values in $\{\rho_{lk} : k = 1, \dots, m, k \neq l\}$ or $\{\rho_{hj} : h = 1, \dots, m, h \neq j\}$. For

both data sets, we specified `AR=1` for `ST.CARar` and `interaction = TRUE` for `ST.CARanova`. For `ST.CARlocalised`, we specified `G=6` for new cases and `G=3` for new deaths. For both `INLA.ST1` and `INLA.STint`, the graph input under a spatial BYM specification ([Besag et al., 1991](#)) is produced from the `Wbinary` matrix. A $\text{logGamma}(1, 0.1)$ prior is imposed on the four precisions in `INLA.ST1` and the five precisions in `INLA.STint`.

To evaluate the adequacy of the aforementioned models, we calculated MAE and Mean Absolute Percentage Error (MAPE). Let $\hat{y}_t(\mathbf{s}_i)$ denote the estimated expectation of the response, where the posterior mean is taken for each MCMC method, in time interval t and country/territory \mathbf{s}_i for each (i, t) , then $\text{MAE} = \frac{1}{mT} \sum_{t=1}^T \sum_{i=1}^m |y_t(\mathbf{s}_i) - \hat{y}_t(\mathbf{s}_i)|$ and $\text{MAPE} = \frac{100\%}{N} \sum_{(i,t) \text{ s.t. } y_t(\mathbf{s}_i) > 0} \left| \frac{y_t(\mathbf{s}_i) - \hat{y}_t(\mathbf{s}_i)}{y_t(\mathbf{s}_i)} \right|$, where $N \leq mT$, $N \in \mathbb{N}$ is the number of (i, t) pairs with non-zero actual $y_t(\mathbf{s}_i)$'s. Out of the $mT = 123 \times 105 = 12915$ actual $y_t(\mathbf{s}_i)$'s, 178 weekly COVID-19 new cases are 0, and 1758 weekly COVID-19 new deaths are 0. We further considered DIC, WAIC, and their estimated effective numbers of parameters.

No matter whether the covariate population is unscaled or scaled, `ST.CARlinear`, `ST.CARanova`, and `ST.CARsepspatial`, with both aforementioned choices for $W_{m \times m}$, and `INLA.ST1` all produced very unsatisfactory model fitting results and were thus excluded from our analyses. With population scaled, among `ST.CARar`, `ST.CARadaptive`, and `ST.CARlocalised`, with both `Wbinary` and `Wcorr` for $W_{m \times m}$, and `INLA.STint`, the only setting that produced an adequate model fit significantly better than its counterpart with unscaled population is `INLA.STint` applied to the weekly COVID-19 new deaths data. Most other model settings led to similarly good results with unscaled and scaled population. We thus only present results with the original unscaled population from settings except `INLA.STint` for the new deaths data, which divided population by 5×10^5 .

Tables 5 and 68 present for both data sets metrics obtained from more suitable ones among all model settings we experimented with. These adequate settings include `autoregWITS`, `autoregCor`, `noselfWITS`, and `noselfCor` from our model, `ST.CARar`, `ST.CARadaptive`,

and **ST.CARlocalised**, with both **Wbinary** and **Wcorr** for $W_{m \times m}$, from **CARBayesST**, and **INLA.STint** fit by **R-INLA**. Tables 5 and 68 suggest that for both data sets, our model's four settings yield performance comparable to that of the best-suited models from R packages **CARBayesST** and **R-INLA**. Moreover, our model clearly beats **CARBayesST** models for the world weekly COVID-19 new cases data set (Table 5).

Metric Method	MAE	MAPE	DIC	p.d.	WAIC	p.w.
autoregWITS	2.248796	1.35548	150922.8	12612.84	151018.5	6656.463
autoregCor	2.272264	1.354982	150932.4	12617.63	150843.5	6565.742
noselfWITS	1.968359	1.422978	150924.3	12620.48	150888.7	6557.625
noselfCor	2.005899	1.41713	150925.8	12620.46	150870.1	6574.339
INLA.STint	0.632495	1.91249	151429.8	12868.29	148388.9	6991.496
ST.CARarWbinary	4.920659	2.988448	153774.1	12346.52	155789.8	9610.862
ST.CARarWcorr	4.531402	1.714859	158076.23	12547.22	160361.6	9826.647
ST.CARadaptiveWbinary	5.874778	2.233535	151254.15	12487.26	148417.63	6918.49
ST.CARadaptiveWcorr	15.64428	2.579549	158116.5	15781.17	216239.24	40352.00
ST.CARlocalisedWbinary	7.098764	0.5548995	190523.03	32576.98	1028955.88	445788.63
ST.CARlocalisedWcorr	16.8224	0.7096886	311732.1	92927.66	20371494.59	10115176.62

Table 5: World weekly COVID-19 new cases: diagnostics metrics from 11 adequate model settings.

We now consider predicting in $h = 18$ new weeks, from May 29, 2022, to September 25, 2022, both ends included, in the $m = 123$ training countries/territories. We also consider predicting in the $T + h = 105 + 18 = 123$ weeks in $r = 4$ new countries/territories—whose ISO 3 codes are HTI, GUM, MNP, and PRI—that do not exhibit zero new COVID-19 cases for multiple consecutive weeks since May 24, 2020. For all settings of our model, each new location \mathbf{s} 's neighbor set $N(\mathbf{s})$ and $w_j(\mathbf{s})$'s in (4.3) are obtained based on the correlations of the actual observed responses in the $T + h$ weeks between \mathbf{s} and the m reference countries/territories. As delineated in Section 5, among all models in **CARBayesST**, only

`ST.CARlinear`, `ST.CARanova`, and `ST.CARar` support out-of-sample predictions. Hence, `ST.CARar` is the only CARBayesST model that fits the world COVID-19 new cases/deaths data adequately and is capable of predicting in new countries/territories and/or future weeks. It, however, performs very poorly (Tables 6 and 7) in out-of-sample predictions.

Method	MedAE	$i = 1 : m$			$i = (m + 1) : (m + r)$	
		$t = T + 1$	$t = (T + 1) : (T + 2)$	$t = (T + 1) : (T + 5)$	$t = (T + 1) : (T + h)$	$t = 1 : T$
<code>autoregWITS</code>	3024.25	3651.0	5980.5	10499.6	600.25	601.00
<code>autoregCor</code>	2933.86	3672.5	6031.9	10468.6	598.19	604.88
<code>noselfWITS</code>	15065.6	15685.7	16437.2	15415.3	733.73	723.05
<code>noselfCor</code>	9878	10160	12211	12128	470.67	471.36
<code>INLA.STint</code>	1362.1	1435.3	1727.7	2764.3	183.83	211.84
<code>ST.CARarWbinary</code>	4.547×10^8	4.610×10^8	4.887×10^8	4.718×10^8	8.267×10^7	9.014×10^7
<code>ST.CARarWcorr</code>	5.382×10^8	5.364×10^8	5.392×10^8	4.958×10^8	7.874×10^7	7.766×10^7

Table 6: World weekly COVID-19 new cases: MedAE for out-of-sample predictions from 7 adequate model settings capable of estimating at new time intervals and spatial locations.

Method	MedAE	$i = 1 : m$			$i = (m + 1) : (m + r)$	
		$t = T + 1$	$t = (T + 1) : (T + 2)$	$t = (T + 1) : (T + 5)$	$t = (T + 1) : (T + h)$	$t = 1 : T$
<code>autoregWITS</code>	17.257	20.798	31.278	56.406	5.2839	5.2839
<code>autoregCor</code>	17.4479	20.1491	31.547	56.599	5.35063	5.35063
<code>noselfWITS</code>	81.698	100.437	122.267	127.852	6.7714	4.7059
<code>noselfCor</code>	74.75	86.27	99.818	103.541	6.7408	5.8654
<code>INLA.STint</code>	8.898	8.630	8.536	10.857	2.1010	2.3678
<code>ST.CARarWbinary</code>	3632411	3537483	3705387	3758511	424443	424443
<code>ST.CARarWcorr</code>	4377532	4426582	4361354	4310342	563653	563653

Table 7: World weekly COVID-19 new deaths: MedAE for out-of-sample predictions from 7 adequate model settings capable of estimating at new time intervals and spatial locations.

Tables 6 and 7 present the Median Absolute Error $\text{MedAE} = \text{median}(|y_t(\mathbf{s}_i) - \hat{y}_t(\mathbf{s}_i)|)$

for out-of-sample predictions in future weeks and/or new countries/territories. Although our model underperforms relative to `INLA.STint`, the performance remains comparable in scale. Our model beats `CARBayesST`, as each of its functions either cannot conduct or performs very unsatisfactorily in out-of-sample predictions. Figures 9 and 10 demonstrate our model setting `autoregWITS`'s adequate out-of-sample prediction performance in all 127 training and testing countries/territories in the first future week with reporting date May 29, 2022. The other three settings of our model produce satisfactory results as well.

7 Discussion

The current work can be extended in several directions. First, although we have modeled the count data using Poisson random variables, the proposed Bayesian framework and sampling strategies are readily applicable to related distributions, such as the zero-inflated Poisson distribution for datasets with many zero responses and the negative binomial distribution viewed as a gamma mixture of Poisson distributions. Second, our theory provides sufficient conditions on the weighting matrix to ensure stationarity of the frailty process. So far, we have investigated the empirical performance of only one such graph built upon nearest neighbors. In general, one can specify other types of sparse graphs for the frailties across spatial and temporal dimensions, as long as the process remains stationary. Third, our current spatiotemporal model is defined on a finite set of time intervals and spatial locations connected through a graph of weights, which does not directly extend to a valid stochastic process over a continuous spatial domain. To achieve such an extension, one possible approach is to represent the latent gamma frailties as the sum of squares of several independent latent Gaussian processes, as in the recent work on Poisson point processes by [Morales-Navarrete et al. \(2024\)](#). We leave these directions to future research.

A Deductions Leading to Posterior Sampling Steps for the Model Given by (2.1), (2.13), and (2.14)

We deduce in detail posterior sampling steps for the model given by (2.1), (2.13), and (2.14).

1. Sampling from the full conditional distribution of c with prior $\pi(c) \sim \mathcal{IG}(\alpha_c, \theta_c)$:

If $m > 1$ and $T > 1$, then

$$\begin{aligned}
f(c|\cdot) &\propto \pi(c) \times \prod_{i=1}^m f(U^1(\mathbf{s}_i) | c) \times \prod_{t=2}^T \prod_{i=1}^m f\left(U^t(\mathbf{s}_i) | Z_{i0}^{t-1}, Z_{i1}^{t-1}, \dots, Z_{i|N(\mathbf{s}_i)|}^{t-1}, c\right) \times \\
&\quad \prod_{t=2}^T \prod_{i=1}^m f(Z_{i0}^{t-1} | U^{t-1}(\mathbf{s}_i), \rho, c) \times \prod_{t=2}^T \prod_{i=1}^m \prod_{j=1}^{|N(\mathbf{s}_i)|} f\left(Z_{ij}^{t-1} | U_{N(\mathbf{s}_i)[j]}^{t-1}, \kappa, c\right) \\
&\propto \left(\frac{1}{c}\right)^{\alpha_c+1} \exp\left\{-\frac{\theta_c}{c}\right\} \times \left(\frac{1}{c}\right)^{m\alpha} \exp\left\{-\frac{1}{c} \sum_{i=1}^m U^1(\mathbf{s}_i)\right\} \times \\
&\quad \prod_{t=2}^T \prod_{i=1}^m \left(\frac{1}{c}\right)^{\alpha + \sum_{j=0}^{|N(\mathbf{s}_i)|} Z_{ij}^{t-1}} \exp\left\{-\frac{U^t(\mathbf{s}_i)}{c}\right\} \cdot \left(\frac{1}{c}\right)^{Z_{i0}^{t-1}} \exp\left\{-\frac{1}{c} \rho U^{t-1}(\mathbf{s}_i)\right\} \times \\
&\quad \prod_{t=2}^T \prod_{i=1}^m \prod_{j=1}^{|N(\mathbf{s}_i)|} \left(\frac{1}{c}\right)^{Z_{ij}^{t-1}} \exp\left\{-\frac{1}{c} [\kappa w_{ij} U_{N(\mathbf{s}_i)[j]}^{t-1}]\right\} \\
&\propto \left(\frac{1}{c}\right)^{Tm\alpha + 2 \sum_{t=2}^T \sum_{i=1}^m \sum_{j=0}^{|N(\mathbf{s}_i)|} Z_{ij}^{t-1} + \alpha_c + 1} \times \exp\left\{-\frac{\theta_c^{\text{post}}}{c}\right\} \\
&\sim \mathcal{IG}\left(\alpha_c + Tm\alpha + 2 \sum_{t=1}^{T-1} \sum_{i=1}^m \sum_{j=0}^{|N(\mathbf{s}_i)|} Z_{ij}^t, \theta_c^{\text{post}}\right), \tag{A.1}
\end{aligned}$$

where $\theta_c^{\text{post}} = \theta_c + \sum_{t=1}^T \sum_{i=1}^m U^t(\mathbf{s}_i) + \rho \cdot \sum_{t=1}^{T-1} \sum_{i=1}^m U^t(\mathbf{s}_i) + \kappa \cdot \sum_{i=1}^m \sum_{j=1}^{|N(\mathbf{s}_i)|} w_{ij} \sum_{t=1}^{T-1} U_{N(\mathbf{s}_i)[j]}^t$.

If $T = 1$, then

$$\begin{aligned}
f(c|\cdot) &\propto \pi(c) \times \prod_{i=1}^m f(U^1(\mathbf{s}_i) | c) \\
&\propto \left(\frac{1}{c}\right)^{m\alpha} \exp\left\{-\frac{1}{c} \sum_{i=1}^m U^1(\mathbf{s}_i)\right\} \times \left(\frac{1}{c}\right)^{\alpha_c+1} \exp\left\{-\frac{\theta_c}{c}\right\} \\
&\propto \left(\frac{1}{c}\right)^{m\alpha + \alpha_c + 1} \exp\left\{-\frac{1}{c} \left[\sum_{i=1}^m U^1(\mathbf{s}_i) + \theta_c\right]\right\}
\end{aligned}$$

$$\sim \mathcal{IG} \left(m\alpha + \alpha_c, \sum_{i=1}^m U^1(\mathbf{s}_i) + \theta_c \right).$$

If $m = 1$ and $T > 1$, then

$$\begin{aligned} f(c|\cdot) &\propto \pi(c) \times f(U^1(\mathbf{s}_1) | c) \times \prod_{t=2}^T f(U^t(\mathbf{s}_1) | Z_{10}^{t-1}, c) \times \prod_{t=1}^{T-1} f(Z_{10}^t | U^t(\mathbf{s}_1), \rho, c) \\ &\propto \left(\frac{1}{c}\right)^{T\alpha+2\sum_{t=1}^{T-1}Z_{10}^t+\alpha_c+1} \exp\left\{-\frac{1}{c}\left[\sum_{t=1}^T U^t(\mathbf{s}_1) + \rho \cdot \sum_{t=1}^{T-1} U^t(\mathbf{s}_1) + \theta_c\right]\right\} \\ &\sim \mathcal{IG}\left(T\alpha + 2\sum_{t=1}^{T-1} Z_{10}^t + \alpha_c, \sum_{t=1}^T U^t(\mathbf{s}_1) + \rho \cdot \sum_{t=1}^{T-1} U^t(\mathbf{s}_1) + \theta_c\right). \end{aligned}$$

2. Sampling from the full conditional distributions of $U^{1:T}(\mathbf{s}_{1:m})$:

Fix any arbitrary $i \in \{1, 2, \dots, m\}$. For each $l \in \{1, 2, \dots, m\}$ such that $\mathbf{s}_i \in N(\mathbf{s}_l)$, we denote $k_l(\mathbf{s}_i)$ as the positive integer less than or equal to h_s such that $\mathbf{s}_i = N(\mathbf{s}_l)[k_l(\mathbf{s}_i)]$. If $m > 1$ and $T > 1$, then for any $t \in \{2, 3, \dots, T-1\}$,

$$\begin{aligned} f(U^t(\mathbf{s}_i)|\cdot) &\propto f(y_t(\mathbf{s}_i) | U^t(\mathbf{s}_i), \boldsymbol{\beta}) \times f(U^t(\mathbf{s}_i) | Z_{i0}^{t-1}, Z_{i1}^{t-1}, \dots, Z_{i|N(\mathbf{s}_i)|}^{t-1}, c) \times \\ &f(Z_{i0}^t | U^t(\mathbf{s}_i), \rho, c) \times \prod_{l:\mathbf{s}_i \in N(\mathbf{s}_l)}^{1 \leq l \leq m} f(Z_{lk_l(\mathbf{s}_i)}^t | U^t(\mathbf{s}_i), \kappa, c) \\ &\propto U^t(\mathbf{s}_i)^{y_t(\mathbf{s}_i)} \exp\left\{-U^t(\mathbf{s}_i) \left[e^{\mathbf{x}_t(\mathbf{s}_i)^T \boldsymbol{\beta}}\right]\right\} \times U^t(\mathbf{s}_i)^{\alpha + \sum_{j=0}^{|N(\mathbf{s}_i)|} Z_{ij}^{t-1}-1} \exp\left\{-\frac{U^t(\mathbf{s}_i)}{c}\right\} \times \\ &U^t(\mathbf{s}_i)^{Z_{i0}^t} \exp\left\{-U^t(\mathbf{s}_i) \cdot \frac{\rho}{c}\right\} \times \prod_{l:\mathbf{s}_i \in N(\mathbf{s}_l)}^{1 \leq l \leq m} U^t(\mathbf{s}_i)^{Z_{lk_l(\mathbf{s}_i)}^t} \exp\left\{-w_{lk_l(\mathbf{s}_i)} U^t(\mathbf{s}_i) \cdot \frac{\kappa}{c}\right\} \\ &\propto U^t(\mathbf{s}_i)^{y_t(\mathbf{s}_i)+\alpha+\sum_{j=0}^{|N(\mathbf{s}_i)|} Z_{ij}^{t-1}-1+Z_{i0}^t+\sum_{l:\mathbf{s}_i \in N(\mathbf{s}_l)}^{1 \leq l \leq m} Z_{lk_l(\mathbf{s}_i)}^t} \times \\ &\exp\left\{-U^t(\mathbf{s}_i) \left[e^{\mathbf{x}_t(\mathbf{s}_i)^T \boldsymbol{\beta}} + \frac{1}{c} \left(1 + \rho + \kappa \sum_{l:\mathbf{s}_i \in N(\mathbf{s}_l)}^{1 \leq l \leq m} w_{lk_l(\mathbf{s}_i)}\right)\right]\right\} \\ &\sim \text{Gamma}\left(y_t(\mathbf{s}_i) + \alpha + \sum_{j=0}^{|N(\mathbf{s}_i)|} Z_{ij}^{t-1} + Z_{i0}^t + \sum_{l:\mathbf{s}_i \in N(\mathbf{s}_l)}^{1 \leq l \leq m} Z_{lk_l(\mathbf{s}_i)}^t, \text{rate}_{U^t(\mathbf{s}_i)}\right), \quad (\text{A.2}) \end{aligned}$$

where $\text{rate}_{U^t(\mathbf{s}_i)} = e^{\mathbf{x}_t(\mathbf{s}_i)^T \boldsymbol{\beta}} + \frac{1}{c} \left(1 + \rho + \kappa \sum_{l:\mathbf{s}_i \in N(\mathbf{s}_l)}^{1 \leq l \leq m} w_{lk_l(\mathbf{s}_i)}\right)$.

$$f(U^t(\mathbf{s}_i)|\cdot) \sim \text{Gamma}\left(y_t(\mathbf{s}_i) + \alpha + Z_{i0}^t + \sum_{l:\mathbf{s}_i \in N(\mathbf{s}_l)}^{1 \leq l \leq m} Z_{lk_l(\mathbf{s}_i)}^t, \text{rate}_{U^t(\mathbf{s}_i)}\right) \text{ for } t = 1, \text{ and}$$

$$f(U^t(\mathbf{s}_i)|\cdot) \sim \text{Gamma} \left(y_t(\mathbf{s}_i) + \alpha + \sum_{j=0}^{|N(\mathbf{s}_i)|} Z_{ij}^{t-1}, e^{\mathbf{x}_t(\mathbf{s}_i)^T \boldsymbol{\beta}} + \frac{1}{c} \right) \text{ for } t = T.$$

$$\text{If } T = 1, \text{ then } f(U^1(\mathbf{s}_i)|\cdot) \sim \text{Gamma} \left(y_1(\mathbf{s}_i) + \alpha, e^{\mathbf{x}_1(\mathbf{s}_i)^T \boldsymbol{\beta}} + \frac{1}{c} \right).$$

If $m = 1$ and $T > 1$, then for any $t \in \{2, \dots, T-1\}$,

$$f(U^t(\mathbf{s}_1)|\cdot) \sim \text{Gamma} \left(y_t(\mathbf{s}_1) + \alpha + Z_{10}^{t-1} + Z_{10}^t, e^{\mathbf{x}_t(\mathbf{s}_1)^T \boldsymbol{\beta}} + \frac{1}{c}(1+\rho) \right),$$

$$f(U^t(\mathbf{s}_1)|\cdot) \sim \text{Gamma} \left(y_t(\mathbf{s}_1) + \alpha + Z_{10}^t, e^{\mathbf{x}_t(\mathbf{s}_1)^T \boldsymbol{\beta}} + \frac{1}{c}(1+\rho) \right) \text{ for } t = 1, \text{ and}$$

$$f(U^t(\mathbf{s}_1)|\cdot) \sim \text{Gamma} \left(y_t(\mathbf{s}_1) + \alpha + Z_{10}^{t-1}, e^{\mathbf{x}_t(\mathbf{s}_1)^T \boldsymbol{\beta}} + \frac{1}{c} \right) \text{ for } t = T.$$

3. Sampling from the full conditional distribution of ρ with prior

$\pi(\rho) \sim \text{Truncated Gamma}(a_\rho, b_\rho, 0, 1)$ when $T > 1$:

$$\begin{aligned} f(\rho|\cdot) &\propto \pi(\rho) \times \prod_{t=1}^{T-1} \prod_{i=1}^m f(Z_{i0}^t | U^t(\mathbf{s}_i), \rho, c) \\ &\propto \rho^{a_\rho-1} \exp\{-b_\rho \cdot \rho\} \mathbb{1}_{\{0 < \rho < 1\}} \times \prod_{t=1}^{T-1} \prod_{i=1}^m \rho^{Z_{i0}^t} \exp\left\{-\frac{\rho}{c} \cdot U^t(\mathbf{s}_i)\right\} \\ &\propto \rho^{a_\rho + \sum_{t=1}^{T-1} \sum_{i=1}^m Z_{i0}^t - 1} \exp\left\{-\rho \left[b_\rho + \frac{1}{c} \sum_{t=1}^{T-1} \sum_{i=1}^m U^t(\mathbf{s}_i) \right]\right\} \mathbb{1}_{\{0 < \rho < 1\}} \\ &\sim \text{Truncated Gamma} \left(a_\rho + \sum_{t=1}^{T-1} \sum_{i=1}^m Z_{i0}^t, b_\rho + \frac{1}{c} \sum_{t=1}^{T-1} \sum_{i=1}^m U^t(\mathbf{s}_i), 0, 1 \right). \quad (\text{A.3}) \end{aligned}$$

4. Sampling from the full conditional distribution of κ with prior

$\pi(\kappa) \sim \text{Truncated Gamma}(a_\kappa, b_\kappa, 0, 1 - \rho)$ when $m > 1$ and $T > 1$:

$$\begin{aligned} f(\kappa|\cdot) &\propto \pi(\kappa) \times \prod_{t=1}^{T-1} \prod_{i=1}^m \prod_{j=1}^{|N(\mathbf{s}_i)|} f(Z_{ij}^t | U_{N(\mathbf{s}_i)[j]}^t, \kappa, c) \\ &\propto \kappa^{a_\kappa-1} \exp\{-b_\kappa \cdot \kappa\} \mathbb{1}_{\{0 < \kappa < 1-\rho\}} \times \prod_{t=1}^{T-1} \prod_{i=1}^m \prod_{j=1}^{|N(\mathbf{s}_i)|} \kappa^{Z_{ij}^t} \exp\left\{-\frac{\kappa}{c} \cdot w_{ij} U_{N(\mathbf{s}_i)[j]}^t\right\} \\ &\propto \kappa^{a_\kappa + \sum_{t=1}^{T-1} \sum_{i=1}^m \sum_{j=1}^{|N(\mathbf{s}_i)|} Z_{ij}^t - 1} \exp\left\{-\kappa \left[b_\kappa + \frac{1}{c} \sum_{i=1}^m \sum_{j=1}^{|N(\mathbf{s}_i)|} w_{ij} \sum_{t=1}^{T-1} U_{N(\mathbf{s}_i)[j]}^t \right]\right\} \mathbb{1}_{\{0 < \kappa < 1-\rho\}} \end{aligned}$$

$$\sim \text{Truncated Gamma} \left(a_\kappa + \sum_{t=1}^{T-1} \sum_{i=1}^m \sum_{j=1}^{|N(\mathbf{s}_i)|} Z_{ij}^t, b_\kappa + \frac{1}{c} \sum_{i=1}^m \sum_{j=1}^{|N(\mathbf{s}_i)|} w_{ij} \sum_{t=1}^{T-1} U_{N(\mathbf{s}_i)[j]}^t, 0, 1 - \rho \right). \quad (\text{A.4})$$

5. Sampling from the full conditional distributions of Z_{ij}^t 's when $T > 1$:

Fix any arbitrary $t \in \{1, 2, \dots, T-1\}$, $i \in \{1, 2, \dots, m\}$. Then

$$\begin{aligned} f(Z_{i0}^t | \cdot) &\propto f(U^{t+1}(\mathbf{s}_i) | Z_{i0}^t, Z_{i1}^t, \dots, Z_{i|N(\mathbf{s}_i)|}^t, c) \times f(Z_{i0}^t | U^t(\mathbf{s}_i), \rho, c) \\ &\propto \frac{\left(\frac{U^{t+1}(\mathbf{s}_i)}{c}\right)^{Z_{i0}^t}}{\Gamma\left(\alpha + \sum_{k=0}^{|N(\mathbf{s}_i)|} Z_{ik}^t\right)} \times \frac{\left[\frac{\rho}{c} \cdot U^t(\mathbf{s}_i)\right]^{Z_{i0}^t}}{Z_{i0}^t!} \\ &\propto \frac{\left(\frac{\rho U^{t+1}(\mathbf{s}_i) U^t(\mathbf{s}_i)}{c^2}\right)^{Z_{i0}^t}}{\Gamma\left(\alpha + \sum_{k=0}^{|N(\mathbf{s}_i)|} Z_{ik}^t\right) \times Z_{i0}^t!} \\ &\sim \text{Bessel} \left(\alpha + \sum_{k=1}^{|N(\mathbf{s}_i)|} Z_{ik}^t - 1, \frac{2}{c} \sqrt{\rho \cdot U^{t+1}(\mathbf{s}_i) U^t(\mathbf{s}_i)} \right). \end{aligned} \quad (\text{A.5})$$

When $m > 1$, we further fix any arbitrary $j \in \{1, 2, \dots, |N(\mathbf{s}_i)|\}$. Then

$$\begin{aligned} f(Z_{ij}^t | \cdot) &\propto f(U^{t+1}(\mathbf{s}_i) | Z_{i0}^t, Z_{i1}^t, \dots, Z_{i|N(\mathbf{s}_i)|}^t, c) \times f(Z_{ij}^t | U_{N(\mathbf{s}_i)[j]}^t, \kappa, c) \\ &\propto \frac{\left(\frac{U^{t+1}(\mathbf{s}_i)}{c}\right)^{Z_{ij}^t}}{\Gamma\left(\alpha + \sum_{k=0}^{|N(\mathbf{s}_i)|} Z_{ik}^t\right)} \times \frac{\left(\frac{\kappa}{c} \cdot w_{ij} U_{N(\mathbf{s}_i)[j]}^t\right)^{Z_{ij}^t}}{Z_{ij}^t!} \\ &\propto \frac{\left(\frac{\kappa U^{t+1}(\mathbf{s}_i)}{c^2} \cdot w_{ij} U_{N(\mathbf{s}_i)[j]}^t\right)^{Z_{ij}^t}}{\Gamma\left(\alpha + \sum_{k=0}^{|N(\mathbf{s}_i)|} Z_{ik}^t\right) \times Z_{ij}^t!} \\ &\sim \text{Bessel} \left(\alpha + \sum_{k=0, k \neq j}^{|N(\mathbf{s}_i)|} Z_{ik}^t - 1, \frac{2}{c} \sqrt{\kappa w_{ij} U^{t+1}(\mathbf{s}_i) U_{N(\mathbf{s}_i)[j]}^t} \right), \end{aligned} \quad (\text{A.6})$$

where $X \sim \text{Bessel}(\nu, a)$ has the probability mass function $\mathbb{P}(X = n | a, \nu) = \frac{(a/2)^{2n+\nu}}{I_\nu(a)\Gamma(n+\nu+1)n!}$ for $n \in \mathbb{N}$, $a > 0$, $\nu > -1$, and $I_\nu(\cdot)$ is the modified Bessel function of the first kind. We generate Bessel random variables via the rejection algorithms in Section 3 of Devroye (2002).

6. Sampling $\beta_{p \times 1}$ via a Metropolis step with prior $\pi(\beta) \sim N_p(\mu_{0\beta}, \Sigma_{0\beta})$:

$$\begin{aligned}
f(\beta|\cdot) &\propto \pi(\beta) \times \prod_{i=1}^m \prod_{t=1}^T f(y_t(s_i) | U^t(s_i), \beta) \\
&\propto \exp \left\{ -\frac{1}{2} (\beta - \mu_{0\beta})^\top \Sigma_{0\beta}^{-1} (\beta - \mu_{0\beta}) \right\} \times \\
&\quad \prod_{i=1}^m \prod_{t=1}^T \exp \left\{ -U^t(s_i) e^{\mathbf{x}_t(s_i)^\top \beta} \right\} \times \left[U^t(s_i) e^{\mathbf{x}_t(s_i)^\top \beta} \right]^{y_t(s_i)} \\
&\propto \exp \left\{ -\frac{1}{2} (\beta - \mu_{0\beta})^\top \Sigma_{0\beta}^{-1} (\beta - \mu_{0\beta}) + \sum_{i=1}^m \sum_{t=1}^T [y_t(s_i) \cdot \mathbf{x}_t(s_i)^\top \beta - U^t(s_i) e^{\mathbf{x}_t(s_i)^\top \beta}] \right\}
\end{aligned} \tag{A.7}$$

is not a standard parametric family, and we resort to a Metropolis step for sampling β from its full conditional distribution.

We consider a symmetric Markov kernel $Q : \mathbb{R}^p \times \mathbb{R}^p \rightarrow \mathbb{R}^+$ with $Q(\beta_a, \beta_b) = Q(\beta_b, \beta_a)$ for all $\beta_a, \beta_b \in \mathbb{R}^p$. $Q(\beta_a, \beta_b)$ equals the density of a $N_p(\beta_a, V)$ random variable evaluated at β_b with probability p and the density of a $N_p(\beta_a, 100V)$ random variable evaluated at β_b with probability $1-p$, where V is an estimate of the inverse Hessian of $\ln[f(\beta|\cdot)]$ and $p \in (0, 1)$ should be quite large to give less probability to big moves in the parameter space. At each MCMC iteration $w \in \mathbb{N}$, we let the current parameter estimate for β be $\beta^{(w)}$. Since

$$\frac{\partial^2}{\partial \beta \partial \beta^\top} \ln f(\beta|\cdot) = -\Sigma_{0\beta}^{-1} - \sum_{i=1}^m \sum_{t=1}^T U^t(s_i) e^{\mathbf{x}_t(s_i)^\top \beta} \mathbf{x}_t(s_i) \mathbf{x}_t(s_i)^\top, \tag{A.8}$$

we set $V^{(w)} = \left[\Sigma_{0\beta}^{-1} + \sum_{i=1}^m \sum_{t=1}^T U^t(s_i) e^{\mathbf{x}_t(s_i)^\top \beta^{(w)}} \mathbf{x}_t(s_i) \mathbf{x}_t(s_i)^\top \right]^{-1}$. We propose a new parameter value β^* from the density $q(\beta|\beta^{(w)}) = Q(\beta^{(w)}, \beta)$ and then set

$$\beta^{(w+1)} = \begin{cases} \beta^*, & \text{with probability } \alpha(\beta^{(w)}, \beta^*) \\ \beta^{(w)}, & \text{with probability } 1 - \alpha(\beta^{(w)}, \beta^*) \end{cases},$$

where $\alpha(\beta^{(w)}, \beta^*) = \min \left\{ \frac{f(\beta^*|\cdot)}{f(\beta^{(w)}|\cdot)}, 1 \right\}$ is the acceptance probability for this multivariate random walk Metropolis algorithm.

B Spatiotemporal Frailty Process Stationarity Condition for the Third Simulation Group Mentioned at the Start of Section 5

Theorem 2. Fix any arbitrary $m \in \mathbb{N}$ and spatial locations $\{\mathbf{s}_1, \dots, \mathbf{s}_m\}$. For each $t = 2, \dots, T$ and \mathbf{s}_i with $i = 2, \dots, m$, we assume

$$\begin{aligned} U^t(\mathbf{s}_i) \mid Z^{t-1}(\mathbf{s}_i) &\stackrel{\text{ind}}{\sim} \text{Gamma}\left(\alpha + Z^{t-1}(\mathbf{s}_i), \frac{1}{c}\right), \\ Z^{t-1}(\mathbf{s}_i) \mid \{U^{t-1}(\mathbf{s}_j) : j = 1, \dots, m\} &\stackrel{\text{ind}}{\sim} \text{Poisson}\left(\frac{1}{c} \sum_{j=1}^m v_{ij} U^{t-1}(\mathbf{s}_j)\right) \end{aligned} \quad (\text{B.1})$$

independent of $U^t(\mathbf{s}_1) \sim \text{Gamma}(\alpha, \frac{1}{c})$ for some hyperparameter $\alpha > 1$, parameter $c > 0$, and nonnegative weights $\mathbf{V} = \{v_{ij} \geq 0 : i, j = 1, \dots, m\}$ such that $\sum_{j=1}^m v_{ij} > 0$ for all $i = 2, \dots, m$ and $v_{1j} = 0$ for all $j = 1, \dots, m$.

Assume \mathbf{V} satisfies at least one of the two following conditions.

- **Condition 1:** $\sum_{i=1}^m v_{ij} \leq 1$ for all $j = 1, \dots, m$;
- **Condition 2:** $\sum_{j=1}^m v_{ij} \leq 1$ for all $i = 1, \dots, m$.

Then the process $\{U^t(\mathbf{s}_{1:m}) : t = 1, 2, \dots, T\}$ defined above in (B.1) is a stationary process with an invariant distribution as $T \rightarrow \infty$.

Proof of Theorem 2. For any vector $\mathbf{x} = (x_1, \dots, x_m)^T \in \mathbb{R}^m$ such that $x_i \geq 0$ for all $i = 1, \dots, m$, we have

$$\begin{aligned} &\mathbb{E} [\exp \{-\mathbf{x}^T U^t(\mathbf{s}_{1:m})\} \mid U^{t-1}(\mathbf{s}_{1:m})] \\ &= \mathbb{E} (\mathbb{E} [\exp \{-\mathbf{x}^T U^t(\mathbf{s}_{1:m})\} \mid Z^{t-1}(\mathbf{s}_{2:m})] \mid U^{t-1}(\mathbf{s}_{1:m})) \\ &= \mathbb{E} \left(\mathbb{E} [\exp \{-x_1 U^t(\mathbf{s}_1)\}] \times \prod_{i=2}^m \mathbb{E} [\exp \{-x_i U^t(\mathbf{s}_i)\} \mid Z^{t-1}(\mathbf{s}_i)] \mid U^{t-1}(\mathbf{s}_{1:m}) \right) \end{aligned}$$

$$\begin{aligned}
&= \mathbb{E} \left(\frac{1}{(cx_1 + 1)^\alpha} \times \prod_{i=2}^m \frac{1}{(cx_i + 1)^{\alpha + Z^{t-1}(\mathbf{s}_i)}} \mid U^{t-1}(\mathbf{s}_{1:m}) \right) \\
&= \frac{1}{(cx_1 + 1)^\alpha} \times \prod_{i=2}^m \mathbb{E} \left(\frac{1}{(cx_i + 1)^{\alpha + Z^{t-1}(\mathbf{s}_i)}} \mid U^{t-1}(\mathbf{s}_{1:m}) \right) \\
&= \frac{1}{(cx_1 + 1)^\alpha} \times \prod_{i=2}^m \sum_{k=0}^{\infty} \frac{\left(\frac{1}{c} \sum_{j=1}^m v_{ij} U^{t-1}(\mathbf{s}_j) \right)^k}{k!} \exp \left\{ -\frac{1}{c} \sum_{j=1}^m v_{ij} U^{t-1}(\mathbf{s}_j) \right\} \cdot \frac{1}{(cx_i + 1)^{\alpha+k}} \\
&= \prod_{i=1}^m \frac{1}{(cx_i + 1)^\alpha} \times \exp \left\{ -\frac{1}{c} \sum_{j=1}^m v_{ij} U^{t-1}(\mathbf{s}_j) \left[1 - \frac{1}{cx_i + 1} \right] \right\} \\
&= \exp \left\{ -\sum_{j=1}^m \left(\sum_{i=1}^m \frac{x_i v_{ij}}{cx_i + 1} \right) U^{t-1}(\mathbf{s}_j) - \alpha \sum_{i=1}^m \log(cx_i + 1) \right\}. \tag{B.2}
\end{aligned}$$

If we define vector-valued function $a(\mathbf{x}) = \left(\sum_{i=1}^m \frac{x_i v_{i1}}{cx_i + 1}, \dots, \sum_{i=1}^m \frac{x_i v_{im}}{cx_i + 1} \right)^T \in \mathbb{R}^m$ and scalar-valued function $b(\mathbf{x}) = -\alpha \sum_{i=1}^m \log(cx_i + 1) \in \mathbb{R}$, then (2.5) implies

$$\mathbb{E} [\exp \{-\mathbf{x}^T U^t(\mathbf{s}_{1:m})\} \mid U^{t-1}(\mathbf{s}_{1:m})] = \exp \{-a(\mathbf{x})^T U^{t-1}(\mathbf{s}_{1:m}) + b(\mathbf{x})\}.$$

Since $v_{ij} \geq 0$ for all (i, j) and $\sum_{j=1}^m v_{ij} > 0$ for all $i = 2, \dots, m$, $a(\mathbf{x}) \neq \mathbf{0}_{m \times 1}$ for all $\mathbf{x} \in \mathbb{R}^m$ with $x_i \geq 0$ for all i and $\sum_{i=2}^m x_i > 0$. Hence, based on Definition 1 in Darolles et al. (2006), the vector process $\{U^t(\mathbf{s}_{1:m}) : t = 1, 2, \dots\}$ is a temporal compound autoregressive process of order 1 for a fixed m and given spatial locations $\{\mathbf{s}_1, \dots, \mathbf{s}_m\}$. By Proposition 6 in Darolles et al. (2006), the process $\{U^t(\mathbf{s}_{1:m}) : t = 1, 2, \dots\}$ converges to a stationary distribution as $T \rightarrow \infty$ if and only if $\lim_{h \rightarrow \infty} a^{\circ h}(\mathbf{x}) = \mathbf{0}_{m \times 1}$ for all $\mathbf{x} \in \mathbb{R}^m$ with $x_i \geq 0$ for all $i = 1, \dots, m$ and $\sum_{i=2}^m x_i > 0$, where $a^{\circ h}(\mathbf{x})$ represents the function $a(\mathbf{x})$ compounded h times with itself. The rest of the proof is exactly the same as that in Theorem 1. \square

C Simulation Results Complementary to Section 5

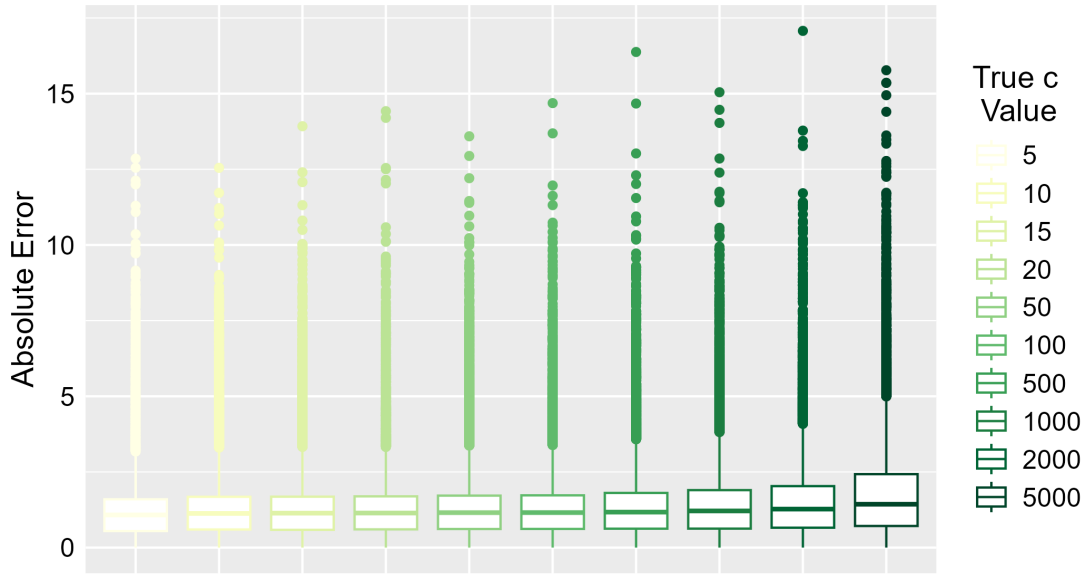


Figure 4: Boxplot: distribution of the mT absolute errors $|y_t(\mathbf{s}_i) - \hat{y}_t(\mathbf{s}_i)|$, where $\hat{y}_t(\mathbf{s}_i)$ denotes the posterior mean in time interval t and spatial location \mathbf{s}_i for each (t, i) , for our model fit with `hypara1` to data simulated from the first simulation group (mentioned at the start of Section 5) and each of the ten true c parameter values.

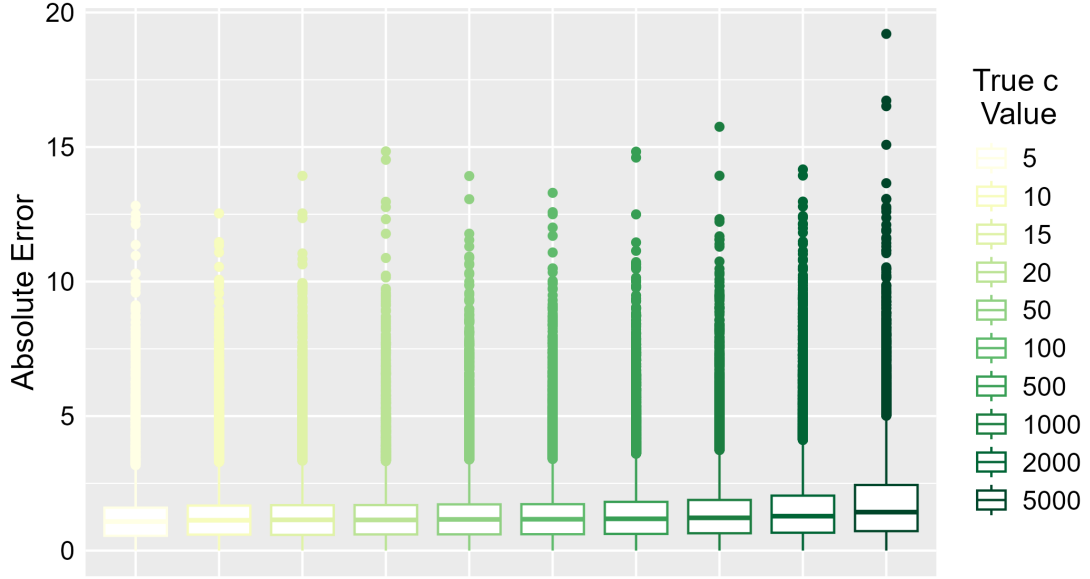


Figure 5: Boxplot: distribution of the mT absolute errors $|y_t(\mathbf{s}_i) - \hat{y}_t(\mathbf{s}_i)|$, where $\hat{y}_t(\mathbf{s}_i)$ denotes the posterior mean in time interval t and spatial location \mathbf{s}_i for each (t, i) , for our model fit with `hypara2` to data simulated from the first simulation group (mentioned at the start of Section 5) and each of the ten true c parameter values.

True c	True $\kappa = 0.35$				True $\kappa = 0.7$			
	2 nd simulation group		3 rd simulation group		2 nd simulation group		3 rd simulation group	
	hypara3	hypara4	hypara3	hypara4	hypara3	hypara4	hypara3	hypara4
$c = 5$	0.739245	0.738330	0.723956	0.721725	1.009475	1.007144	0.942227	0.939763
$c = 10$	0.766734	0.76466	0.750299	0.748261	1.041290	1.040639	0.976482	0.974455
$c = 15$	0.775026	0.773128	0.757853	0.756802	1.049664	1.049141	0.979377	0.978869
$c = 20$	0.779227	0.778088	0.762157	0.760419	1.052398	1.052027	0.987071	0.985950
$c = 50$	0.789033	0.788211	0.774082	0.773347	1.067943	1.06694	1.00299	1.00351
$c = 100$	0.794015	0.794397	0.779964	0.781459	1.074548	1.079313	1.006237	1.007725
$c = 500$	0.818645	0.818356	0.805213	0.800317	1.114351	1.11053	1.039833	1.029073
$c = 1000$	0.847104	0.847053	0.825729	0.831444	1.160870	1.15175	1.08213	1.076918
$c = 2000$	0.894481	0.891117	0.874451	0.880667	1.228211	1.23757	1.139403	1.149787
$c = 5000$	1.018098	1.016191	1.004142	1.00886	1.426702	1.450810	1.324379	1.326022

Table 8: Mean Absolute Error (MAE) for each of the $2 \times 2 \times 2 \times 10 = 80$ simulation settings for the second and the third simulation groups.

True c	True $\kappa = 0.35$				True $\kappa = 0.7$			
	2 nd simulation group		3 rd simulation group		2 nd simulation group		3 rd simulation group	
	hypara3	hypara4	hypara3	hypara4	hypara3	hypara4	hypara3	hypara4
$c = 5$	0.3722	0.3696	0.3399	0.3343	0.7010	0.7003	0.7175	0.7164
$c = 10$	0.3711	0.3680	0.3408	0.3379	0.6990	0.6989	0.7175	0.7171
$c = 15$	0.3699	0.3684	0.3371	0.3357	0.7010	0.7012	0.7103	0.7099
$c = 20$	0.3677	0.3674	0.3431	0.3389	0.6995	0.6991	0.7149	0.7147
$c = 50$	0.3690	0.3662	0.3416	0.3407	0.7000	0.6998	0.7147	0.7152
$c = 100$	0.3696	0.3675	0.3468	0.3468	0.6988	0.6986	0.7142	0.7137
$c = 500$	0.3679	0.3685	0.3426	0.3425	0.6992	0.6992	0.7141	0.7138
$c = 1000$	0.3685	0.3688	0.3417	0.3404	0.6990	0.6993	0.7137	0.7136
$c = 2000$	0.3672	0.3672	0.3399	0.3412	0.6993	0.6993	0.7141	0.7139
$c = 5000$	0.3674	0.3682	0.3410	0.3406	0.6996	0.6993	0.7143	0.7138

Table 9: Mean value of the kept 10^4 posterior samples of the parameter κ for each of the $2 \times 2 \times 2 \times 10 = 80$ simulation settings for the second and the third simulation groups.

True c	True $\kappa = 0.35$				True $\kappa = 0.7$			
	2 nd simulation group		3 rd simulation group		2 nd simulation group		3 rd simulation group	
	hypara3	hypara4	hypara3	hypara4	hypara3	hypara4	hypara3	hypara4
$c = 5$	4.941	4.964	5.217	5.257	5.067	5.081	4.808	4.828
$c = 10$	9.849	9.901	10.414	10.459	10.164	10.170	9.725	9.747
$c = 15$	14.83	14.87	15.75	15.78	15.21	15.20	14.74	14.75
$c = 20$	19.86	19.87	20.85	20.97	20.35	20.38	19.49	19.50
$c = 50$	49.58	49.79	52.20	52.25	50.80	50.87	48.72	48.64
$c = 100$	99.07	99.38	103.31	103.26	102.02	102.1	97.48	97.54
$c = 500$	496.2	495.6	520.4	520.6	509.9	509.8	488.1	488.6
$c = 1000$	991.2	990.9	1042.3	1043.9	1019.9	1019.4	978.1	978.0
$c = 2000$	1987	1987	2089	2086	2037	2038	1954	1955
$c = 5000$	4967	4959	5215	5218	5087	5093	4884	4889

Table 10: Mean value of the kept 10^4 posterior samples of the parameter c for each of the $2 \times 2 \times 2 \times 10 = 80$ simulation settings for the second and the third simulation groups.

		Minimum	1st Quantile	Median	Mean	3rd Quantile	Maximum
Actual $y_t(\mathbf{s}_i)$'s		0.00	11.00	21.00	24.72	34.00	127.00
$U_t(\mathbf{s}_i)$'s	hypara1	0.00	11.92	21.36	24.72	33.93	156.96
	hypara2	0.00	11.92	21.36	24.72	33.93	160.24
c	hypara1	4.743	4.933	4.986	4.987	5.041	5.249
	hypara2	4.654	4.945	4.997	4.997	5.049	5.409
κ	hypara1	0.3673	0.3958	0.4022	0.4023	0.4090	0.4411
	hypara2	0.3682	0.3966	0.4030	0.4030	0.4092	0.4383
ρ	hypara1	0.3662	0.3975	0.4041	0.4040	0.4104	0.4406
	hypara2	0.3671	0.3970	0.4030	0.4031	0.4094	0.4387

Table 11: Summary statistics of the actual observed counts $y_{1:T}(\mathbf{s}_{1:m})$ and the kept 10^4 posterior samples of the parameters $c, \kappa, \rho, U_{1:T}(\mathbf{s}_{1:m})$ for hyperparameter specifications **hypara1** and **hypara2** with true parameter values $(\kappa, \rho, c) = (0.4, 0.4, 5)$ and undirected spatial locations from the first simulation group.

		Minimum	1st Quantile	Median	Mean	3rd Quantile	Maximum
Actual $y_t(\mathbf{s}_i)$'s		0.00	23.00	42.00	49.46	68.00	258.00
$U_t(\mathbf{s}_i)$'s	hypara1	0.00	23.88	42.73	49.46	67.79	315.09
	hypara2	0.00	23.88	42.73	49.46	67.79	317.33
c	hypara1	9.405	9.834	9.934	9.936	10.034	10.656
	hypara2	9.413	9.853	9.946	9.949	10.043	10.480
κ	hypara1	0.3660	0.3970	0.4031	0.4031	0.4092	0.4396
	hypara2	0.3630	0.3963	0.4025	0.4025	0.4086	0.4393
ρ	hypara1	0.3726	0.3975	0.4034	0.4035	0.4096	0.4376
	hypara2	0.3636	0.3978	0.4042	0.4040	0.4102	0.4371

Table 12: Summary statistics of the actual observed counts $y_{1:T}(\mathbf{s}_{1:m})$ and the kept 10^4 posterior samples of the parameters $c, \kappa, \rho, U_{1:T}(\mathbf{s}_{1:m})$ for hyperparameter specifications **hypara1** and **hypara2** with true parameter values $(\kappa, \rho, c) = (0.4, 0.4, 10)$ and undirected spatial locations from the first simulation group.

		Minimum	1st Quantile	Median	Mean	3rd Quantile	Maximum
Actual $y_t(\mathbf{s}_i)$'s		0.00	35.00	64.00	74.13	102.00	382.00
$U_t(\mathbf{s}_i)$'s	hypara1	0.00	35.87	64.03	74.13	101.36	459.63
	hypara2	0.00	35.87	64.03	74.13	101.36	443.33
c	hypara1	14.19	14.75	14.91	14.91	15.06	15.69
	hypara2	14.07	14.77	14.93	14.92	15.08	15.67
κ	hypara1	0.3722	0.4027	0.4088	0.4088	0.4151	0.4412
	hypara2	0.3715	0.4010	0.4076	0.4074	0.4138	0.4418
ρ	hypara1	0.3604	0.3919	0.3976	0.3979	0.4039	0.4348
	hypara2	0.3645	0.3928	0.3990	0.3991	0.4054	0.4287

Table 13: Summary statistics of the actual observed counts $y_{1:T}(\mathbf{s}_{1:m})$ and the kept 10^4 posterior samples of the parameters $c, \kappa, \rho, U_{1:T}(\mathbf{s}_{1:m})$ for hyperparameter specifications **hypara1** and **hypara2** with true parameter values $(\kappa, \rho, c) = (0.4, 0.4, 15)$ and undirected spatial locations from the first simulation group.

		Minimum	1st Quantile	Median	Mean	3rd Quantile	Maximum
Actual $y_t(\mathbf{s}_i)$'s		0.00	47.00	85.00	98.84	135.00	517.00
$U_t(\mathbf{s}_i)$'s	hypara1	0.00	47.56	85.25	98.84	135.15	596.63
	hypara2	0.00	47.55	85.25	98.84	135.15	604.63
c	hypara1	18.91	19.70	19.88	19.89	20.08	21.29
	hypara2	18.90	19.68	19.87	19.87	20.06	20.95
κ	hypara1	0.3728	0.3998	0.4068	0.4064	0.4132	0.4402
	hypara2	0.3748	0.4008	0.4070	0.4072	0.4134	0.4432
ρ	hypara1	0.3682	0.3937	0.3998	0.4001	0.4063	0.4357
	hypara2	0.3642	0.3933	0.3995	0.3995	0.4058	0.4320

Table 14: Summary statistics of the actual observed counts $y_{1:T}(\mathbf{s}_{1:m})$ and the kept 10^4 posterior samples of the parameters $c, \kappa, \rho, U_{1:T}(\mathbf{s}_{1:m})$ for hyperparameter specifications **hypara1** and **hypara2** with true parameter values $(\kappa, \rho, c) = (0.4, 0.4, 20)$ and undirected spatial locations from the first simulation group.

		Minimum	1st Quantile	Median	Mean	3rd Quantile	Maximum
Actual $y_t(\mathbf{s}_i)$'s		0.0	118.0	213.0	247.1	338.0	1282.0
$U_t(\mathbf{s}_i)$'s	hypara1	0.0	118.6	213.2	247.1	338.8	1405.3
	hypara2	0.0	118.6	213.2	247.1	338.8	1418.8
c	hypara1	47.18	49.37	49.84	49.86	50.33	52.88
	hypara2	47.24	49.35	49.84	49.84	50.33	52.37
κ	hypara1	0.3713	0.3999	0.4060	0.4061	0.4121	0.4390
	hypara2	0.3765	0.4007	0.4068	0.4069	0.4132	0.4390
ρ	hypara1	0.3643	0.3938	0.3999	0.3998	0.4060	0.4304
	hypara2	0.3679	0.3931	0.3992	0.3991	0.4051	0.4313

Table 15: Summary statistics of the actual observed counts $y_{1:T}(\mathbf{s}_{1:m})$ and the kept 10^4 posterior samples of the parameters $c, \kappa, \rho, U_{1:T}(\mathbf{s}_{1:m})$ for the two hyperparameter specifications (**hypara1** and **hypara2**) when the true parameter values are $(\kappa, \rho, c) = (0.4, 0.4, 50)$ and the spatial locations are undirected from the first simulation group.

		Minimum	1st Quantile	Median	Mean	3rd Quantile	Maximum
Actual $y_t(\mathbf{s}_i)$'s		0.0	237.0	426.0	494.2	674.0	2454.0
$U_t(\mathbf{s}_i)$'s	hypara1	0.0	237.9	426.5	494.2	675.2	2631.5
	hypara2	0.0	237.9	426.5	494.2	675.2	2637.0
c	hypara1	94.82	98.58	99.56	99.57	100.55	105.36
	hypara2	94.58	98.55	99.48	99.53	100.50	104.58
κ	hypara1	0.3696	0.3999	0.4063	0.4061	0.4125	0.4369
	hypara2	0.3733	0.4008	0.4067	0.4068	0.4128	0.4387
ρ	hypara1	0.3685	0.3941	0.4000	0.4002	0.4059	0.4332
	hypara2	0.3653	0.3937	0.3995	0.3995	0.4052	0.4318

Table 16: Summary statistics of the actual observed counts $y_{1:T}(\mathbf{s}_{1:m})$ and the kept 10^4 posterior samples of the parameters $c, \kappa, \rho, U_{1:T}(\mathbf{s}_{1:m})$ for hyperparameter specifications **hypara1** and **hypara2** with true parameter values $(\kappa, \rho, c) = (0.4, 0.4, 100)$ and undirected spatial locations from the first simulation group.

		Minimum	1st Quantile	Median	Mean	3rd Quantile	Maximum
Actual $y_t(\mathbf{s}_i)$'s		0	1188	2130	2471	3378	12125
$U_t(\mathbf{s}_i)$'s	hypara1	0	1189	2129	2471	3378	12547
	hypara2	0	1189	2129	2471	3378	12556
c	hypara1	470.3	492.3	497.3	497.5	502.5	525.9
	hypara2	466.7	492.8	497.7	497.7	502.6	531.9
κ	hypara1	0.3697	0.4005	0.4066	0.4065	0.4127	0.4417
	hypara2	0.3710	0.4001	0.4062	0.4062	0.4123	0.4374
ρ	hypara1	0.3658	0.3940	0.3999	0.3999	0.4058	0.4371
	hypara2	0.3715	0.3942	0.4000	0.4001	0.4058	0.4338

Table 17: Summary statistics of the actual observed counts $y_{1:T}(\mathbf{s}_{1:m})$ and the kept 10^4 posterior samples of the parameters $c, \kappa, \rho, U_{1:T}(\mathbf{s}_{1:m})$ for hyperparameter specifications **hypara1** and **hypara2** with true parameter values $(\kappa, \rho, c) = (0.4, 0.4, 500)$ and undirected spatial locations from the first simulation group.

		Minimum	1st Quantile	Median	Mean	3rd Quantile	Maximum
Actual $y_t(\mathbf{s}_i)$'s		1	2369	4252	4941	6736	24221
$U_t(\mathbf{s}_i)$'s	hypara1	0.019	2373.657	4255.920	4941.258	6739.421	24875.179
	hypara2	0.008	2373.594	4255.815	4941.266	6739.462	24775.287
c	hypara1	945.6	986.8	997.2	996.9	1007.2	1044.5
	hypara2	937.7	985.6	994.8	994.9	1004.0	1046.7
κ	hypara1	0.3727	0.4007	0.4066	0.4067	0.4128	0.4399
	hypara2	0.3755	0.4009	0.4072	0.4073	0.4134	0.4400
ρ	hypara1	0.3672	0.3935	0.3993	0.3993	0.4052	0.4348
	hypara2	0.3696	0.3930	0.3992	0.3991	0.4053	0.4260

Table 18: Summary statistics of the actual observed counts $y_{1:T}(\mathbf{s}_{1:m})$ and the kept 10^4 posterior samples of the parameters $c, \kappa, \rho, U_{1:T}(\mathbf{s}_{1:m})$ for hyperparameter specifications **hypara1** and **hypara2** with true parameter values $(\kappa, \rho, c) = (0.4, 0.4, 1000)$ and undirected spatial locations from the first simulation group.

		Minimum	1st Quantile	Median	Mean	3rd Quantile	Maximum
Actual $y_t(\mathbf{s}_i)$'s		5	4767	8529	9882	13464	48245
$U_t(\mathbf{s}_i)$'s	hypara1	0.63	4756.08	8533.04	9882.26	13479.89	49040.28
	hypara2	0.82	4756.05	8533.17	9882.24	13479.89	49053.01
c	hypara1	1886	1971	1990	1990	2009	2100
	hypara2	1904	1974	1994	1994	2013	2105
κ	hypara1	0.3673	0.3999	0.4061	0.4061	0.4123	0.4407
	hypara2	0.3702	0.4006	0.4072	0.4072	0.4138	0.4389
ρ	hypara1	0.3694	0.3941	0.4000	0.4001	0.4062	0.4398
	hypara2	0.3634	0.3927	0.3989	0.3989	0.4051	0.4328

Table 19: Summary statistics of the actual observed counts $y_{1:T}(\mathbf{s}_{1:m})$ and the kept 10^4 posterior samples of the parameters $c, \kappa, \rho, U_{1:T}(\mathbf{s}_{1:m})$ for hyperparameter specifications **hypara1** and **hypara2** with true parameter values $(\kappa, \rho, c) = (0.4, 0.4, 2000)$ and undirected spatial locations from the first simulation group.

		Minimum	1st Quantile	Median	Mean	3rd Quantile	Maximum
Actual $y_t(\mathbf{s}_i)$'s		11	11893	21324	24706	33732	121817
$U_t(\mathbf{s}_i)$'s	hypara1	3.52	11889.96	21319.67	24706.13	33733.67	123024.56
	hypara2	2.17	11890.13	21319.76	24706.12	33733.53	123114.89
c	hypara1	4730	4933	4981	4983	5033	5258
	hypara2	4736	4926	4972	4973	5020	5244
κ	hypara1	0.3788	0.4012	0.4074	0.4072	0.4133	0.4432
	hypara2	0.3727	0.4003	0.4064	0.4064	0.4125	0.4380
ρ	hypara1	0.3594	0.3933	0.3988	0.3989	0.4047	0.4283
	hypara2	0.3672	0.3939	0.4000	0.3999	0.4058	0.4338

Table 20: Summary statistics of the actual observed counts $y_{1:T}(\mathbf{s}_{1:m})$ and the kept 10^4 posterior samples of the parameters $c, \kappa, \rho, U_{1:T}(\mathbf{s}_{1:m})$ for hyperparameter specifications **hypara1** and **hypara2** with true parameter values $(\kappa, \rho, c) = (0.4, 0.4, 5000)$ and undirected spatial locations from the first simulation group.

		Minimum	1st Quantile	Median	Mean	3rd Quantile	Maximum
Actual $y_t(\mathbf{s}_i)$'s		0.00	7.00	14.00	16.56	23.00	92.00
$U_t(\mathbf{s}_i)$'s	hypara3	0.000	7.261	14.010	16.557	23.091	122.156
	hypara4	0.000	7.258	14.009	16.557	23.093	116.952
c	hypara3	4.725	5.008	5.065	5.067	5.124	5.448
	hypara4	4.743	5.019	5.080	5.081	5.143	5.430
κ	hypara3	0.6682	0.6961	0.7010	0.7010	0.7061	0.7317
	hypara4	0.6732	0.6951	0.7002	0.7003	0.7054	0.7312

Table 21: Summary statistics of the actual observed counts $y_{1:T}(\mathbf{s}_{1:m})$ and the kept 10^4 posterior samples of the parameters $c, \kappa, U_{1:T}(\mathbf{s}_{1:m})$ for the two hyperparameter specifications (hypara3 and hypara4) when the true parameter values are $(\kappa, c) = (0.7, 5)$ and the spatial locations are undirected from the second simulation group.

		Minimum	1st Quantile	Median	Mean	3rd Quantile	Maximum
Actual $y_t(\mathbf{s}_i)$'s		0.00	14.00	28.00	33.11	46.00	181.00
$U_t(\mathbf{s}_i)$'s	hypara3	0.00	14.50	27.98	33.11	46.12	222.57
	hypara4	0.00	14.50	27.99	33.11	46.12	221.75
c	hypara3	9.455	10.051	10.162	10.164	10.275	10.819
	hypara4	9.657	10.053	10.170	10.170	10.283	10.791
κ	hypara3	0.6717	0.6941	0.6990	0.6990	0.7040	0.7281
	hypara4	0.6720	0.6941	0.6989	0.6989	0.7038	0.7244

Table 22: Summary statistics of the actual observed counts $y_{1:T}(\mathbf{s}_{1:m})$ and the kept 10^4 posterior samples of the parameters $c, \kappa, U_{1:T}(\mathbf{s}_{1:m})$ for the two hyperparameter specifications (hypara3 and hypara4) when the true parameter values are $(\kappa, c) = (0.7, 10)$ and the spatial locations are undirected from the second simulation group.

		Minimum	1st Quantile	Median	Mean	3rd Quantile	Maximum
Actual $y_t(\mathbf{s}_i)$'s		0.0	21.0	42.0	49.8	70.0	287.0
$U_t(\mathbf{s}_i)$'s	hypara3	0.00	21.94	42.29	49.80	69.36	342.79
	hypara4	0.00	21.94	42.29	49.80	69.36	341.63
c	hypara3	14.30	15.04	15.21	15.21	15.38	16.24
	hypara4	14.25	15.04	15.21	15.20	15.37	16.22
κ	hypara3	0.6732	0.6961	0.7010	0.7010	0.7058	0.7284
	hypara4	0.6737	0.6964	0.7012	0.7012	0.7060	0.7265

Table 23: Summary statistics of the actual observed counts $y_{1:T}(\mathbf{s}_{1:m})$ and the kept 10^4 posterior samples of the parameters $c, \kappa, U_{1:T}(\mathbf{s}_{1:m})$ for the two hyperparameter specifications (hypara3 and hypara4) when the true parameter values are $(\kappa, c) = (0.7, 15)$ and the spatial locations are undirected from the second simulation group.

		Minimum	1st Quantile	Median	Mean	3rd Quantile	Maximum
Actual $y_t(\mathbf{s}_i)$'s		0.00	28.00	56.00	66.32	92.00	381.00
$U_t(\mathbf{s}_i)$'s	hypara3	0.00	29.06	56.08	66.32	92.60	440.38
	hypara4	0.00	29.06	56.08	66.32	92.61	444.60
c	hypara3	19.27	20.13	20.35	20.35	20.57	21.66
	hypara4	19.13	20.16	20.38	20.38	20.60	21.73
κ	hypara3	0.6719	0.6947	0.6994	0.6995	0.7044	0.7262
	hypara4	0.6714	0.6942	0.6991	0.6991	0.7040	0.7283

Table 24: Summary statistics of the actual observed counts $y_{1:T}(\mathbf{s}_{1:m})$ and the kept 10^4 posterior samples of the parameters $c, \kappa, U_{1:T}(\mathbf{s}_{1:m})$ for the two hyperparameter specifications (hypara3 and hypara4) when the true parameter values are $(\kappa, c) = (0.7, 20)$ and the spatial locations are undirected from the second simulation group.

		Minimum	1st Quantile	Median	Mean	3rd Quantile	Maximum
Actual $y_t(\mathbf{s}_i)$'s		0.0	72.0	140.0	165.8	233.0	976.0
$U_t(\mathbf{s}_i)$'s	hypara3	0.00	73.22	140.37	165.75	232.27	1081.72
	hypara4	0.00	73.22	140.37	165.75	232.27	1102.49
c	hypara3	48.10	50.23	50.79	50.80	51.33	53.55
	hypara4	47.44	50.34	50.87	50.87	51.40	54.16
κ	hypara3	0.6718	0.6952	0.7001	0.7000	0.7048	0.7295
	hypara4	0.6732	0.6949	0.6998	0.6998	0.7046	0.7304

Table 25: Summary statistics of the actual observed counts $y_{1:T}(\mathbf{s}_{1:m})$ and the kept 10^4 posterior samples of the parameters $c, \kappa, U_{1:T}(\mathbf{s}_{1:m})$ for the two hyperparameter specifications (hypara3 and hypara4) when the true parameter values are $(\kappa, c) = (0.7, 50)$ and the spatial locations are undirected from the second simulation group.

		Minimum	1st Quantile	Median	Mean	3rd Quantile	Maximum
Actual $y_t(\mathbf{s}_i)$'s		0.0	145.0	279.0	331.8	463.0	1936.0
$U_t(\mathbf{s}_i)$'s	hypara3	0.0	145.7	280.3	331.8	462.9	2094.2
	hypara4	0.0	145.7	280.3	331.8	462.9	2109.4
c	hypara3	96.44	100.96	101.99	102.02	103.06	107.52
	hypara4	95.7	101.0	102.0	102.1	103.1	108.6
κ	hypara3	0.6717	0.6940	0.6989	0.6988	0.7037	0.7237
	hypara4	0.6722	0.6938	0.6986	0.6986	0.7035	0.7292

Table 26: Summary statistics of the actual observed counts $y_{1:T}(\mathbf{s}_{1:m})$ and the kept 10^4 posterior samples of the parameters $c, \kappa, U_{1:T}(\mathbf{s}_{1:m})$ for the two hyperparameter specifications (hypara3 and hypara4) when the true parameter values are $(\kappa, c) = (0.7, 100)$ and the spatial locations are undirected from the second simulation group.

		Minimum	1st Quantile	Median	Mean	3rd Quantile	Maximum
Actual $y_t(\mathbf{s}_i)$'s		0	725	1401	1659	2327	9047
$U_t(\mathbf{s}_i)$'s	hypara3	0.0	726.5	1402.4	1658.8	2324.5	9380.4
	hypara4	0.0	726.6	1402.3	1658.8	2324.5	9428.0
c	hypara3	481.8	504.6	509.8	509.9	515.1	539.0
	hypara4	484.4	504.4	509.8	509.8	515.0	541.7
κ	hypara3	0.6730	0.6944	0.6992	0.6992	0.7040	0.7293
	hypara4	0.6676	0.6943	0.6992	0.6992	0.7041	0.7245

Table 27: Summary statistics of the actual observed counts $y_{1:T}(\mathbf{s}_{1:m})$ and the kept 10^4 posterior samples of the parameters $c, \kappa, U_{1:T}(\mathbf{s}_{1:m})$ for the two hyperparameter specifications (hypara3 and hypara4) when the true parameter values are $(\kappa, c) = (0.7, 500)$ and the spatial locations are undirected from the second simulation group.

		Minimum	1st Quantile	Median	Mean	3rd Quantile	Maximum
Actual $y_t(\mathbf{s}_i)$'s		0	1451	2814	3318	4644	18528
$U_t(\mathbf{s}_i)$'s	hypara3	0	1451	2809	3318	4644	19012
	hypara4	0	1451	2809	3318	4644	18996
c	hypara3	964.3	1009.6	1019.7	1019.9	1029.9	1081.7
	hypara4	964.8	1009.2	1019.2	1019.4	1029.3	1078.8
κ	hypara3	0.6718	0.6943	0.6991	0.6990	0.7038	0.7289
	hypara4	0.6735	0.6944	0.6992	0.6993	0.7041	0.7235

Table 28: Summary statistics of the actual observed counts $y_{1:T}(\mathbf{s}_{1:m})$ and the kept 10^4 posterior samples of the parameters $c, \kappa, U_{1:T}(\mathbf{s}_{1:m})$ for the two hyperparameter specifications (hypara3 and hypara4) when the true parameter values are $(\kappa, c) = (0.7, 1000)$ and the spatial locations are undirected from the second simulation group.

		Minimum	1st Quantile	Median	Mean	3rd Quantile	Maximum
Actual $y_t(\mathbf{s}_i)$'s		1	2909	5608	6636	9279	36824
$U_t(\mathbf{s}_i)$'s	hypara3	0.02	2906.28	5611.68	6635.58	9283.75	37839.95
	hypara4	0.01	2906.44	5611.76	6635.57	9283.54	37524.77
c	hypara3	1914	2017	2036	2037	2057	2170
	hypara4	1922	2017	2038	2038	2059	2136
κ	hypara3	0.6704	0.6946	0.6994	0.6993	0.7041	0.7252
	hypara4	0.6731	0.6944	0.6993	0.6993	0.7041	0.7265

Table 29: Summary statistics of the actual observed counts $y_{1:T}(\mathbf{s}_{1:m})$ and the kept 10^4 posterior samples of the parameters $c, \kappa, U_{1:T}(\mathbf{s}_{1:m})$ for the two hyperparameter specifications (hypara3 and hypara4) when the true parameter values are $(\kappa, c) = (0.7, 2000)$ and the spatial locations are undirected from the second simulation group.

		Minimum	1st Quantile	Median	Mean	3rd Quantile	Maximum
Actual $y_t(\mathbf{s}_i)$'s		5	7286	14010	16589	23207	92135
$U_t(\mathbf{s}_i)$'s	hypara3	0.68	7274.32	14023.42	16588.77	23197.09	93506.65
	hypara4	0.81	7274.13	14023.49	16588.73	23197.07	93122.49
c	hypara3	4803	5035	5087	5087	5139	5353
	hypara4	4836	5041	5092	5093	5146	5396
κ	hypara3	0.6716	0.6949	0.6997	0.6996	0.7044	0.7246
	hypara4	0.6695	0.6944	0.6993	0.6993	0.7041	0.7259

Table 30: Summary statistics of the actual observed counts $y_{1:T}(\mathbf{s}_{1:m})$ and the kept 10^4 posterior samples of the parameters $c, \kappa, U_{1:T}(\mathbf{s}_{1:m})$ for the two hyperparameter specifications (hypara3 and hypara4) when the true parameter values are $(\kappa, c) = (0.7, 5000)$ and the spatial locations are undirected from the second simulation group.

		Minimum	1st Quantile	Median	Mean	3rd Quantile	Maximum
Actual $y_t(\mathbf{s}_i)$'s		0.000	2.000	6.000	7.829	11.000	63.000
$U_t(\mathbf{s}_i)$'s	hypara3	0.000	2.431	5.701	7.829	10.994	87.799
	hypara4	0.000	2.430	5.700	7.829	10.993	89.944
c	hypara3	4.472	4.850	4.938	4.941	5.030	5.416
	hypara4	4.511	4.874	4.961	4.964	5.049	5.569
κ	hypara3	0.3089	0.3604	0.3722	0.3722	0.3841	0.4362
	hypara4	0.3047	0.3585	0.3698	0.3696	0.3811	0.4336

Table 31: Summary statistics of the actual observed counts $y_{1:T}(\mathbf{s}_{1:m})$ and the kept 10^4 posterior samples of the parameters $c, \kappa, U_{1:T}(\mathbf{s}_{1:m})$ for the two hyperparameter specifications (hypara3 and hypara4) when the true parameter values are $(\kappa, c) = (0.35, 5)$ and the spatial locations are undirected from the second simulation group.

		Minimum	1st Quantile	Median	Mean	3rd Quantile	Maximum
Actual $y_t(\mathbf{s}_i)$'s		0.00	4.00	11.00	15.59	22.00	135.00
$U_t(\mathbf{s}_i)$'s	hypara3	0.000	4.828	11.338	15.589	21.872	175.830
	hypara4	0.000	4.826	11.338	15.589	21.873	170.927
c	hypara3	9.005	9.673	9.844	9.849	10.024	10.819
	hypara4	9.168	9.725	9.890	9.901	10.062	11.089
κ	hypara3	0.3100	0.3598	0.3711	0.3711	0.3824	0.4283
	hypara4	0.3005	0.3575	0.3686	0.3680	0.3792	0.4226

Table 32: Summary statistics of the actual observed counts $y_{1:T}(\mathbf{s}_{1:m})$ and the kept 10^4 posterior samples of the parameters $c, \kappa, U_{1:T}(\mathbf{s}_{1:m})$ for the two hyperparameter specifications (hypara3 and hypara4) when the true parameter values are $(\kappa, c) = (0.35, 10)$ and the spatial locations are undirected from the second simulation group.

		Minimum	1st Quantile	Median	Mean	3rd Quantile	Maximum
Actual $y_t(\mathbf{s}_i)$'s		0.00	7.00	17.00	23.43	33.00	184.00
$U_t(\mathbf{s}_i)$'s	hypara3	0.000	7.277	17.021	23.430	32.701	232.022
	hypara4	0.000	7.276	17.020	23.432	32.705	233.137
c	hypara3	13.47	14.58	14.83	14.83	15.07	16.38
	hypara4	13.55	14.61	14.86	14.87	15.12	16.22
κ	hypara3	0.3102	0.3594	0.3704	0.3699	0.3809	0.4235
	hypara4	0.3078	0.3580	0.3688	0.3684	0.3794	0.4218

Table 33: Summary statistics of the actual observed counts $y_{1:T}(\mathbf{s}_{1:m})$ and the kept 10^4 posterior samples of the parameters $c, \kappa, U_{1:T}(\mathbf{s}_{1:m})$ for the two hyperparameter specifications (hypara3 and hypara4) when the true parameter values are $(\kappa, c) = (0.35, 15)$ and the spatial locations are undirected from the second simulation group.

		Minimum	1st Quantile	Median	Mean	3rd Quantile	Maximum
Actual $y_t(\mathbf{s}_i)$'s		0.00	9.00	22.00	31.26	43.00	246.00
$U_t(\mathbf{s}_i)$'s	hypara3	0.000	9.672	22.692	31.255	43.562	304.002
	hypara4	0.000	9.669	22.692	31.255	43.562	301.296
c	hypara3	17.81	19.52	19.86	19.86	20.20	21.58
	hypara4	18.30	19.53	19.85	19.87	20.19	21.81
κ	hypara3	0.3155	0.3568	0.3678	0.3677	0.3786	0.4340
	hypara4	0.3059	0.3570	0.3679	0.3674	0.3782	0.4232

Table 34: Summary statistics of the actual observed counts $y_{1:T}(\mathbf{s}_{1:m})$ and the kept 10^4 posterior samples of the parameters $c, \kappa, U_{1:T}(\mathbf{s}_{1:m})$ for the two hyperparameter specifications (hypara3 and hypara4) when the true parameter values are $(\kappa, c) = (0.35, 20)$ and the spatial locations are undirected from the second simulation group.

		Minimum	1st Quantile	Median	Mean	3rd Quantile	Maximum
Actual $y_t(\mathbf{s}_i)$'s		0.00	24.00	57.00	78.22	109.00	604.00
$U_t(\mathbf{s}_i)$'s	hypara3	0.00	24.16	56.96	78.22	109.14	692.00
	hypara4	0.00	24.16	56.96	78.22	109.14	687.09
c	hypara3	44.94	48.83	49.55	49.58	50.33	54.34
	hypara4	45.71	49.00	49.77	49.79	50.53	54.50
κ	hypara3	0.3062	0.3594	0.3694	0.3690	0.3793	0.4321
	hypara4	0.3035	0.3564	0.3665	0.3662	0.3764	0.4174

Table 35: Summary statistics of the actual observed counts $y_{1:T}(\mathbf{s}_{1:m})$ and the kept 10^4 posterior samples of the parameters $c, \kappa, U_{1:T}(\mathbf{s}_{1:m})$ for the two hyperparameter specifications (hypara3 and hypara4) when the true parameter values are $(\kappa, c) = (0.35, 50)$ and the spatial locations are undirected from the second simulation group.

		Minimum	1st Quantile	Median	Mean	3rd Quantile	Maximum
Actual $y_t(\mathbf{s}_i)$'s		0.0	47.0	114.0	156.4	218.0	1176.0
$U_t(\mathbf{s}_i)$'s	hypara3	0.00	47.94	114.01	156.36	217.71	1314.87
	hypara4	0.00	47.94	114.02	156.36	217.72	1302.91
c	hypara3	91.18	97.44	99.02	99.07	100.65	107.99
	hypara4	92.23	97.75	99.33	99.38	100.86	109.62
κ	hypara3	0.3092	0.3593	0.3700	0.3696	0.3802	0.4243
	hypara4	0.3070	0.3578	0.3680	0.3675	0.3779	0.4164

Table 36: Summary statistics of the actual observed counts $y_{1:T}(\mathbf{s}_{1:m})$ and the kept 10^4 posterior samples of the parameters $c, \kappa, U_{1:T}(\mathbf{s}_{1:m})$ for the two hyperparameter specifications (hypara3 and hypara4) when the true parameter values are $(\kappa, c) = (0.35, 100)$ and the spatial locations are undirected from the second simulation group.

		Minimum	1st Quantile	Median	Mean	3rd Quantile	Maximum
Actual $y_t(\mathbf{s}_i)$'s		0.0	241.0	569.5	781.4	1091.0	5862.0
$U_t(\mathbf{s}_i)$'s	hypara3	0.0	240.8	569.2	781.4	1089.8	6162.7
	hypara4	0.0	240.8	569.2	781.4	1089.7	6130.4
c	hypara3	456.6	488.3	495.7	496.2	503.9	548.7
	hypara4	457.1	488.1	495.6	495.6	502.9	538.8
κ	hypara3	0.3070	0.3580	0.3683	0.3679	0.3782	0.4190
	hypara4	0.3148	0.3589	0.3687	0.3685	0.3781	0.4273

Table 37: Summary statistics of the actual observed counts $y_{1:T}(\mathbf{s}_{1:m})$ and the kept 10^4 posterior samples of the parameters $c, \kappa, U_{1:T}(\mathbf{s}_{1:m})$ for the two hyperparameter specifications (hypara3 and hypara4) when the true parameter values are $(\kappa, c) = (0.35, 500)$ and the spatial locations are undirected from the second simulation group.

		Minimum	1st Quantile	Median	Mean	3rd Quantile	Maximum
Actual $y_t(\mathbf{s}_i)$'s		0	480	1137	1562	2178	11699
$U_t(\mathbf{s}_i)$'s	hypara3	0.0	479.9	1138.1	1562.5	2177.0	12164.6
	hypara4	0.0	479.9	1138.1	1562.5	2177.0	12094.0
c	hypara3	912.7	975.2	991.0	991.2	1006.4	1111.3
	hypara4	908.1	975.8	990.4	990.9	1005.4	1097.2
κ	hypara3	0.2967	0.3583	0.3687	0.3685	0.3790	0.4226
	hypara4	0.3046	0.3594	0.3690	0.3688	0.3785	0.4316

Table 38: Summary statistics of the actual observed counts $y_{1:T}(\mathbf{s}_{1:m})$ and the kept 10^4 posterior samples of the parameters $c, \kappa, U_{1:T}(\mathbf{s}_{1:m})$ for the two hyperparameter specifications (hypara3 and hypara4) when the true parameter values are $(\kappa, c) = (0.35, 1000)$ and the spatial locations are undirected from the second simulation group.

		Minimum	1st Quantile	Median	Mean	3rd Quantile	Maximum
Actual $y_t(\mathbf{s}_i)$'s		0	964	2279	3126	4364	23165
$U_t(\mathbf{s}_i)$'s	hypara3	0.0	961.2	2277.8	3125.6	4361.2	23735.7
	hypara4	0.0	961.2	2277.7	3125.6	4361.1	23786.4
c	hypara3	1823	1955	1985	1987	2018	2173
	hypara4	1828	1957	1987	1987	2017	2142
κ	hypara3	0.3044	0.3571	0.3678	0.3672	0.3778	0.4208
	hypara4	0.3181	0.3574	0.3671	0.3672	0.3768	0.4270

Table 39: Summary statistics of the actual observed counts $y_{1:T}(\mathbf{s}_{1:m})$ and the kept 10^4 posterior samples of the parameters $c, \kappa, U_{1:T}(\mathbf{s}_{1:m})$ for the two hyperparameter specifications (hypara3 and hypara4) when the true parameter values are $(\kappa, c) = (0.35, 2000)$ and the spatial locations are undirected from the second simulation group.

		Minimum	1st Quantile	Median	Mean	3rd Quantile	Maximum
Actual $y_t(\mathbf{s}_i)$'s		0	2407	5694	7814	10878	58052
$U_t(\mathbf{s}_i)$'s	hypara3	0	2403	5695	7814	10881	59029
	hypara4	0	2403	5695	7814	10881	58955
c	hypara3	4575	4884	4964	4967	5045	5428
	hypara4	4533	4879	4958	4959	5036	5496
κ	hypara3	0.3060	0.3574	0.3677	0.3674	0.3778	0.4168
	hypara4	0.2977	0.3577	0.3681	0.3682	0.3787	0.4184

Table 40: Summary statistics of the actual observed counts $y_{1:T}(\mathbf{s}_{1:m})$ and the kept 10^4 posterior samples of the parameters $c, \kappa, U_{1:T}(\mathbf{s}_{1:m})$ for the two hyperparameter specifications (hypara3 and hypara4) when the true parameter values are $(\kappa, c) = (0.35, 5000)$ and the spatial locations are undirected from the second simulation group.

		Minimum	1st Quantile	Median	Mean	3rd Quantile	Maximum
Actual $y_t(\mathbf{s}_i)$'s		0.00	5.00	11.00	13.73	19.00	74.00
$U_t(\mathbf{s}_i)$'s	hypara3	0.000	5.488	11.206	13.734	19.178	101.142
	hypara4	0.000	5.486	11.206	13.734	19.180	100.537
c	hypara3	4.514	4.750	4.809	4.808	4.865	5.178
	hypara4	4.535	4.769	4.826	4.828	4.885	5.173
κ	hypara3	0.6746	0.7113	0.7176	0.7175	0.7237	0.7505
	hypara4	0.6754	0.7102	0.7165	0.7164	0.7226	0.7490

Table 41: Summary statistics of the actual observed counts $y_{1:T}(\mathbf{s}_{1:m})$ and the kept 10^4 posterior samples of the parameters $c, \kappa, U_{1:T}(\mathbf{s}_{1:m})$ for the two hyperparameter specifications (hypara3 and hypara4) when the true parameter values are $(\kappa, c) = (0.7, 5)$ and the spatial locations are directed from the third simulation group.

		Minimum	1st Quantile	Median	Mean	3rd Quantile	Maximum
Actual $y_t(\mathbf{s}_i)$'s		0.00	11.00	22.00	27.51	39.00	166.00
$U_t(\mathbf{s}_i)$'s	hypara3	0.00	10.95	22.37	27.51	38.53	208.85
	hypara4	0.00	10.95	22.37	27.51	38.53	212.36
c	hypara3	9.175	9.616	9.729	9.725	9.833	10.395
	hypara4	9.164	9.638	9.744	9.747	9.856	10.338
κ	hypara3	0.6868	0.7117	0.7176	0.7175	0.7234	0.7511
	hypara4	0.6846	0.7111	0.7171	0.7171	0.7230	0.7488

Table 42: Summary statistics of the actual observed counts $y_{1:T}(\mathbf{s}_{1:m})$ and the kept 10^4 posterior samples of the parameters $c, \kappa, U_{1:T}(\mathbf{s}_{1:m})$ for the two hyperparameter specifications (hypara3 and hypara4) when the true parameter values are $(\kappa, c) = (0.7, 10)$ and the spatial locations are directed from the third simulation group.

		Minimum	1st Quantile	Median	Mean	3rd Quantile	Maximum
Actual $y_t(\mathbf{s}_i)$'s		0.00	16.00	34.00	41.21	58.00	240.00
$U_t(\mathbf{s}_i)$'s	hypara3	0.00	16.30	33.70	41.21	57.78	292.69
	hypara4	0.00	16.30	33.70	41.22	57.78	293.47
c	hypara3	13.81	14.58	14.74	14.74	14.91	15.75
	hypara4	13.95	14.59	14.75	14.75	14.91	15.71
κ	hypara3	0.6768	0.7044	0.7104	0.7103	0.7162	0.7430
	hypara4	0.6730	0.7040	0.7100	0.7099	0.7159	0.7409

Table 43: Summary statistics of the actual observed counts $y_{1:T}(\mathbf{s}_{1:m})$ and the kept 10^4 posterior samples of the parameters $c, \kappa, U_{1:T}(\mathbf{s}_{1:m})$ for the two hyperparameter specifications (hypara3 and hypara4) when the true parameter values are $(\kappa, c) = (0.7, 15)$ and the spatial locations are directed from the third simulation group.

		Minimum	1st Quantile	Median	Mean	3rd Quantile	Maximum
Actual $y_t(\mathbf{s}_i)$'s		0.00	21.00	44.00	54.96	77.00	342.00
$U_t(\mathbf{s}_i)$'s	hypara3	0.00	21.82	44.82	54.96	76.92	413.15
	hypara4	0.00	21.82	44.82	54.96	76.93	414.19
c	hypara3	18.38	19.27	19.48	19.49	19.70	20.71
	hypara4	18.22	19.29	19.50	19.50	19.72	20.60
κ	hypara3	0.6856	0.7090	0.7150	0.7149	0.7207	0.7489
	hypara4	0.6829	0.7089	0.7146	0.7147	0.7206	0.7488

Table 44: Summary statistics of the actual observed counts $y_{1:T}(\mathbf{s}_{1:m})$ and the kept 10^4 posterior samples of the parameters $c, \kappa, U_{1:T}(\mathbf{s}_{1:m})$ for the two hyperparameter specifications (hypara3 and hypara4) when the true parameter values are $(\kappa, c) = (0.7, 20)$ and the spatial locations are directed from the third simulation group.

		Minimum	1st Quantile	Median	Mean	3rd Quantile	Maximum
Actual $y_t(\mathbf{s}_i)$'s		0.0	54.0	112.0	137.5	192.0	822.0
$U_t(\mathbf{s}_i)$'s	hypara3	0.00	54.77	112.14	137.52	192.49	920.54
	hypara4	0.00	54.76	112.13	137.52	192.49	918.93
c	hypara3	45.74	48.16	48.72	48.72	49.26	51.92
	hypara4	45.70	48.13	48.63	48.64	49.17	51.68
κ	hypara3	0.6830	0.7089	0.7147	0.7147	0.7205	0.7479
	hypara4	0.6840	0.7093	0.7151	0.7152	0.7209	0.7528

Table 45: Summary statistics of the actual observed counts $y_{1:T}(\mathbf{s}_{1:m})$ and the kept 10^4 posterior samples of the parameters $c, \kappa, U_{1:T}(\mathbf{s}_{1:m})$ for the two hyperparameter specifications (hypara3 and hypara4) when the true parameter values are $(\kappa, c) = (0.7, 50)$ and the spatial locations are directed from the third simulation group.

		Minimum	1st Quantile	Median	Mean	3rd Quantile	Maximum
Actual $y_t(\mathbf{s}_i)$'s		0.0	108.0	225.0	274.9	385.0	1591.0
$U_t(\mathbf{s}_i)$'s	hypara3	0.0	108.8	225.3	274.9	384.7	1764.8
	hypara4	0.0	108.8	225.3	274.9	384.7	1746.9
c	hypara3	92.21	96.38	97.42	97.48	98.55	105.09
	hypara4	91.77	96.43	97.55	97.54	98.60	102.89
κ	hypara3	0.6791	0.7084	0.7143	0.7142	0.7201	0.7466
	hypara4	0.6825	0.7079	0.7139	0.7137	0.7195	0.7464

Table 46: Summary statistics of the actual observed counts $y_{1:T}(\mathbf{s}_{1:m})$ and the kept 10^4 posterior samples of the parameters $c, \kappa, U_{1:T}(\mathbf{s}_{1:m})$ for the two hyperparameter specifications (hypara3 and hypara4) when the true parameter values are $(\kappa, c) = (0.7, 100)$ and the spatial locations are directed from the third simulation group.

		Minimum	1st Quantile	Median	Mean	3rd Quantile	Maximum
Actual $y_t(\mathbf{s}_i)$'s		0	550	1122	1375	1921	8447
$U_t(\mathbf{s}_i)$'s	hypara3	0.0	549.3	1122.8	1374.8	1922.7	8856.2
	hypara4	0.0	549.4	1122.8	1374.8	1922.7	8787.0
c	hypara3	460.3	483.0	488.0	488.1	493.2	514.5
	hypara4	463.1	483.3	488.4	488.6	493.9	519.5
κ	hypara3	0.6815	0.7084	0.7142	0.7141	0.7200	0.7504
	hypara4	0.6815	0.7083	0.7139	0.7138	0.7195	0.7452

Table 47: Summary statistics of the actual observed counts $y_{1:T}(\mathbf{s}_{1:m})$ and the kept 10^4 posterior samples of the parameters $c, \kappa, U_{1:T}(\mathbf{s}_{1:m})$ for the two hyperparameter specifications (hypara3 and hypara4) when the true parameter values are $(\kappa, c) = (0.7, 500)$ and the spatial locations are directed from the third simulation group.

		Minimum	1st Quantile	Median	Mean	3rd Quantile	Maximum
Actual $y_t(\mathbf{s}_i)$'s		0	1095	2252	2750	3850	16684
$U_t(\mathbf{s}_i)$'s	hypara3	0	1096	2249	2750	3843	17186
	hypara4	0	1096	2249	2750	3843	17235
c	hypara3	923.3	967.5	977.7	978.1	988.6	1036.0
	hypara4	919.6	967.1	977.7	978.0	988.8	1033.4
κ	hypara3	0.6802	0.7080	0.7139	0.7137	0.7196	0.7459
	hypara4	0.6827	0.7079	0.7137	0.7136	0.7195	0.7443

Table 48: Summary statistics of the actual observed counts $y_{1:T}(\mathbf{s}_{1:m})$ and the kept 10^4 posterior samples of the parameters $c, \kappa, U_{1:T}(\mathbf{s}_{1:m})$ for the two hyperparameter specifications (hypara3 and hypara4) when the true parameter values are $(\kappa, c) = (0.7, 1000)$ and the spatial locations are directed from the third simulation group.

		Minimum	1st Quantile	Median	Mean	3rd Quantile	Maximum
Actual $y_t(\mathbf{s}_i)$'s		0	2199	4496	5499	7683	33144
$U_t(\mathbf{s}_i)$'s	hypara3	0	2195	4495	5499	7683	33899
	hypara4	0	2195	4495	5499	7683	33818
c	hypara3	1848	1933	1954	1954	1976	2082
	hypara4	1851	1934	1955	1955	1976	2060
κ	hypara3	0.6829	0.7083	0.7140	0.7141	0.7200	0.7442
	hypara4	0.6810	0.7080	0.7139	0.7139	0.7198	0.7461

Table 49: Summary statistics of the actual observed counts $y_{1:T}(\mathbf{s}_{1:m})$ and the kept 10^4 posterior samples of the parameters $c, \kappa, U_{1:T}(\mathbf{s}_{1:m})$ for the two hyperparameter specifications (hypara3 and hypara4) when the true parameter values are $(\kappa, c) = (0.7, 2000)$ and the spatial locations are directed from the third simulation group.

		Minimum	1st Quantile	Median	Mean	3rd Quantile	Maximum
Actual $y_t(\mathbf{s}_i)$'s		0	5498	11290	13749	19200	83046
$U_t(\mathbf{s}_i)$'s	hypara3	0	5491	11273	13749	19191	84107
	hypara4	0	5491	11273	13749	19191	84140
c	hypara3	4627	4832	4884	4884	4935	5145
	hypara4	4576	4836	4889	4889	4941	5167
κ	hypara3	0.6812	0.7086	0.7144	0.7143	0.7201	0.7430
	hypara4	0.6780	0.7080	0.7138	0.7138	0.7195	0.7448

Table 50: Summary statistics of the actual observed counts $y_{1:T}(\mathbf{s}_{1:m})$ and the kept 10^4 posterior samples of the parameters $c, \kappa, U_{1:T}(\mathbf{s}_{1:m})$ for the two hyperparameter specifications (hypara3 and hypara4) when the true parameter values are $(\kappa, c) = (0.7, 5000)$ and the spatial locations are directed from the third simulation group.

		Minimum	1st Quantile	Median	Mean	3rd Quantile	Maximum
Actual $y_t(\mathbf{s}_i)$'s		0.000	2.000	5.000	7.748	11.000	76.000
$U_t(\mathbf{s}_i)$'s	hypara3	0.000	2.411	5.634	7.749	10.829	99.658
	hypara4	0.000	2.409	5.632	7.748	10.827	98.062
c	hypara3	4.677	5.119	5.213	5.217	5.315	5.753
	hypara4	4.734	5.148	5.256	5.257	5.362	5.923
κ	hypara3	0.2690	0.3267	0.3405	0.3399	0.3530	0.4124
	hypara4	0.2582	0.3204	0.3345	0.3343	0.3488	0.4051

Table 51: Summary statistics of the actual observed counts $y_{1:T}(\mathbf{s}_{1:m})$ and the kept 10^4 posterior samples of the parameters $c, \kappa, U_{1:T}(\mathbf{s}_{1:m})$ for the two hyperparameter specifications (hypara3 and hypara4) when the true parameter values are $(\kappa, c) = (0.35, 5)$ and the spatial locations are directed from the third simulation group.

		Minimum	1st Quantile	Median	Mean	3rd Quantile	Maximum
Actual $y_t(\mathbf{s}_i)$'s		0.00	4.00	11.00	15.49	22.00	143.00
$U_t(\mathbf{s}_i)$'s	hypara3	0.000	4.813	11.194	15.485	21.729	178.855
	hypara4	0.000	4.811	11.193	15.486	21.730	180.091
c	hypara3	9.513	10.231	10.410	10.414	10.589	11.351
	hypara4	9.613	10.273	10.452	10.459	10.637	11.510
κ	hypara3	0.2764	0.3293	0.3408	0.3408	0.3529	0.4064
	hypara4	0.2733	0.3256	0.3384	0.3379	0.3508	0.3991

Table 52: Summary statistics of the actual observed counts $y_{1:T}(\mathbf{s}_{1:m})$ and the kept 10^4 posterior samples of the parameters $c, \kappa, U_{1:T}(\mathbf{s}_{1:m})$ for the two hyperparameter specifications (hypara3 and hypara4) when the true parameter values are $(\kappa, c) = (0.35, 10)$ and the spatial locations are directed from the third simulation group.

		Minimum	1st Quantile	Median	Mean	3rd Quantile	Maximum
Actual $y_t(\mathbf{s}_i)$'s		0.00	7.00	17.00	23.27	32.00	209.00
$U_t(\mathbf{s}_i)$'s	hypara3	0.000	7.196	16.840	23.275	32.375	259.715
	hypara4	0.000	7.195	16.839	23.274	32.371	256.028
c	hypara3	14.47	15.48	15.74	15.75	16.02	17.90
	hypara4	14.05	15.51	15.77	15.78	16.04	17.52
κ	hypara3	0.2547	0.3253	0.3375	0.3371	0.3493	0.3912
	hypara4	0.2573	0.3237	0.3362	0.3357	0.3482	0.4076

Table 53: Summary statistics of the actual observed counts $y_{1:T}(\mathbf{s}_{1:m})$ and the kept 10^4 posterior samples of the parameters $c, \kappa, U_{1:T}(\mathbf{s}_{1:m})$ for the two hyperparameter specifications (hypara3 and hypara4) when the true parameter values are $(\kappa, c) = (0.35, 15)$ and the spatial locations are directed from the third simulation group.

		Minimum	1st Quantile	Median	Mean	3rd Quantile	Maximum
Actual $y_t(\mathbf{s}_i)$'s		0.0	9.0	22.5	31.1	43.0	246.0
$U_t(\mathbf{s}_i)$'s	hypara3	0.000	9.726	22.584	31.098	43.238	312.579
	hypara4	0.000	9.726	22.583	31.098	43.239	297.549
c	hypara3	18.81	20.48	20.83	20.85	21.20	23.11
	hypara4	19.08	20.59	20.96	20.97	21.34	22.92
κ	hypara3	0.2686	0.3313	0.3438	0.3431	0.3555	0.4096
	hypara4	0.2740	0.3264	0.3392	0.3389	0.3516	0.4011

Table 54: Summary statistics of the actual observed counts $y_{1:T}(\mathbf{s}_{1:m})$ and the kept 10^4 posterior samples of the parameters $c, \kappa, U_{1:T}(\mathbf{s}_{1:m})$ for the two hyperparameter specifications (hypara3 and hypara4) when the true parameter values are $(\kappa, c) = (0.35, 20)$ and the spatial locations are directed from the third simulation group.

		Minimum	1st Quantile	Median	Mean	3rd Quantile	Maximum
Actual $y_t(\mathbf{s}_i)$'s		0.00	24.00	56.00	77.69	108.25	643.00
$U_t(\mathbf{s}_i)$'s	hypara3	0.00	24.27	56.22	77.69	108.40	734.59
	hypara4	0.00	24.27	56.22	77.69	108.39	757.83
c	hypara3	47.11	51.31	52.16	52.20	53.03	58.14
	hypara4	47.59	51.33	52.21	52.25	53.14	57.18
κ	hypara3	0.2698	0.3305	0.3419	0.3416	0.3531	0.4052
	hypara4	0.2731	0.3288	0.3410	0.3407	0.3529	0.4023

Table 55: Summary statistics of the actual observed counts $y_{1:T}(\mathbf{s}_{1:m})$ and the kept 10^4 posterior samples of the parameters $c, \kappa, U_{1:T}(\mathbf{s}_{1:m})$ for the two hyperparameter specifications (hypara3 and hypara4) when the true parameter values are $(\kappa, c) = (0.35, 50)$ and the spatial locations are directed from the third simulation group.

		Minimum	1st Quantile	Median	Mean	3rd Quantile	Maximum
Actual $y_t(\mathbf{s}_i)$'s		0	48	112	155	215	1290
$U_t(\mathbf{s}_i)$'s	hypara3	0.00	48.71	112.17	154.99	215.58	1434.44
	hypara4	0.00	48.71	112.17	154.98	215.58	1421.74
c	hypara3	95.59	101.59	103.24	103.31	105.02	112.11
	hypara4	95.25	101.47	103.14	103.26	104.97	112.23
κ	hypara3	0.2892	0.3352	0.3471	0.3468	0.3585	0.4063
	hypara4	0.2826	0.3352	0.3476	0.3468	0.3585	0.4077

Table 56: Summary statistics of the actual observed counts $y_{1:T}(\mathbf{s}_{1:m})$ and the kept 10^4 posterior samples of the parameters $c, \kappa, U_{1:T}(\mathbf{s}_{1:m})$ for the two hyperparameter specifications (hypara3 and hypara4) when the true parameter values are $(\kappa, c) = (0.35, 100)$ and the spatial locations are directed from the third simulation group.

		Minimum	1st Quantile	Median	Mean	3rd Quantile	Maximum
Actual $y_t(\mathbf{s}_i)$'s		0.0	239.0	562.0	775.9	1078.2	6582.0
$U_t(\mathbf{s}_i)$'s	hypara3	0.0	240.5	561.0	775.9	1079.1	6936.0
	hypara4	0.0	240.5	561.0	775.9	1079.1	6850.5
c	hypara3	480.3	512.1	520.2	520.4	528.4	565.2
	hypara4	478.0	511.7	520.5	520.6	529.2	572.9
κ	hypara3	0.2761	0.3317	0.3425	0.3426	0.3538	0.4001
	hypara4	0.2785	0.3309	0.3427	0.3425	0.3543	0.3981

Table 57: Summary statistics of the actual observed counts $y_{1:T}(\mathbf{s}_{1:m})$ and the kept 10^4 posterior samples of the parameters $c, \kappa, U_{1:T}(\mathbf{s}_{1:m})$ for the two hyperparameter specifications (hypara3 and hypara4) when the true parameter values are $(\kappa, c) = (0.35, 500)$ and the spatial locations are directed from the third simulation group.

		Minimum	1st Quantile	Median	Mean	3rd Quantile	Maximum
Actual $y_t(\mathbf{s}_i)$'s		0	483	1120	1552	2155	13105
$U_t(\mathbf{s}_i)$'s	hypara3	0.0	482.4	1120.6	1551.5	2153.7	13526.8
	hypara4	0.0	482.4	1120.6	1551.5	2153.6	13522.2
c	hypara3	950.2	1024.3	1041.2	1042.3	1060.0	1136.8
	hypara4	951.4	1025.5	1043.2	1043.9	1061.9	1147.9
κ	hypara3	0.2836	0.3299	0.3423	0.3417	0.3538	0.4044
	hypara4	0.2788	0.3283	0.3407	0.3404	0.3527	0.4006

Table 58: Summary statistics of the actual observed counts $y_{1:T}(\mathbf{s}_{1:m})$ and the kept 10^4 posterior samples of the parameters $c, \kappa, U_{1:T}(\mathbf{s}_{1:m})$ for the two hyperparameter specifications (hypara3 and hypara4) when the true parameter values are $(\kappa, c) = (0.35, 1000)$ and the spatial locations are directed from the third simulation group.

		Minimum	1st Quantile	Median	Mean	3rd Quantile	Maximum
Actual $y_t(\mathbf{s}_i)$'s		0	964	2236	3103	4302	26189
$U_t(\mathbf{s}_i)$'s	hypara3	0.0	964.3	2237.2	3103.5	4305.6	26774.4
	hypara4	0.0	964.4	2237.2	3103.4	4305.5	26744.6
c	hypara3	1887	2054	2088	2089	2124	2310
	hypara4	1904	2050	2084	2086	2120	2309
κ	hypara3	0.2706	0.3283	0.3402	0.3399	0.3521	0.4062
	hypara4	0.2638	0.3296	0.3414	0.3412	0.3527	0.4028

Table 59: Summary statistics of the actual observed counts $y_{1:T}(\mathbf{s}_{1:m})$ and the kept 10^4 posterior samples of the parameters $c, \kappa, U_{1:T}(\mathbf{s}_{1:m})$ for hyperparameter specifications **hypara3** and **hypara4** with true parameter values $(\kappa, c) = (0.35, 2000)$ and directed spatial locations from the third simulation group.

		Minimum	1st Quantile	Median	Mean	3rd Quantile	Maximum
Actual $y_t(\mathbf{s}_i)$'s		0	2417	5602	7758	10756	65568
$U_t(\mathbf{s}_i)$'s	hypara3	0	2412	5604	7758	10757	66557
	hypara4	0	2412	5604	7758	10757	66657
c	hypara3	4776	5125	5213	5215	5301	5720
	hypara4	4710	5130	5214	5218	5302	5710
κ	hypara3	0.2712	0.3294	0.3412	0.3410	0.3536	0.4028
	hypara4	0.2734	0.3294	0.3408	0.3406	0.3524	0.3999

Table 60: Summary statistics of the actual observed counts $y_{1:T}(\mathbf{s}_{1:m})$ and the kept 10^4 posterior samples of the parameters $c, \kappa, U_{1:T}(\mathbf{s}_{1:m})$ for hyperparameter specifications **hypara3** and **hypara4** with true parameter values $(\kappa, c) = (0.35, 5000)$ and directed spatial locations from the third simulation group.

	Minimum	1st Quantile	Median	Mean	3rd Quantile	Maximum
$y_t(\mathbf{s}_i)$'s	0.0	32.0	73.0	97.6	138.0	877.0
$U_t(\mathbf{s}_i)$'s	0.00	32.14	73.47	97.60	137.74	975.15
$ y_t(\mathbf{s}_i) - U_t(\mathbf{s}_i) $'s	1.910×10^{-5}	0.4108	0.7546	0.8700	0.9926	13.30
c	48.80	49.76	50.00	50.00	50.25	51.45
κ	0.3799	0.3964	0.3996	0.3996	0.4027	0.4139
ρ	0.08676	0.09662	0.09869	0.09880	0.10089	0.11156

Table 61: Data simulated from our model with $T = 50$ and $m = 1600$: summary statistics of the actual observed counts $y_{1:T}(\mathbf{s}_{1:m})$, absolute error $|y_t(\mathbf{s}_i) - \hat{y}_t(\mathbf{s}_i)|$ for all (t, i) , and the kept 5000 posterior samples of the parameters $c, \kappa, \rho, U_{1:T}(\mathbf{s}_{1:m})$ for hyperparameter specification `hypara1`. The true parameter values are $(\kappa, \rho, c) = (0.4, 0.1, 50)$ and the spatial locations are undirected.

	Minimum	1st Quantile	Median	Mean	3rd Quantile	Maximum
$y_t(\mathbf{s}_i)$'s	0.00	32.00	73.00	97.95	138.00	827.00
$U_t(\mathbf{s}_i)$'s	0.00	32.39	73.24	97.95	137.65	920.08
$ y_t(\mathbf{s}_i) - U_t(\mathbf{s}_i) $'s	0.000032	0.409718	0.752823	0.871786	0.990895	11.581919
c	48.59	49.97	50.30	50.30	50.61	52.00
κ	0.3669	0.3857	0.3900	0.3900	0.3943	0.4112
ρ	0.08974	0.10334	0.10647	0.10644	0.10961	0.12243

Table 62: Data simulated from our model with $T = 50$ and $m = 900$: summary statistics of the actual observed counts $y_{1:T}(\mathbf{s}_{1:m})$, absolute error $|y_t(\mathbf{s}_i) - \hat{y}_t(\mathbf{s}_i)|$ for all (t, i) , and the kept 5000 posterior samples of the parameters $c, \kappa, \rho, U_{1:T}(\mathbf{s}_{1:m})$ for hyperparameter specification `hypara1`. The true parameter values are $(\kappa, \rho, c) = (0.4, 0.1, 50)$ and the spatial locations are undirected.

Measure Model	runtime	$\overline{\text{ESS}}$	MAE	DIC	p.d.	WAIC	p.w.
ST.CARlinear	198.8	1744.6	0.8895834	130032.4521	726.3246	130041.1649	721.4034
our model	3960	1796	0.6724177	132245.9	10784.88	146306.7	12800.52
INLA.ST1	0.06	N.A.	0.8152582	121443.7	644.4155	121442.9	634.4881
INLA.STint	0.17	N.A.	0.8029276	121437.9	1296.044	121447.7	1268.957
ST.CARsepspatial	413.4	1763.44	0.8791573	130912.3594	584.5215	130905.9726	591.2164
our model	2811.6	≈ 5000	0.4222	137704.1	20851.72	142312.5	13164.35
INLA.ST1	0.05	N.A.	0.8629758	127409.9	332.8639	127414.2	334.6194
INLA.STint	0.16	N.A.	0.8458735	127388.5	1196.434	127411.9	1188.314
ST.CARanova	340	1591.8	0.7733028	116189.0105	392.9050	116188.5211	388.8913
our model	3888	1690.4	0.5987155	117326.7	9040.101	129505.7	10961.21
INLA.ST1	0.05	N.A.	0.7334602	110367.8	340.7747	110369.1	339.5231
INLA.STint	0.15	N.A.	0.7221786	110356.6	997.812	110371.4	991.0257
ST.CARar	438.5	160.81	0.7643704	118770.380	3364.181	118963.927	3286.991
our model	3600	2059	0.587558	118839.3	10885.02	134954.3	13914.49
INLA.ST1	0.05	N.A.	0.9683906	134942	524.072	135072.5	646.7803
INLA.STint	0.21	N.A.	0.7966171	133244.5	8108.409	133422.4	7083.456
ST.CARadaptive	8394.6	553.73	2.499	257256.44	15379.43	257808.92	12680.56
ST.CARlocalised	2278.8	1052.194	2.086	256728.10	16717.58	259627.62	15125.71
our model	3708	4161	1.568243	268834.9	32390.91	273852.9	19207.85
INLA.STint	0.24	N.A.	1.578	276148.6	30308.05	272842.8	19945.11

Table 63: Data simulated from five CARBayesST settings (ST.CARadaptive and ST.CARlocalised share the same simulated data set) with $T = 50$ and $m = 900$: overall computation time (`runtime`) in seconds, mean response ESS ($\overline{\text{ESS}}$) at the 5000 kept post-burn-in MCMC iterations, and diagnostics metrics from the corresponding CARBayesST models, our model, and INLA.STint. INLA.ST1 performs poorly on the last simulated data set, and that row is thus excluded from the table.

Measure Model	runtime	ESS	MAE	DIC	p.d.	WAIC	p.w.
our model	3105	≈ 5000	0.871786	354027.7	43160.52	356793.3	23600.63
ST.CARar	454.3	1836.4	0.726032	357016.49	43727.37	346145.25	23725.93
ST.CARsepspatial	438.8	1837.5	0.721146	357247.67	43862.85	346378.54	23818.88
ST.CARadaptive	8455.8	1832.1	0.72530	357026.62	43734.17	346157.38	23730.59
ST.CARlocalised	2376.7	1821.0	1.386163	330143.28	14034.64	351824.76	25731.95
INLA.STint	0.30	N.A.	0.7423270	358961	44208.66	352875	26861.97

Table 64: Data simulated from our model with $T = 50$ and $m = 900$: overall computation time (`runtime`) in seconds, mean response ESS (`ESS`) at the 5000 kept post-burn-in MCMC iterations, and diagnostics metrics from our model and adequate CARBayesST, INLA models. ST.CARlinear, ST.CARanova, and INLA.ST1 perform very poorly and are thus not included in the table.

Measure Model	runtime	ESS	DIC	p.d.	WAIC	p.w.
ST.CARlinear	354.1	1654.5	180652.004	1087.128	180662.097	1077.577
our model	5832	1834.3	182552.5	15187.24	203970.8	18801.85
INLA.ST1	0.11	N.A.	180806.4	981.5026	180809.1	970.7971
INLA.STint	0.34	N.A.	180785.6	1951.996	180809.3	1922.594
ST.CARanova	565.7	1342.47	185764.3132	523.3728	185769.0505	524.0533
our model	5724	1990.3	188700.5	17032.12	212612	20975.82
INLA.ST1	0.08	N.A.	185803.7	477.9899	185806.7	477.7393
INLA.STint	0.26	N.A.	185784.7	1498.866	185807.9	1491.158
ST.CARar	705.5	153.72	194680.446	5827.903	194951.276	5594.397
our model	5904	1929.8	195367.1	17007.77	220530.1	21572.76
INLA.ST1	0.08	N.A.	204053.4	838.319	204242.3	1015.105
INLA.STint	0.34	N.A.	201731.7	12100.4	202004.7	10637.6

Table 65: Data simulated from ST.CARlinear, ST.CARanova, and ST.CARar with $T + h = 48 + 2 = 50$ consecutive time periods and $m + r = 1500 + 21 = 1521 = 39^2$ spatial locations: overall computation time (`runtime`) in seconds, mean response ESS (`ESS`) at the 5000 kept post-burn-in MCMC iterations, and diagnostics metrics from the corresponding CARBayesST models, our model, INLA.ST1, and INLA.STint.

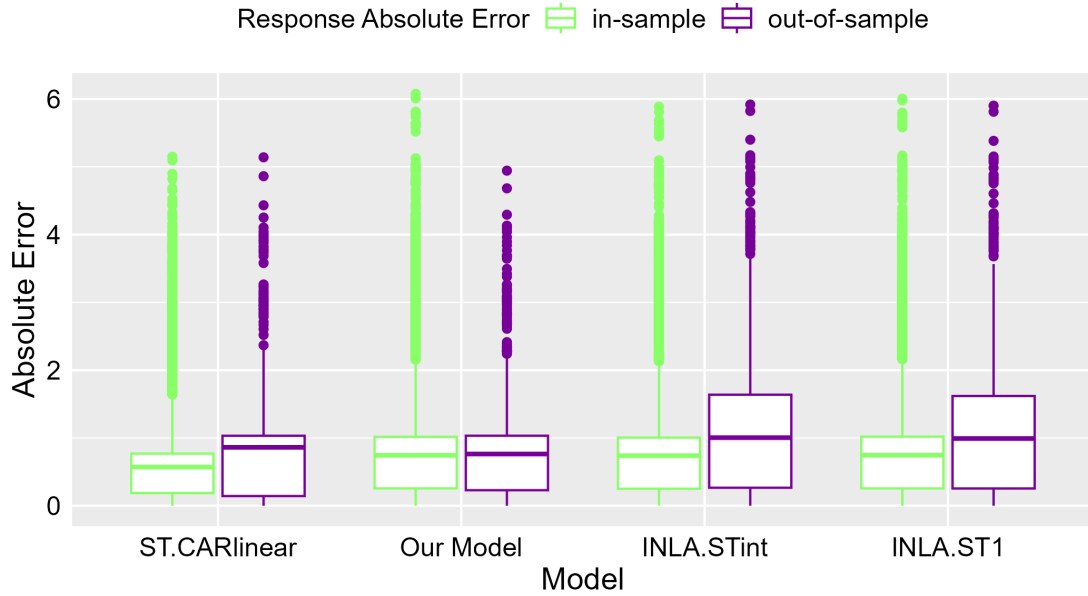


Figure 6: Boxplot for data simulated from ST.CARlinear with 50 consecutive time periods and $m+r = 1521 = 39^2$ spatial locations: distribution of the absolute errors $|y_t(\mathbf{s}_i) - \hat{y}_t(\mathbf{s}_i)|$, where $\hat{y}_t(\mathbf{s}_i)$ is the posterior mean for each (t, i) .

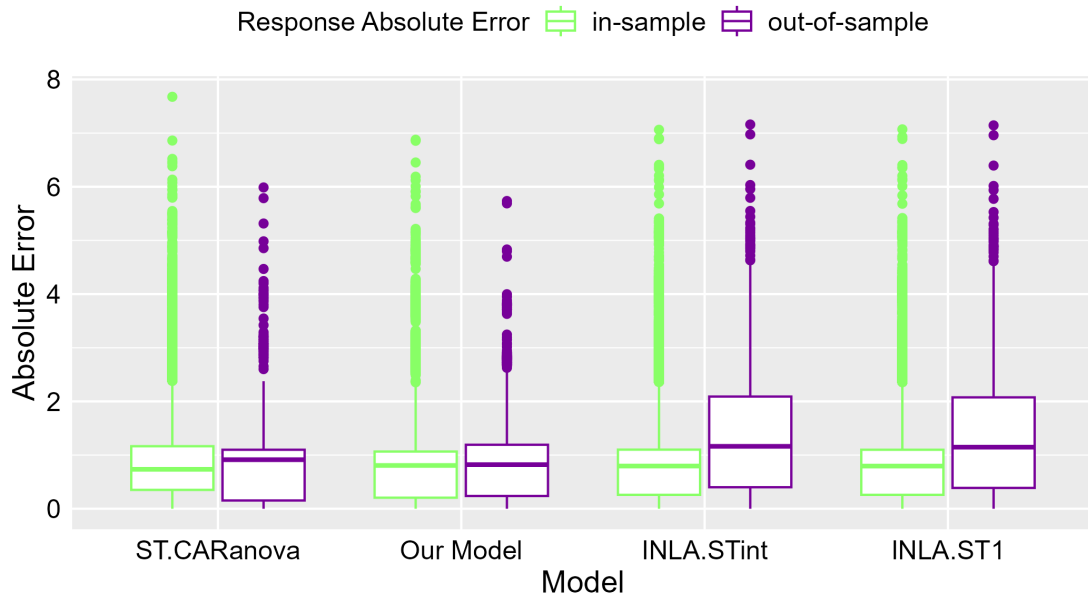


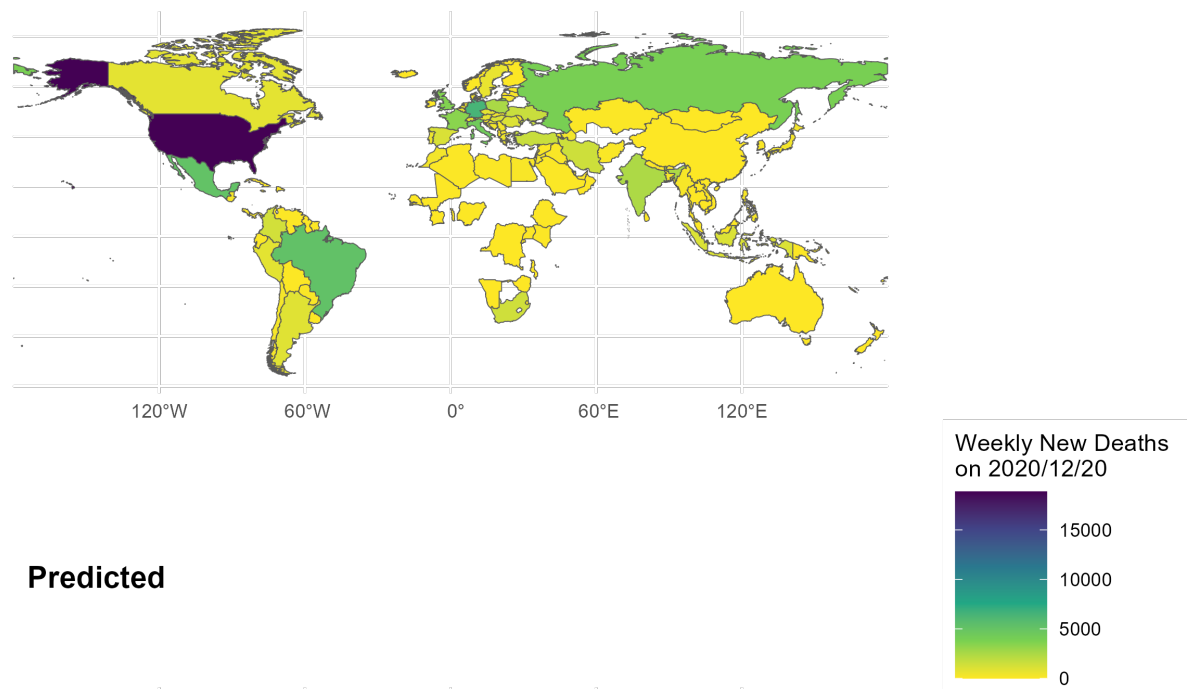
Figure 7: Boxplot for data simulated from ST.CARanova with 50 consecutive time periods and $m+r = 1521 = 39^2$ spatial locations: distribution of the absolute errors $|y_t(\mathbf{s}_i) - \hat{y}_t(\mathbf{s}_i)|$, where $\hat{y}_t(\mathbf{s}_i)$ is the posterior mean for each (t, i) .

D World Weekly COVID-19 Data Results Complementary to Section 6

		Minimum	1st Quantile	Median	Mean	3rd Quantile	Maximum
Actual $y_t(\mathbf{s}_i)$'s		0	504	3633	39190	16957	5650933
$\hat{y}_t(\mathbf{s}_i) = \bar{U}_t(\mathbf{s}_i) \times e^{\mathbf{x}_t(\mathbf{s}_i)\beta}$, S	autoregWITS	1	506	3633	39190	16954	5650904
	autoregCor	1	506	3632	39190	16956	5650902
	noselfWITS	1	505	3631	39190	16955	5650942
	noselfCor	1	505	3631	39190	16951	5650865
c	autoregWITS	0.993	1.022	1.030	1.030	1.038	1.079
	autoregCor	0.9899	1.0192	1.0271	1.0273	1.0349	1.0710
	noselfWITS	4.257	4.417	4.449	4.450	4.483	4.608
	noselfCor	2.714	2.803	2.824	2.825	2.846	2.950
κ	autoregWITS	0.000	$7.257 \cdot 10^{-6}$	$3.122 \cdot 10^{-5}$	$6.216 \cdot 10^{-5}$	$8.260 \cdot 10^{-5}$	$8.317 \cdot 10^{-4}$
	autoregCor	$1.000 \cdot 10^{-9}$	$2.510 \cdot 10^{-3}$	$3.472 \cdot 10^{-3}$	$3.497 \cdot 10^{-3}$	$4.527 \cdot 10^{-3}$	$8.207 \cdot 10^{-3}$
	noselfWITS	0.3843	0.4033	0.4082	0.4082	0.4130	0.4347
	noselfCor	0.5009	0.5157	0.5195	0.5195	0.5232	0.5376
ρ	autoregWITS	0.8555	0.8679	0.8708	0.8708	0.8737	0.8865
	autoregCor	0.8487	0.8638	0.8669	0.8669	0.8699	0.8847

Table 66: World weekly COVID-19 new cases: summary statistics of the actual observed counts $y_{1:T}(\mathbf{s}_{1:m})$, the predicted responses $\hat{y}_t(\mathbf{s}_i) = \bar{U}_t(\mathbf{s}_i) \times \exp\{\mathbf{x}_t(\mathbf{s}_i)\beta\}$ for all (t, i) , where β is fixed as described earlier and $\bar{U}_t(\mathbf{s}_i)$ is the mean of the kept posterior samples of $U_t(\mathbf{s}_i)$ for each (t, i) , and the kept 5000 posterior samples of c, κ for the four settings—autoregWITS, autoregCor, noselfWITS, and noselfCor—and of ρ for the first two settings.

Actual



Predicted

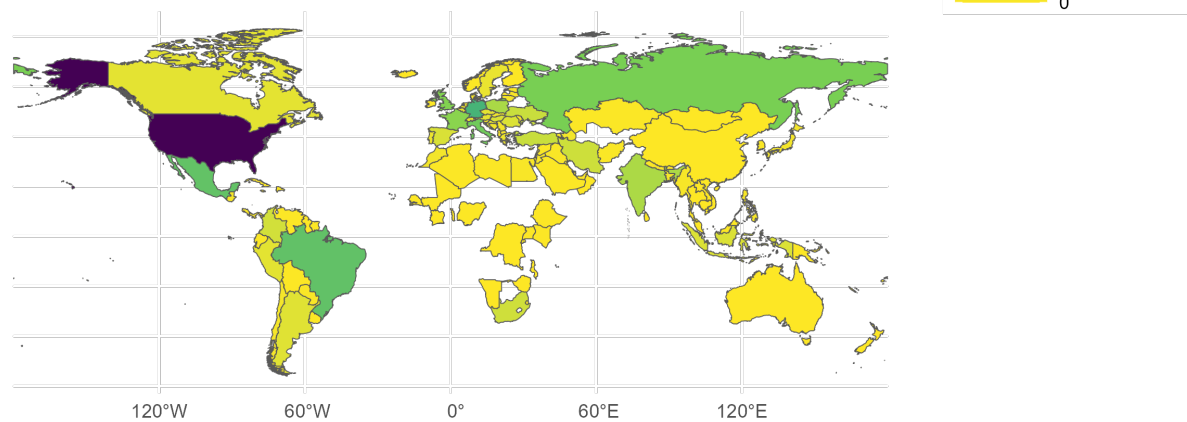


Figure 8: Actual and predicted (from the `noselfWITS` setting) new COVID-19 deaths in the $m = 123$ training countries/territories in the week reported on December 20, 2020. The shapefile is obtained from [Opendatasoft](#).

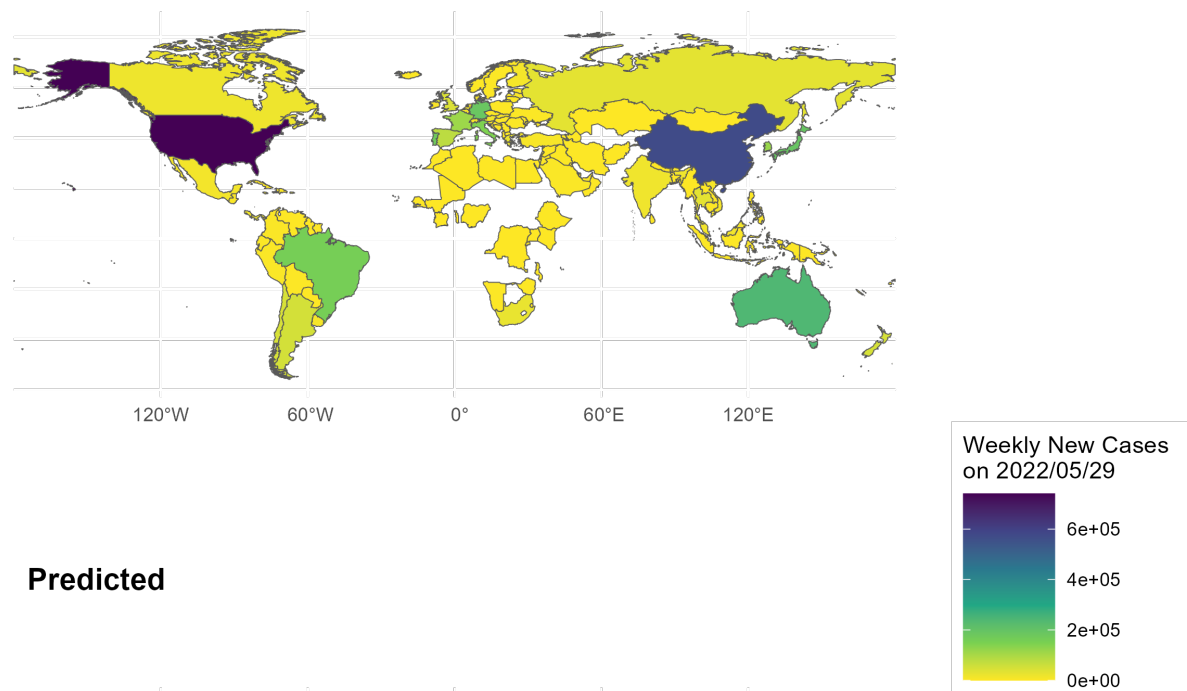
		Minimum	1st Quantile	Median	Mean	3rd Quantile	Maximum
Actual $y_t(\mathbf{s}_i)$'s		0.0	5.0	41.0	447.6	213.0	28982.0
$\hat{y}_t(\mathbf{s}_i) = \bar{U}_t(\mathbf{s}_i) \times e^{\mathbf{x}_t(\mathbf{s}_i)\boldsymbol{\beta}}$	autoregWITS	0.166	4.882	41.798	447.580	213.936	28982.182
	autoregCor	0.164	4.889	41.723	447.585	214.045	28982.409
	noselfWITS	0.663	5.119	41.866	447.578	213.347	28979.238
	noselfCor	0.541	5.034	41.828	447.581	213.384	28985.861
c	autoregWITS	0.4660	0.4782	0.4807	0.4807	0.4832	0.4950
	autoregCor	0.4674	0.4780	0.4806	0.4806	0.4831	0.4944
	noselfWITS	3.433	3.549	3.578	3.578	3.605	3.719
	noselfCor	2.968	3.071	3.096	3.095	3.119	3.262
κ	autoregWITS	0.000	$5.475 \cdot 10^{-6}$	$2.171 \cdot 10^{-5}$	$4.362 \cdot 10^{-5}$	$5.821 \cdot 10^{-5}$	$5.054 \cdot 10^{-4}$
	autoregCor	0.000	6.068×10^{-6}	2.501×10^{-5}	4.755×10^{-5}	6.494×10^{-5}	4.973×10^{-4}
	noselfWITS	0.4529	0.4770	0.4828	0.4827	0.4884	0.5164
	noselfCor	0.4392	0.4591	0.4633	0.4634	0.4677	0.4889
ρ	autoregWITS	0.9162	0.9251	0.9274	0.9274	0.9296	0.9400
	autoregCor	0.9163	0.9251	0.9274	0.9273	0.9295	0.9385

Table 67: World weekly COVID-19 new deaths: summary statistics of the actual observed counts $y_{1:T}(\mathbf{s}_{1:m})$, the predicted responses $\hat{y}_t(\mathbf{s}_i) = \bar{U}_t(\mathbf{s}_i) \times \exp\{\mathbf{x}_t(\mathbf{s}_i)\boldsymbol{\beta}\}$ for all (t, i) , where $\boldsymbol{\beta}$ is fixed as described earlier and $\bar{U}_t(\mathbf{s}_i)$ is the mean of the kept posterior samples of $U_t(\mathbf{s}_i)$ for each (t, i) , and the kept 5000 posterior samples of c, κ for the four settings—autoregWITS, autoregCor, noselfWITS, and noselfCor—and of ρ for the first two settings.

Metric Method	MAE	MAPE	DIC	p.d.	WAIC	p.w.
autoregWITS	1.663053	8.244734	90033.79	9549.816	95707.1	7880.353
autoregCor	1.663616	8.238353	90036.46	9551.499	94828.54	7452.335
noselfWITS	1.208447	9.702637	91735.95	10393.63	94901.5	7101.675
noselfCor	1.188701	9.391659	91613.89	10380.57	95029.55	7175.584
INLA.STint	0.6212796	9.18734	93428.45	12055.36	93801.81	8511.567
ST.CARarWbinary	1.559777	12.13594	89079.418	8702.329	87505.799	5265.140
ST.CARarWcorr	1.535569	12.07959	88601.097	8549.985	86870.359	5050.861
ST.CARadaptiveWbinary	1.912252	12.48362	88208.038	8419.877	86989.594	5263.732
ST.CARadaptiveWcorr	1.474775	11.83246	89026.926	8886.574	87508.425	5387.956
ST.CARlocalisedWbinary	0.8899884	4.244823	93041.34	11800.16	110737.68	17358.49
ST.CARlocalisedWcorr	0.8595571	3.696582	94486.38	12652.32	122573.85	23243.61

Table 68: Weekly COVID-19 new deaths: diagnostics metrics from 11 adequate model settings.

Actual



Predicted

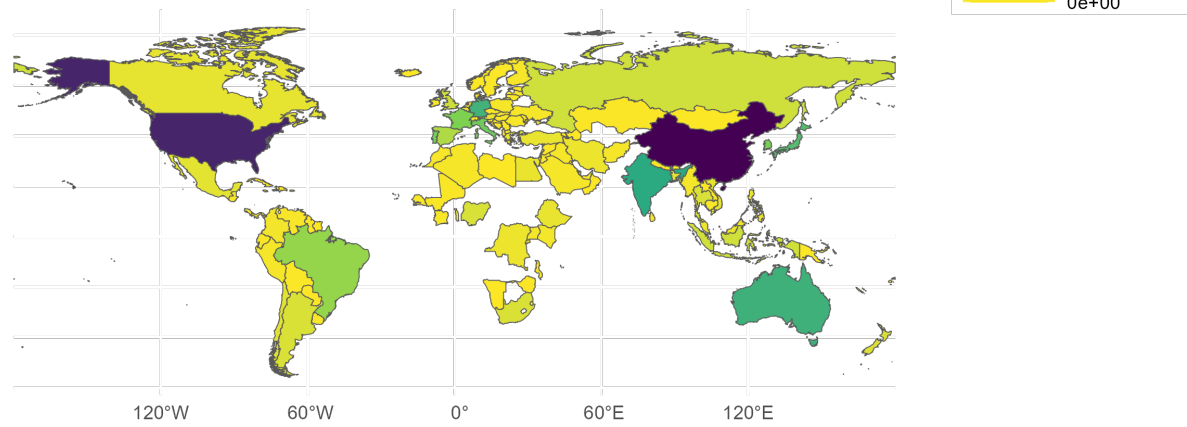
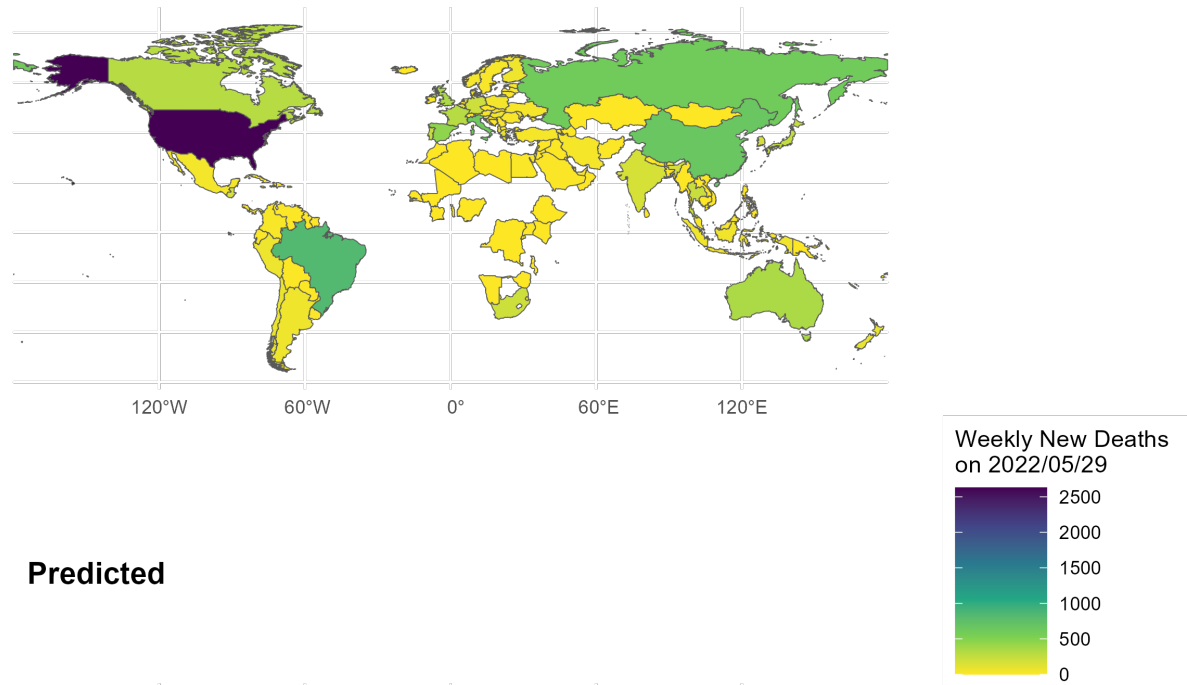


Figure 9: Actual and predicted (from the `autoregWITS` setting) new COVID-19 cases in the $m + r = 123 + 4 = 127$ training and testing countries/territories in the week reported on May 29, 2022. The shapefile is obtained from [Opendatasoft](#).

Actual



Predicted

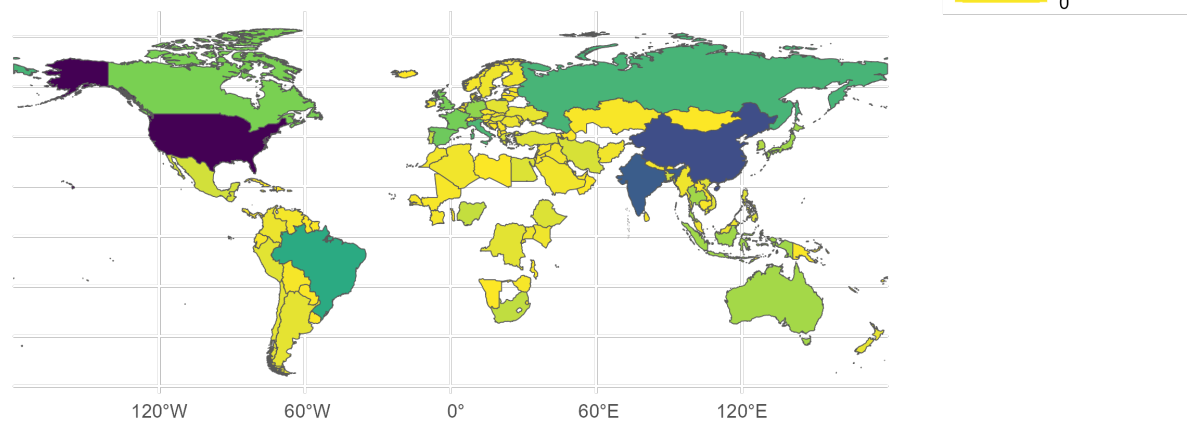


Figure 10: Actual and predicted (from the autoregWITS setting) new COVID-19 deaths in the $m+r = 123+4 = 127$ training and testing countries/territories in the week reported on May 29, 2022. The shapefile is obtained from [Opendatasoft](#).

References

- Bansal, P., R. Krueger, and D. J. Graham (2021). Fast Bayesian estimation of spatial count data models. *Computational Statistics and Data Analysis* 157, 107152.
- Besag, J. (1974). Spatial interaction and the statistical analysis of lattice systems (with discussion). *Journal of the Royal Statistical Society, Series B* 36(2), 192–236.
- Besag, J. and C. Kooperberg (1995). On conditional and intrinsic autoregressions. *Biometrika* 82(4), 733–746.
- Besag, J., J. York, and A. Mollié (1991). Bayesian image restoration, with two applications in spatial statistics. *Annals of the Institute of Statistical Mathematics* 43, 1–20.
- Blangiardo, M., M. Cameletti, G. Baio, and H. Rue (2013). Spatial and spatio-temporal models with R-INLA. *Spatial and Spatio-temporal Epidemiology* 7, 39–55.
- Bradley, J. R. and M. Clinch (2025). Generating independent replicates directly from the posterior distribution for a class of spatial hierarchical models. *Journal of Computational and Graphical Statistics* 34(1), 123–139.
- Bradley, J. R., S. H. Holan, and C. K. Wikle (2018). Computationally efficient multivariate spatio-temporal models for high-dimensional count-valued data (with discussion). *Bayesian Analysis* 13(1), 253–310.
- Christensen, O. F. and R. Waagepetersen (2004). Bayesian prediction of spatial count data using generalized linear mixed models. *Biometrics* 58(2), 280–286.
- Creal, D. D. (2017). A Class of Non-Gaussian State Space Models With Exact Likelihood Inference. *Journal of Business and Economic Statistics* 35(4), 585–597.
- D’Angelo, L. and A. Canale (2023). Efficient posterior sampling for Bayesian Poisson regression. *Journal of Computational and Graphical Statistics* 32(3), 917–926.
- Darolles, S., C. Gourieroux, and J. Jasiak (2006). Structural Laplace transform and compound autoregressive models. *Journal of Time Series Analysis* 27(4), 477–503.

- Datta, A., S. Banerjee, A. O. Finley, and A. E. Gelfand (2016). Hierarchical nearest-neighbor Gaussian process models for large geostatistical datasets. *Journal of the American Statistical Association* 111(514), 800–812.
- De Oliveira, V. (2013). Hierarchical Poisson models for spatial count data. *Journal of Multivariate Analysis* 122, 393–408.
- De Oliveira, V. (2014). Poisson kriging: A closer investigation. *Spatial Statistics* 7, 1–20.
- Devroye, L. (2002). Simulating Bessel random variables. *Statistics and Probability Letters* 57(3), 249–257.
- Diggle, P. J., J. A. Tawn, and R. A. Moyeed (1998). Model-based geostatistics (with discussion). *Journal of the Royal Statistical Society: Series C* 47(3), 299–350.
- Estes, L., P. R. Elsen, T. Treuer, L. Ahmed, K. Caylor, J. Chang, C. J. J., and E. C. Ellis (2018). The spatial and temporal domains of modern ecology. *Nature Ecology & Evolution* 2, 819–826.
- Gourieroux, C. and J. Jasiak (2006). Autoregressive gamma processes. *Journal of Forecasting* 25(2), 129–152.
- Katzfuss, M. and J. Guinness (2021). A general framework for Vecchia approximations of Gaussian processes. *Statistical Science* 36(1), 124–141.
- Lee, D., A. Rushworth, and G. Napier (2018). Spatio-temporal areal unit modeling in R with conditional autoregressive priors using the CARBayesST package. *Journal of Statistical Software* 84, 1–39.
- Mardia, K. V. (1988). Multi-dimensional multivariate Gaussian Markov random fields with application to image processing. *Journal of Multivariate Analysis* 24(2), 265–284.
- Morales-Navarrete, D., M. Bevilacqua, C. Caamaño Carrillo, and L. M. Castro (2024). Modelling point referenced spatial count data: A Poisson process approach. *Journal of the American Statistical Association* 119(545), 664–677.
- Nazia, N., Z. A. Butt, M. L. Bedard, W.-C. Tang, H. Sehar, and J. Law (2022). Methods

- used in the spatial and spatiotemporal analysis of COVID-19 epidemiology: A systematic review. *International Journal of Environmental Research and Public Health* 19, 8267.
- Rue, H., S. Martino, and N. Chopin (2009). Approximate Bayesian inference for latent Gaussian models by using integrated nested Laplace approximations. *Journal of the Royal Statistical Society, Series B* 71(2), 319–392.
- Vecchia, A. V. (1988). Estimation and model identification for continuous spatial processes. *Journal of the Royal Statistical Society: Series B (Methodological)* 50(2), 297–312.
- Ward, T., M. Morris, A. Gelman, B. Carpenter, W. Ferguson, C. Overton, and M. Fyles (2023). Bayesian spatial modelling of localised SARSCoV-2 transmission through mobility networks across England. *PLoS Computational Biology* 19(11), e1011580.
- Zhai, Q., Z. Ye, C. Li, M. Revie, and D. B. Dunson (2025). Modeling recurrent failures on large directed networks. *Journal of the American Statistical Association* 120(549), 251–265.
- Zhao, E., M. R. Stone, X. Ren, J. Guenthoer, K. S. Smythe, T. Pulliam, S. R. Williams, C. R. Uytingco, S. E. B. Taylor, P. Nghiem, J. H. Bielas, and R. Gottardo (2021). Spatial transcriptomics at subspot resolution with BayesSpace. *Nature Biotechnology* 39(11), 1375–1384.
- Zhu, Y., M. Peruzzi, C. Li, and D. B. Dunson (2024). Radial neighbors for provably accurate scalable approximations of Gaussian processes. *Biometrika* 111(4), 1151–1167.